2009

Vesicle Targeting In Plasmodium Falciparum: The Identification and Molecular Characterization of Plasmodium Falciparum Family of of Snare Proteins

Lawrence Sumanjah Ayong
University of Central Florida

VESICLE TARGETING IN PLASMODIUM FALCIPARUM: IDENTIFICATION AND MOLECULAR CHARACTERIZATION OF P. FALCIPARUM FAMILY OF SNARE PROTEINS

By

LAWRENCE SUMANJAH AYONG
D.Sc. in Biochemistry, University of Yaounde I, Cameroon, 2002

A dissertation presented in partial fulfillment of the requirements
for the degree of Doctor of Philosophy in Biomedical Sciences
in the Burnett School of Biomedical Sciences
in the College of Medicine
at the University of Central Florida
Orlando, Florida

Fall Term 2009

Major Professor:
Debopam Chakrabarti, Professor

ABSTRACT

Proteins of the SNARE (Soluble N-ethylmaleimide sensitive factor attachment protein receptor) super-family have been characterized as playing an essential role in vesicle targeting and fusion in all eukaryotes. The intracellular malaria parasite *Plasmodium falciparum* exhibits an unusual endomembrane system that is characterized by an unstacked Golgi apparatus, a developmentally induced apical complex, and various organellar structures of parasite origin in the infected host cells. How malaria parasites target nuclear-encoded proteins to these novel compartments is a central question in *Plasmodium* cell biology. Ultrastructural studies elsewhere have implicated the participation of specialized vesicular elements in transport of virulence proteins, including various cytoadherance and host cell remodeling factors, into the infected erythrocyte cytoplasm. However, little is known about the machineries that define the directionality of vesicle trafficking in malaria parasites.

We hypothesized that the *P. falciparum* SNARE proteins would exhibit novel features required for vesicle targeting to the parasite-specific compartments. We then identified for the first time and confirmed the expression of eighteen SNARE genes in *P. falciparum*. Members of the PfSNAREs exhibit atypical structural features (Ayong *et al*., 2007, *Molecular & Biochemical Parasitology*, **152**(2), 113-122). Among the atypical PfSNAREs, PfSec22 contains an unusual insertion of the *Plasmodium* export element (PEXEL) within its profilin-like longin domain, preceded by an N-terminal hydrophobic segment.

Localization analyses suggest that PfSec22 is predominantly a vesicle-associated SNARE of the ER/Golgi interface, but which associates partially with mobile extraparasitic

vesicles in *P. falciparum*-infected erythrocytes at trophozoite stages. We showed that PfSec22 export into host cells occurs via a two-step model that involves extraparasitic vesicle budding from the parasite plasma membrane and fusion with the parasitophorous vacuolar membrane. Export of PfSec22 was independent of its membrane-insertion suggesting that this protein might cross the vacuolar space as a single-pass type IV membrane protein. We demonstrated that the atypical longin domain dictates the steady-state localization of PfSec22, regulating its ER/Golgi trafficking and export into host cells. Our study provides the first experimental evidence for SNARE protein export in *P. falciparum*, and suggests a role of PfSec22 in vesicle trafficking within the infected host cell (Ayong *et al*, *Eukaryotic Cell*, Epub Jul 17, 2009)

Next, to define the physiological function of the PfSec22 protein in *Plasmodium* parasites, we investigated its cognate partners. Using purified recombinant proteins we showed that PfSec22 forms direct binding interactions with six other PfSNAREs *in vitro*. These included the PfSyn5, PfBet1, PfGS27, PfSyn6, PfSyn16 and PfSyn18 PfSNAREs. By generating GFP-expressing parasites, we successfully localized the SNARE proteins PfSyn5, PfBet1 and PfGS27 to the parasite *cis*-Golgi compartment. We confirmed the association of PfSec22 with PfSyn5, PfBet1 and PfGS27 *in vivo* by immunoprecipitation analyses. Our data indicate a conserved ER-to-Golgi SNARE assembly in *P. falciparum*, and suggest that the malaria Sec22 protein might form novel SNARE complexes required for vesicle traffic within *P. falciparum*-infected erythrocytes.

ACKNOWLEDGMENTS

My first and very pleasant duty is to acknowledge my indebtedness to my Advisor, Dr. Debopam Chakrabarti, for his trust, guidance and constant support for my training. His uncompromising demand for excellence and perfection was a driving force behind my academic performance and professional development.

I am profoundly thankful to my committee members, Dr. Kenneth Teter, Dr. Suren Tatulian and Dr. Mark Muller, whose insightful comments and suggestions were critical in shaping the work presented in this dissertation.

I would like to express my profound gratitude to all faculty members and the administrative staff in the Biomedical Sciences Ph.D program for their contributions to my professional development at UCF.

I am particularly grateful to all members of the Chakrabarti lab, whose team spirit and curiosity made my lab work a necessary calling.

Special thanks go to Drs. David Fidock and Marcus Lee of Columbia University, Drs. Theodore Taraschi and Timothy Schneider of Thomas Jefferson University, and to Drs. Ratna Chakrabarti, Christina Fernandez-Valle, James Tuckson and Wei Zhao of the University of Central Florida for their material and technical support during this study.

I am particularly thankful to Dondrea Thompson and to my family for their encouragement, love and support throughout my academic career.

Finally, I am thankful to the Fulbright fellowship program for giving me the opportunity to pursue my academic dreams here in the United States of America

TABLE OF CONTENTS

LIST OF FIGURES

LIST OF TABLES

CHAPTER 1:
GENERAL INTRODUCTION

1.1 HYPOTHESIS AND SPECIFIC OBJECTIVES

The malaria parasite *Plasmodium falciparum* exhibits an unusual endomembrane system that is characterized by 1) presence of a digestive vacuole that is specialized in hemoglobin uptake and degradation, 2) presence of an apical complex; a collection of specialized secretory organelles that are involved in host cell invasion and immune evasion, 3) absence of a classical Golgi apparatus, and 4) presence of a complex network of parasite-induced tubovesicular structures in the infected host cell compartment. The cellular processes involved in the biogenesis and maintenance of these unique organellar structures in *P. falciparum*-infected cells are not understood. Additionally, asexual forms of the parasite export hundreds of virulence factors into the host cell cytoplasm (erythrocytes and hepatocytes) that are essential for the disease pathogenesis and immune evasion. The signals and machineries involved in protein sorting and targeting to the parasite-specific organelles are elusive.

It is believed that both tubular and vesicle transport processes play a key role in protein trafficking in *Plasmodium* parasites. Vesicle trafficking in eukaryotic cells is a multi-step process that involves vesicle budding from a donor compartment, migration along cytoskeletal arrays and fusion with a specific target compartment. Proteins of the SNARE superfamily have been characterized to play an essential role in specifying the directionality of vesicle transport in yeast, plants and mammalian cells. However, no studies have characterized the role of this important protein family in vesicle targeting in malaria parasites.

This study was aimed at understanding the role of *P. falciparum* family of SNAREs (PfSNAREs) in vesicle targeting to the parasite-specific destinations. In this seminal study, we hypothesized that members of the PfSNAREs would exhibit novel features that might be required for their localization to pathways that are unique to the malaria parasite. A systematic analysis of the *Plasmodium* genome database was undertaken to identify the *P. falciparum* complement of SNAREs and to dissect any unique structural features. To test our central hypothesis, we investigated the steady-state locations of the *P. falciparum* Sec22 gene product (PfSec22), which contains an unusual insertion of the *Plasmodium* export element (PEXEL) within its N-terminal sequence preceded by a recessed hydrophobic segment. This PfSec22 protein, unlike its yeast counterpart (Sec22p), was unable to complement a Sec22-3 temperature-sensitive allele in *Saccharomyces cerevisiae* when expressed in *trans*. By generating various deletion and point mutation constructs, we further investigated the role of the atypical N-terminal domain and the hydrophobic segments in PfSec22 trafficking. Together, our data indicate that *P. falciparum* targets this ER/Golgi v-SNARE into the infected host cell, at trophozoite stages, where it associates with mobile extraparasitic vesicles. Furthermore, we show that PfSec22 export to the infected host cell is independent of the PEXEL and C-terminal hydrophobic segments, and that the N-terminal hydrophobic domain regulates the Golgi exit of PfSec22 in malaria parasites.

In an effort to identify other SNARE proteins that might assemble into fusogenic SNARE complexes with PfSec22 at the extraparasitic locations, we investigated the PfSec22 interacting PfSNAREs and examined their intracellular locations. We showed that PfSec22 potentially forms SNARE complexes with PfSyn5, PfBet1, PfGS27, PfSyn6, PfSyn16 and PfSyn18.

Interaction of PfSec22 with PfSyn5, PfBet1 and PfGS27 *in vivo* was confirmed by co-immunoprecipitation analyses. Surprisingly, these three PfSNAREs localized exclusively to the Golgi-like structure suggesting that PfSec22 might form novel complexes within the extraparasitic vesicular transport pathways. Studies are underway to define the subcellular locations of PfSyn6, PfSyn16, PfSyn18 and other atypical PfSNAREs that might sequentially assemble into fusogenic SNARE complexes with PfSec22 at the extraparasitic locations.

Taken together, the data presented in this study demonstrate that 1) some members of the *Plasmodium* SNARE homologues indeed exhibit structural features that are unique to the malaria parasite, 2) that the *P. falciparum* Sec22 gene product partially associates with non-canonical trafficking pathways in the infected host cell, 3) that the atypical longin domain regulates the steady-state dynamics of PfSec22 in malaria parasites, and 4) that PfSec22 forms novel SNARE complexes with the *Plasmodium* complements of Syn6 and Syn16, presumably required for vesicle targeting to yet an uncharacterized trafficking pathway. This study is the first detailed analysis of SNARE proteins in malaria parasites, and provides new insights into the organization of the secretory system in *P. falciparum*.

1.2 LITERATURE REVIEW

1.2.1. Plasmodium falciparum: the most virulent form of malaria parasites

Malaria is caused by protozoans of the genus *Plasmodium*. At least 200 *Plasmodium* species have been described that infect mammals, reptiles, or birds [1]. Of the four species that infect humans (*P. falciparum*, *P. vivax*, *P. malariae*, and *P. ovale*), *P. falciparum* causes the most lethal form of malaria, resulting in 1 to 3 million deaths annually. Between 300 and 660 million clinical cases of *P. falciparum* malaria are reported each year, a majority of whom are children under five years old and pregnant women [2]. An estimated 2.2 billion people worldwide are at risk of *P. falciparum* infection each year, a majority (>90%) of whom live in Sub-Saharan Africa [3-5]. Outside Africa, *P. falciparum* accounts for an estimated 85 million cases of malaria especially in the Amazon basin of the Americas and in Asia [6]. Although malaria once occurred in the United States and several parts of Western Europe, the disease receded with economic development and following widespread implementation of improved public health policies. Present day malaria in the United States and Europe is primarily imported from the Amazon basin, Asia, the Middle East, and Africa. Of the 1,528 reported cases of malaria in the United States in 2005, 48.6% were due to *P. falciparum* alone [7]. Some profound effects of human infection with *P. falciparum* include severe anaemia, cerebral malaria, acute respiratory distress, epilepsy, hypoglycaemia, acidosis, and multi-organ failures. In pregnant women, especially during the first and second pregnancies, *P. falciparum* infection may result in spontaneous abortion, stillbirth, low birth weights, maternal anaemia and death [2].

More than a deadly disease, the socio-economic impacts of *P. falciparum* malaria are enormous. About 58% of all malaria cases occur in the 20% world's poorest population who, unfortunately, are also victims of the world's two leading infectious agents, HIV/AIDS and tuberculosis [8].The disease significantly strains global economic development, debilitates the world's most active populations, endangers children's education, and impairs cognitive development in young children [8-11].

Significant strides have been made by both residents of endemic countries and by the international community to reduce the mortality and morbidity of malaria in some highest hit areas [6]. However, a major gap still exists between the new-found interest in malaria research and the tools needed to eliminate the disease in all affected areas. Some major challenges include 1) absence of a malaria vaccine with operational implications, 2) the unprecedented rise and spread of multi-drug resistant parasites, 3) the limited number of antimalarials available in the market, 4) the rapid spread of insecticide-resistant mosquitoes, and 5) the worsening world economy as well as global climate changes that favor parasite development and spread.

1.2.2. Life cycle of P. falciparum

Plasmodium parasites exhibit a complex life-cycle that is characterized by three invasive forms (sporozoites, merozoites, and ookinetes), and several morphologically distinct intermediary forms. The developmental cycle consist of two asexual phases (exo-erythrocytic schizogony in the liver and erythrocytic schizogony in enucleated human erythrocytes) and one sexual cycle also known as sporogony occurring within the mosquito mid gut (Fig. 1) [12].

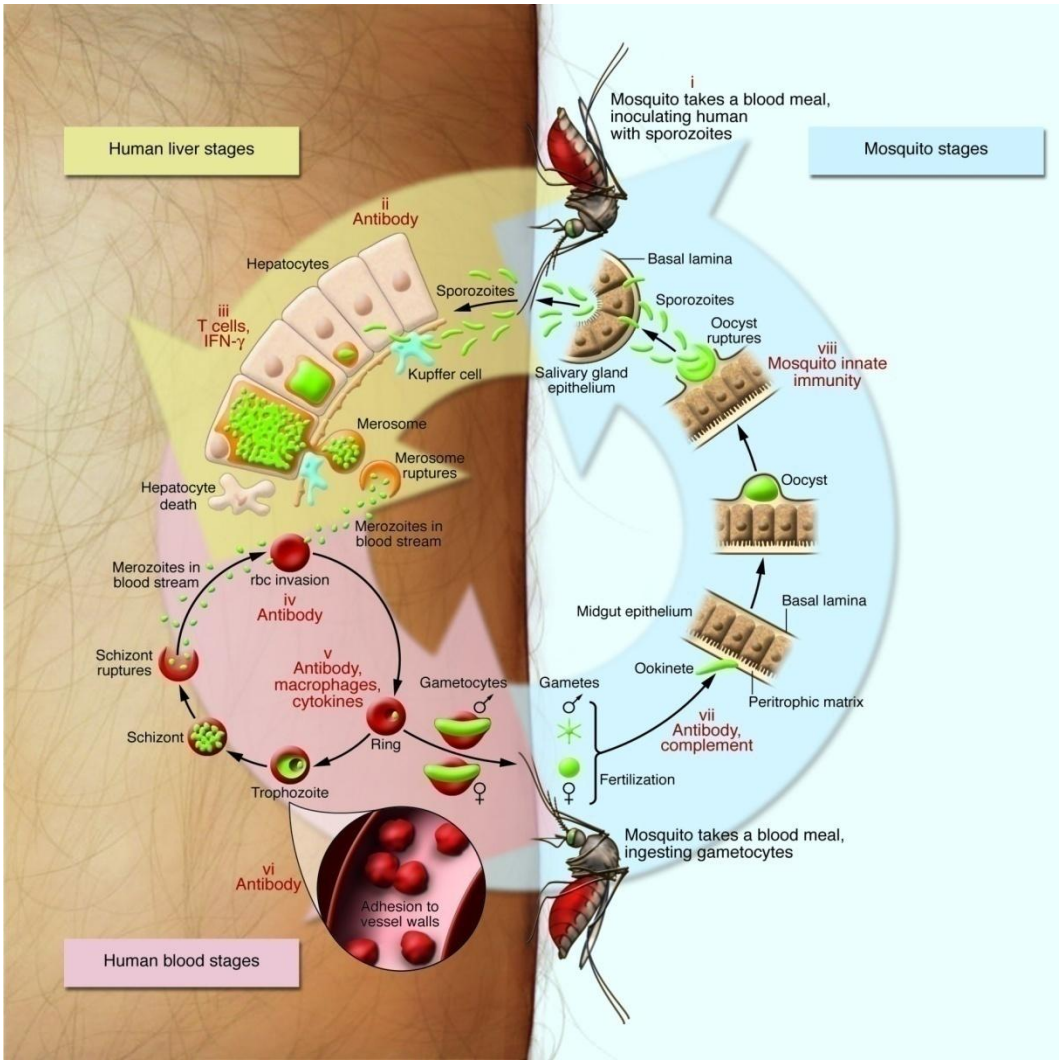

Figure 1: Life cycle of human malaria parasites

Infection of the human host is initiated when haploid sporozoites are injected along with saliva into the bloodstream by a feeding mosquito. The motile sporozoites then move with the general circulation into the liver where they invade hepatocytes and undergo an asexual replication known as exo-erythrocytic schizogony. Unlike *P. vivax* and *P. ovale* which go through a dormant period in the form of hypnozoites, liver stages of *P. falciparum* infection often last about 6 days and are usually asymptomatic. Exo-erythrocytic schizogony culminates in the production of several merozoites, which initially are released into the bloodstream as large

aggregates called merosomes [13]. Upon rupture of the merosomes, free-moving merozoites attach and invade enucleated erythrocytes where the parasite undergoes a complex series of morphological transitions resulting in a new population of merozoites. The merozoite stage comprises the only extracellular form (lasting about 20 seconds) of the intraerythrocytic cycle, which last approximately 48 hours. This cycle includes two sexual forms called gametocytes and three asexual forms that are subjectively referred to as rings (0-24 hpi), trophozoite (24-36 hpi) and schizonts or segmenters (36-48 hpi) [14, 15]. Parasite development into the trophozoite stage is accompanied by an active metabolism that involves ingestion of host cell cytoplasm and proteolysis of the ingested hemoglobin. The trophic period ends with four successive rounds of nuclear division without cytokinesis known as erythrocytic schizogony that occur approximately 28-36 hpi [14, 16, 17]. Schizogony results in multinucleated schizont stage parasites that ultimately mature into 16-32 daughter merozoites [18, 19]. This cycle of growth and asexual replication repeats every 48 hours, causing parasitaemia to rise rapidly to levels as high as 10^{13} in some patients. Blood stage forms of the infection are responsible for the pathologies associated with severe malaria. These include acute anemia caused by the massive destruction of host erythrocytes, and cerebral and placental malarias arising from sequestration of mature stage parasites in the brain and placenta. In response to stimuli not well understood, a small proportion of the ring stage parasites differentiate into sexual gametocytic forms namely microgametocytes (male gametocytes) and macrogametocytes (female gametocytes). Gametocyte maturation takes 7 to 10 days after merozoite invasion, and involves five stages designated stages I to V. Ingestion of gametocytes by a feeding *Anopheles* vector induces gametogenesis and escape of the resulting gametes (microgamete and macrogamete) from the host erythrocyte [20]. Upon fertilization of

the macrogamete by a flagellated microgamete, a diploid zygote is formed that differentiates into a motile ookinete. The ookinete penetrates the gut epithelial cells where it encysts to form an oocyst. Eventually the oocyst undergoes a meiotic reduction in chromosome number and multiple rounds of asexual replication (sporogony) resulting in the production of over 2000 sporozoites. Upon rupture of the mature oocyst, the released sporozoites migrate through the hemocoel to the salivary gland of the mosquito where they await transfer to the vertebrate host during a next blood meal.

1.2.3. Ultrastructural features of P. falciparum: presence of strange organelles

The development of *P. falciparum* parasites inside human erythrocytes is a continuous dynamic process that involves many intermediate stages and endomembrane complexities, only a few of which are discernable at the ultrastructural level [18]. In addition to an endoplasmic reticulum (ER), an 'unstacked' Golgi, and a mitochondria, the parasite has evolved a distinct set of novel organelles in response to its intracellular life-style that include a pigment vacuole, also known as food or digestive vacuole involved in host cell hemoglobin digestion, and a remnant plastid called apicoplast that is thought to have been acquired in a secondary endosymbiosis event [21-23]. Also present in the invasive stages is a set of secretory organelles, collectively known as the apical complex that include the rhoptries, micronemes and dense granules, which contain proteases, adhesions, and various membrane-active substances involved in host cell recognition and modifications [24]. During invasion of erythrocytes, the parasite becomes enclosed within an additional lipid bilayer called the parasitophorous vacuole membrane (PVM), which acts as a semipermeable barrier, separating the parasite from the host erythrocyte

cytoplasm [15, 25]. Beginning at the early trophozoite stage, a tubulovesicular network (TVN) and cleft structures called Maurer's clefts (MC) are visible within the host cell compartment.

Ultrastructurally, merozoite (~ 1.6μm long and 1.0μm wide) comprise a thick bristly coat of thin filaments anchored to the plasma membrane with major component being the merozoite surface protein (MSP) 1 complex involved in host cell capture and entry [18, 26]. Beneath the plasma membrane lie two other membranes called alveola, which together with the plasma membrane form the pellicle. At the apical end lies three membranous structures that are collectively known as apical organelles and include two rhoptries (~650 nm long and 300 nm wide), several micronemes (120 x 40 nm), and multiple rounded bodies known as dense granules (~80 nm diameter) [18, 27]. Between the rhoptries and nucleus is a region containing closely packed free ribosomes, a resource for accelerating protein synthesis in the newly invaded ring stage parasite [18, 28]. A single mitochondrion and a single plastid (apicoplast) lie beneath a band of subpellicular microtubules to which the plastid is attached.

Upon invasion of host erythrocytes, the parasite transforms into a thin discoidal, flat or cup-shaped ring form of the trophozoite stage [26]. Ring stage parasites comprise a thick rim of cytoplasm containing the chief organelles: nucleus, mitochondrion, plastid, ribosomes and endoplasmic reticulum (ER). Nuclear shape varies from a sausage-like form to a disc. The mitochondrion and plastid are always attached to each other at one end [29]. Although, the Golgi is not evident by transmission electron microscopy, clusters of vesicles and smooth and rough ER close to the nucleus suggest a Golgi body [18]. Various dense structures called cytostomes and at least one pigment vacuole (also known as digestive or food vacuole) are observed within the cytoplasm. Initially there are several small vacuoles, which then fuse at later stages to form a

single large pigment vacuole [30]. As the parasite develops, the surrounding parasitophorous vacuole membrane (PVM) extends membranous blebs and finger-like projections into the erythrocyte cytosol, called tubovesicular networks (TVN). The ring stage parasite eventually changes shape into the more rounded or irregular trophozoite form at about 24 hours post invasion.

Distinction between the ring and trophozoite stages depends on cell size and shape rather than any fundamental internal difference, thus the ring is more properly called the ring form of the trophozoite stage [28]. In mature trophozoites, the ER enlarges and the numbers of free ribosomes multiply greatly. A more elaborate but unusual type of Golgi (unstacked Golgi) is evident close to the nuclear envelope [31]. The mitochondrion and plastid lengthen considerably; and their membrane whorls come in contact with the pigment vacuole. Enlargement of the trophozoite within the parasitophorous vacuole (PV) is accompanied by significant modifications in the host cell compartment [14, 18]. The PVM embraces the PM closely with little intervening space, and in a few places it forms more elaborate sets of loops, whorls, various membranous stacks and configurations that penetrate deep into the erythrocyte cytosol. Some of these configurations reach the underside of the erythrocyte plasma membrane (EPM), but no instances of fusion with the EPM to form an open pore has been discovered. These membranous stacks correspond to the basophilic dots seen in the cytoplasm of Giemsa-stained cells called Maurer's clefts. At the ultrastructural level, Maurer's clefts can be classified as long clefts, often continuous with the PVM, or as short clefts that presumably correspond to branches of long clefts or detached, independent structures [27]. At the mid-trophozoite stage, the rough ER has proliferated considerably, and the Golgi-like complex has increased in size and number. Various

dense materials accumulate in the PV, suggesting of increased export of parasite factors. In certain strains of the parasite, the EPM is greatly deformed into knob-like structures that facilitate cell adhesion and sequestration of trophozoites and schizonts in deep visceral bloods vessels.

The schizont stage represents intraerythrocytic parasites that are undergoing or have undergone repetitive nuclear division following trophic development. The nucleus divides about four times, with alternating bouts of DNA synthesis, resulting in 16 to 20 nuclei. Numerous cytoplasmic changes accompany nuclear division including great proliferation of the rough ER and ribosomes throughout the parasite cytoplasm, duplication of mitochondria and plastids, and accumulation of large lipid vacuoles required for future membrane provenance [18]. Various centers of merozoite formation are evident, including an ordered assembly of the apical organelles [28, 32]. During the last nuclear division, the merozoite-forming foci appear around the circumference of the parasite each containing the apical organelles. Coated vesicles bud off from the nuclear membrane, coalescing into the Golgi body, which in turn produces a second set of vesicles that fuse to create the two rhoptries, or transform individually into micronemes and dense granules [18, 28]. Before complete separation of each nascent merozoite, a nucleus, mitochondrion and plastid migrate from the central region of schizont cytoplasm into each cell, and the merozoite coat is added in yet an undefined process to its surface. A constriction ring then separates the merozoites from the residual body of the schizont containing the pigment vacuole, and the separate merozoites cluster within the PV. Merozoite release then follows disruption of the PVM and EPM, presumably triggered by apical organelle secretions.

1.2.4. Parasite-induced modifications in P. falciparum-infected erythrocytes

Entry of malaria parasites into human red blood cells involves the invagination of a protein-free patch of the erythrocyte membrane, resulting in formation of a parasitophorous vacuole (PV) in which parasite development occurs [25]. This entry process is initiated by interactions between surface molecules of the merozoites (e.g. EBA175 and EBA140) and RBC membrane sialoglycophorins as well as glycophorins A and C that results in the establishment of a tight junction between the parasite and the RBC [33-35]. Following activation of an actin-myosin motor in the pellicle of the invading merozoite, the merozoite then uses a gliding motility to enter the host cell [36].

Upon entry into human red blood cells (RBC), the parasite modifies the permeability and adhesive characteristics of the host cell to promote nutrient uptake and immune evasion [37, 38]. Transmission electron microscopy studies revealed that ring stage parasites are surrounded by a parasitophorous vacuolar membrane (PVM) [39]. Multiple membrane-bound organelles, including tubular extensions and whorls that emanate from the PV membrane known as the tubulovesicular network (TVN), also appear in the host cell cytoplasm [40]. A second set of slender-like structures (~20 nm wide) with an electron-dense coat and electron-lucent lumen called Maurer's clefts (~30 nm wide) is also observed in the infected erythrocyte cytoplasm beginning at the ring stage [18, 41, 42]. Electron tomography analyses revealed that the MC are flat and disc-shaped, and are connected to each other by slender profiles. These organelles, which are thought to arise from the PVM, are connected to the RBC membrane via tubular tethers of diameter about 30 nm [43, 44]. Maurer's clefts appear to serve as secretory organelles involved in virulence protein packaging and delivery to the RBC membrane [45-47]. Non-

membrane-bound aggregates and rare vesicle-like structures of variable sizes (ranging from 25 nm to 800 nm diameters) have also been observed in the cytoplasm of *P. falciparum*-infected erythrocytes [44, 48-52], suggesting that the parasite has developed a novel system for membrane trafficking outside its plasma membrane.

A prominent morphological alteration of *P. falciparum*-infected RBCs is the formation of electron-dense structures, called knobs, at the erythrocyte plasma membrane [14, 53]. Knobs serve as concentration sites for immuno-variant adhesins, collectively called *P. falciparum* erythrocyte membrane protein 1 (PfEMP1), required for cytoadherence of mature stage parasites to the vascular endothelial linings and immune evasion [40, 54, 55]. This adhesion and subsequent accumulation of infected erythrocytes in the microvasculature are pivotal events in the pathogenesis of *P. falciparum*, and represent major virulence factors.

1.2.5. Unusual transport pathways in blood stages of P. falciparum

In contrast to a number of other intracellular pathogens, which invade and multiply within nucleated host cells, *P. falciparum* develops inside terminally differentiated human erythrocytes that are devoid of all intracellular organelles and protein trafficking machineries [56-58]. To survive within the enucleated cells, *P. falciparum* traffics a large number of proteins to, and through, the host erythrocyte where they mediate numerous functions such as nutrient acquisition, cytoadherence and immune evasion [14, 59-63]. The *P. falciparum* endomembranes comprise a dynamic system of overlapping compartmental boundaries, and multidirectional protein trafficking pathways [62, 64]. Protein trafficking to the erythrocyte surface membrane involves several levels of sophistication as blood stages of the parasite reside inside a

parasitophorous vacuole (PV); thus, are separated from the external milieu by three lipid bilayers: the parasite plasma membrane (PPM), the parasitophorous vacuole membrane (PVM), and the erythrocyte plasma membrane (Fig. 2) [62].

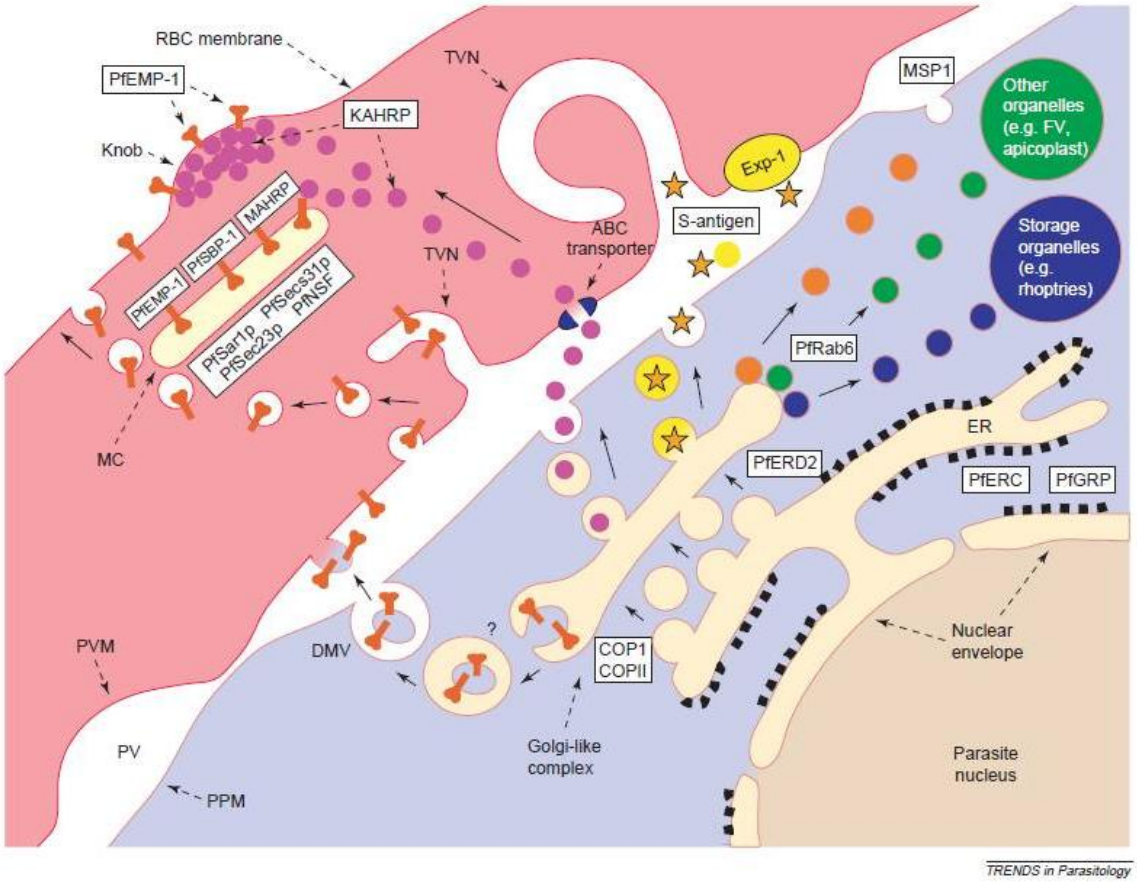

Figure 2: Putative transport pathways in *P. falciparum*-infected erythrocytes

Soluble malaria proteins that are destined for export into the infected host cell enter the secretory system via the ER, and then are directed through a rudimentary Golgi to the PV. It is believed that some exported proteins (e.g. KAHRP, S-antigen and MSP-1) presumably are transported in separate vesicles to distinct sub-compartments of the PV, or might be co-transported to the PV in mixed cargo vesicles, and sorted into resident and forward-destined proteins within this compartment. Along the secretory system, some proteins might be retrieved

from the PM or diverted from the ER or Golgi to intracellular organelles that include the digestive vacuole, the apicoplast, or the apical organelles. Proteins destined for locations beyond the PVM are first released into the PV. It has been proposed that recognition of a translocation motif in the exported proteins results in translocation across the PVM, via a putative ATP-dependent transporter (ABC transporter). The exported soluble proteins then diffuse across the RBC cytosol to the MC or erythrocyte surface. Exported integral membrane proteins, such as membrane-associated histidine-rich proteins (MAHRP), are thought to traffic via a vesicle-mediated pathway. Evidence from ultrastructural examinations suggests the presence of double membrane vesicles (DMVs) in the parasite cytosol, which might be involved in delivery of membrane-associated proteins to the PVM.

Although a classical secretory pathway appears to operate in *P. falciparum*, intracellular traffic in this parasite is unusual in several respects. Firstly, protein transport in *P. falciparum* involves a range of destinations not found in other eukaryotes. These include the three secretory organelles (micronemes, rhoptries and dense granules), the PV and PVM, and various locations within the infected host erythrocyte. Secondly, most electron micrographs reveal no obvious Golgi in the parasite, although some studies have found membrane-enclosed structures resembling a single Golgi cisterna [18, 30, 65]. Evidence for presence of an unusual Golgi structure has also been provided by immunolocalization experiments using homologues of eukaryotic *cis*- and *trans*-Golgi antigens, which suggest that the parasite Golgi exists in a highly modified and 'unstacked' form [66-68]. Thirdly, the export of some of the secreted proteins follows a brefeldin A-insensitive pathway, suggesting a Golgi-independent secretory process for the some parasite proteins. Fourthly, protein trafficking into the infected erythrocyte cytosol

necessitates novel machineries for translocation across the PV, the PVM, and the host cell cytosol. Two models have been proposed to account for protein translocation across the surrounding PV (~10 nm thick): a one-step and a two-step model (Fig. 3) [63, 69].

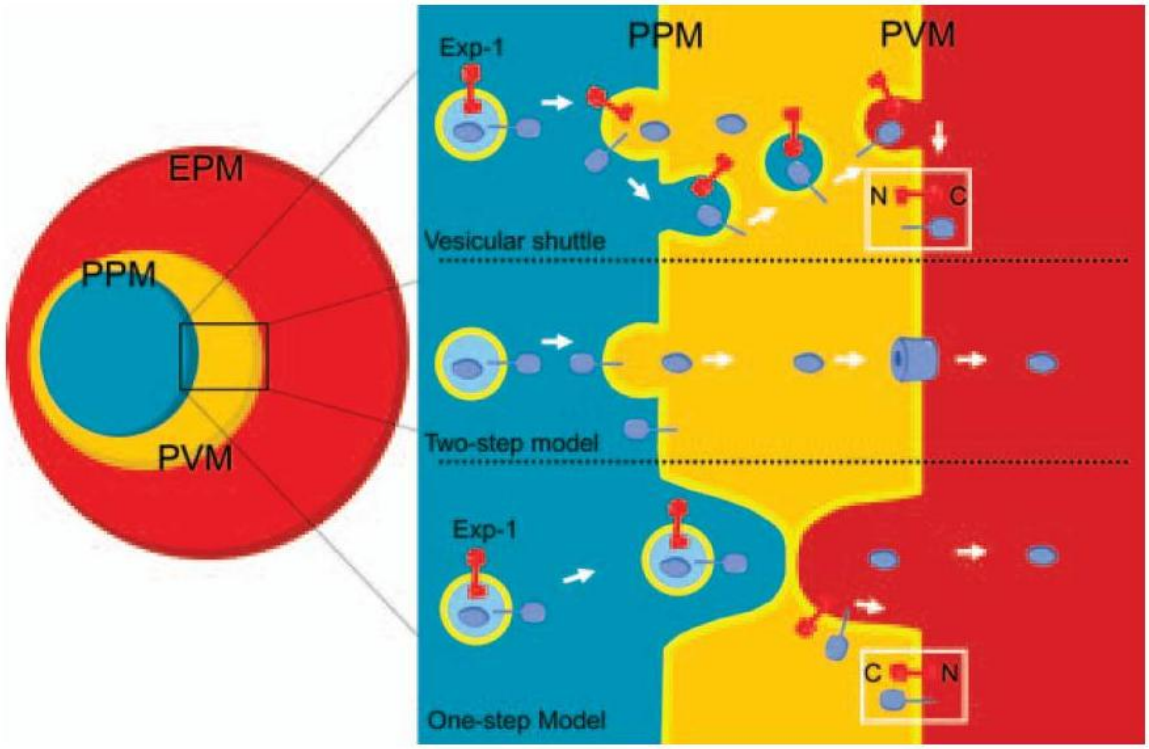

Figure 3: Models for protein transport across the PVM

The one-step model proposes that fusion of secretory vesicles at regions where the PPM appears to coalesce with the PVM would result in translocation into the erythrocyte cytosol [63, 66]. In contrast, the two-step model suggests that proteins secreted into the PV would subsequently be translocated across the PVM, either by protein complexes or by vesicle budding [62, 63].

1.2.6. Membrane traffic in P. falciparum: Tubular versus Vesicle-mediated traffic

Intracellular membrane traffic is an essential process in all eukaryotic cells. It involves the rapid and selective transport of proteins and lipids from a donor compartment to an acceptor membrane, required for the biogenesis and maintenance of cellular organization and functions. Eukaryotic membrane traffic is mediated largely by distinct transport vesicles as well as by continuous tubular connections that link conservative intracellular compartments.

Digitized fluorescence and electron microscopy studies have revealed the presence of both transport vesicles and tubular structures in *P. falciparum* [39, 51, 65, 70, 71]. Tubular transport processes, known as cytostomal tubes, have been implicated in hemoglobin uptake and transport to the digestive vacuole[70]. These double membrane-bound cytostomal tubes, which are mostly detected in trophozoite-stage (~30-hour) parasites, appear to bud off double membrane-bound vesicles containing host cell hemoglobin into the parasite cytoplasm [30, 70]. Serial optical sections of Bodipy ceramide-stained cells, followed by three-dimensional reconstruction, have also revealed a network of interconnected tubules (termed TVN or tubovesicular network) in *P. falciparum*-infected erythrocytes [39]. The TVN is thought to develop as a series of interconnected vesicles in ring-stage parasites, which, in trophozoite stages, acquire a more prominent tubular morphology with a few attached vesicles [39, 72].

Freely mobile vesicular elements have been detected in the infected erythrocyte cytosol [48, 52], and within the parasite cytoplasm [73]. However, the free moving vesicles in the infected host cell do not appear to be a dominant feature and remain poorly characterized [39].

1.2.7 Vesicular traffic and the SNARE hypotheses

Vesicular transport is a fundamental process in all eukaryotic cells, and mutations in components of the vesicle trafficking machineries results in various forms of human diseases [74-78]. According to a vesicular transport hypothesis, vesicular traffic is a multi-step process in which, (1) vesicles bud from a donor compartment (vesicle budding) in a process that allows retention of resident proteins (protein sorting), (2) budded vesicles are targeted to a specific acceptor compartment (vesicle targeting), and (3) the vesicle and acceptor membranes fuse into a single compartment (vesicle fusion) (Fig. 4)[79].

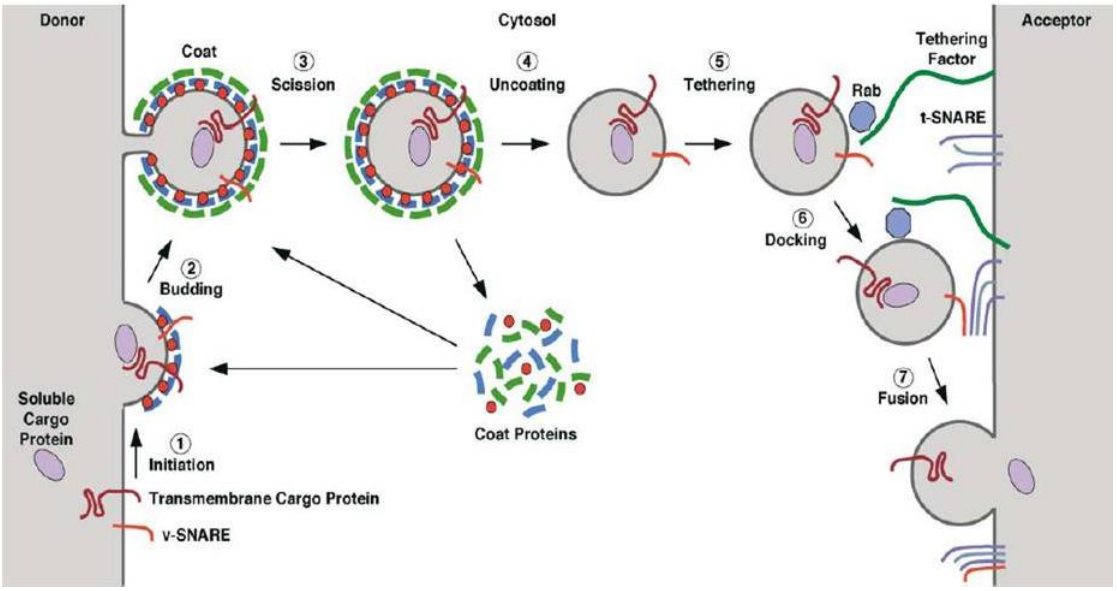

Figure 4: Steps in vesicle budding and fusion

The process of budding and fusion are iterated at the consecutive transport pathways until the cargo reaches its final destination [79, 80]. To balance the forward movement of organeller membranes (anterograde transport), and to maintain organelle homeostasis, some components of the transport machinery and escaped resident proteins are retrieved from the acceptor compartment back to the corresponding donor membrane (retrograde transport).

A central dogma in vesicular transport is that the process is vectorial; vesicles generated from one compartment will only fuse with a cognate acceptor membrane. Compartmental specificity is provided by distinct members of protein families, such as those involved in sorting (e.g. membrane coats, adaptor proteins, and cargo receptors), small GTPases of the rab family, tethering factors, and members of the SNARE superfamily [80, 81]. The docking and fusion steps of vesicular traffic are accomplished by specific interactions between vesicle-associated SNAREs (v-SNAREs) and cognate partners on the acceptor or target membrane (t-SNAREs).

1.2.7.1. The SNARE superfamily: Discovery, domain architecture and functions

SNAREs (Soluble N-ethylmaleimide sensitive factor Attachment protein Receptors) represent a superfamily of membrane-anchored proteins that are now widely believed to play a key role in vesicle targeting and fusion in all eukaryotes [81-85]. A crucial step in the discovery of SNAREs was the identification in a cell-free assay of an N-ethylmaleimide sensitive factor (NSF) that was required for intra-Golgi membrane fusion [86]. Inactivation of NSF with N-ethylmaleimide resulted in accumulation of uncoated vesicles on Golgi membranes, suggesting a role in vesicle fusion [87]. It thereafter became apparent that NSF was involved in a wide range of membrane fusion steps both in the secretory and endocytic transport pathways [88-90]. A key step toward understanding NSF function was the identification of the adaptor protein, alpha-SNAP (soluble NSF attachment protein), which binds NSF to membranes [91]. By using NSF/alpha-SNAP as an affinity reagent to fractionate a brain homogenate, Söllner and colleagues identified a set of three membrane-associated “SNAP receptors”, or SNAREs, which had previously been implicated in synaptic vesicle fusion with the plasma membrane [92]. One

of these SNAREs, synaptobrevin or vesicle-associated membrane protein (VAMP), was known to be located in synaptic vesicles whereas the other two proteins, syntaxin and synaptosome-associated protein of 25-kDa (SNAP25), had been localized to the presynaptic plasma membrane. The discovery of the link between NSF, the adaptor protein alpha-SNAP, and the SNARE proteins SNAP25, synaptobravin, and Syn1 revolutionalized future analysis of synaptic transmission and intracellular membrane traffic. Today, several homologues of the founding SNAREs have been discovered, and their role in membrane traffic elucidated.

SNAREs are functionally referred to as v- or t-SNAREs based on their localization to transport vesicles (v) or to the target (t) membrane during fusion. Support for a function of SNAREs as fusogens came from *in vitro* reconstitution experiments showing that purified recombinant SNAREs can promote liposome fusion provided that v- and t-SNAREs are in different liposomes [93]. The role of SNAREs in membrane fusion has recently be demonstrated in an *in vivo* model wherein cells were engineered to expressed 'flipped' SNARE that faced the outside of the cell rather than the cytoplasm [94]. Efficient fusion was observed between the cells only when cells containing the flipped v-SNAREs were mixed with cells containing the cognate flipped t-SNAREs. *In vitro* studies of various SNARE complexes from yeast and mammals have validated that each v-SNARE is specific for a limited number of t-SNAREs. This selectivity of v- and t-SNARE interactions is encoded in the respective SNARE motifs [95], and contributes to the specificity of SNARE-dependent fusion *in vivo*. Additional the selectivity of SNARE-mediated fusion is provided by spatial segregation of the cognate t-SNAREs from the non-cognate counterparts during fusion, and by diverse proofreading interactions that involve specific inhibitory SNAREs [96].

SNAREs are also divided into distinct subfamilies on the basis of whether they contain one or two SNARE motifs, on the sequences of the SNARE motifs, and on the type of flanking domains. Most SNAREs contain a single SNARE motif that is preceded by a variable N-terminal sequence and is followed by a C-terminal transmembrane domain [83, 97]. Other SNAREs do not possess transmembrane domains and are membrane anchored by post-translational lipid modification events. For example, SNAP25 and its relatives contain a palmitoylation cysteine-motif between the two SNARE motifs that mediate their post-translational insertion to membranes [98]. Some single SNARE motif-containing SNAREs without a transmembrane domain also contain cysteine-motifs at the C-terminal end that can be palmitoylated or prenylated, resulting in membrane attachment of the protein [83, 99, 100].

SNAREs also differ in the sequences that surround the SNARE motif or membrane attachment motifs. For example, the N-termini of syntaxins are composed of separate domains (designated helix a, b, and c or Habc), which are conserved between syntaxins that function at distinct trafficking pathways [101]. On the basis of the presence or absence of a conserved N-terminal extension in VAMP homologues, this subfamily have been divided into long VAMPs (or longins) and short VAMPs (brevins) [102]. Other N-terminal domains include the PX domain of Vam7 (yeast homologue of SNAP25) that binds to phosphoinositide-3-phosphate [103].

The SNARE motif On the basis of a conserved arginine or glutamine at the central ionic layer position of various SNARE motifs, SNAREs have also been classified as R- or Q-SNAREs [104]. According to the ‘SNARE hypothesis’, vesicle fusion is mediated by ordered interactions between a single R-SNARE (often located on vesicles) and three Q-SNAREs resulting in a highly stable quaternary complex called a SNAREpin [93]. This 3Q:1R requirement for fusion-

competent SNARE complexes in membrane has been confirmed by mutagenesis studies [105-107]. Replacing one of the glutamines with arginine in the yeast exocytic SNARE complex causes a growth defect that could be compensated for by replacing the R-SNARE arginine with glutamine. SNARE complexes of lower orders (1:1 and 2:1) are also common in biological systems, but their physiological relevance is not known. It has, however, been demonstrated that liposome fusion to deposited bilayers can be accomplished with just synaptobrevin and syntaxin in different membranes [108-110]. Isolated SNARE domains are largely unstructured. Upon binary and ternary complex assembly, major structural changes occur resulting in a disorder-to-order transition, presumably required to supply the fusion energy [111-113].

Intracellular membrane traffic is a fundamental process in all eukaryotic cells. It involves the generation of transport vesicles from a donor compartment, movement of vesicles along cytoskeleton arrays, and fusion with target membranes [79, 114]. Vesicle fusion is mediated by a family of evolutionary conserved coiled coil domain containing proteins known as soluble N-ethylmaleimide-sensitive factor attachment protein receptors (SNAREs) [81, 84, 115-117]. Increasing evidence indicates that SNAREs are both (a) the specificity determinants in the vectorial transport of proteins and (b) the actual catalysts in the fusion event [118, 119]. SNAREs are structurally characterized by a conserved stretch of 60-70 amino acids called the SNARE motif, a single transmembrane (TM) domain or lipid modification motif located at the C-terminal end of each polypeptide, and a structurally variable N-terminal segment [81, 84, 120]. The SNARE motif consists of a heptad repeat of hydrophobic residues that serve as points of contact between interacting SNAREs during complex assembly.

Distinct sets of SNARE proteins localize to distinct intracellular trafficking pathways where they selectively interact with other family members to form stable *trans* complexes called SNAREpins [121]. Each complex contains four distinct SNARE motifs that are intertwined to form sixteen stacked layers of interacting side chains. Conventionally, these layers are numbered from -7 to +8 [104, 122]. The central '0' layer residue of the SNARE complex is highly conserved and is typically comprised of three glutamine (Q) residues and one arginine (R) residue. Depending on the zero layer amino acid, SNAREs are structurally classified into R- or Q-types. Multiple sequence alignments of various SNARE domains reveal that the '0' layer arginine residue is a characteristic of SNAREs called VAMPs (Vesicle-Associated Membrane Proteins) while glutamine at this position is a characteristic of syntaxins and synaptosome-associated protein (SNAP)-like SNAREs. Depending on the presence or absence of a profilin-like fold at their N-terminal domains, VAMPs are further divided into longins (long-VAMPs) or brevins (short-VAMPs) [81, 83, 84]. Subunit variations within the SNARE motif have also led to subdivision of the two major families (Q- and R-SNAREs) into Qa (Syntaxin), Qb (SNAP25N/Membrin-like), Qc (SNAP25C/Bet1-like), RG (Longins), and RD (Brevin) subfamilies [102, 123]. Assembly of the SNARE complex under physiological conditions often follows a "3Q:1R" rule that involves the interaction of SNARE motifs from each of the subfamilies that include 1Qa-, 1Qb-, 1Qc-, and 1R-SNARE [96, 106, 121].

Genome sequencing of model organisms has revealed interspecies variations in the number and functions of most eukaryotic SNARE families. These include 16 putative SNARE genes in Giardia, 20 in Drosophila melanogaster, 23 in C. elegans, 24 in Saccharomyces

cerevisiae, 36 in Homo sapiens, and as many as 54 SNARE genes in Arabidopsis thaliana [124-126]. In the malaria parasite, the number of SNARE family members is unknown.

1.2.7.2. Synthesis and intracellular targeting of SNAREs

SNAREs belong to a family of tail-anchored proteins, which insert into the ER membrane following a post-translational process involving various chaperones and a transmembrane domain (TMD) recognition complex (TRC) [127-133]. Specific sets of SNAREs reside predominantly in specific intracellular trafficking pathways (Fig. 5)[84]. However, the steady state localization of SNAREs depends on their rates of synthesis, fusion and recycling.

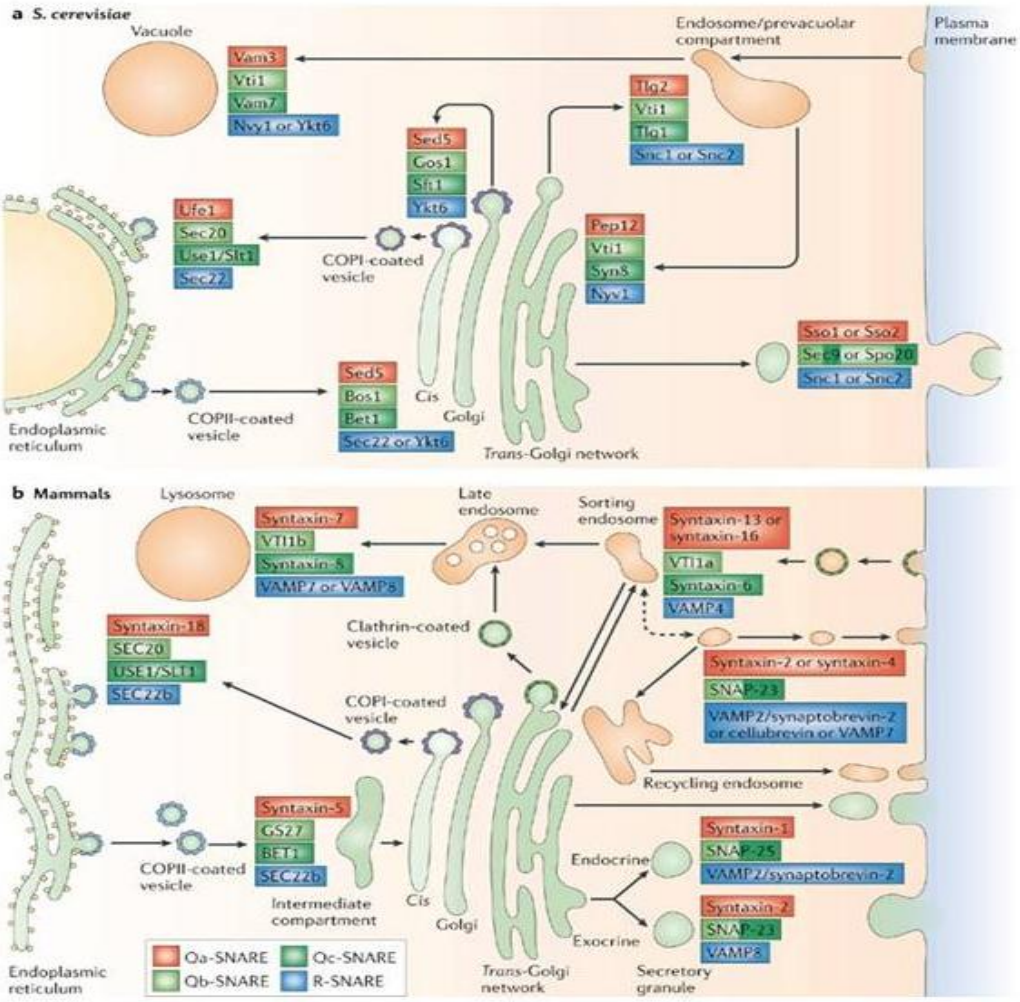

Figure 5: Subcellular distribution of SNAREs in yeast and mammals

Little is known about the signals and machineries involved in SNARE protein targeting in different cell types. For the few SNAREs that have been examined, the targeting determinants may be located in the C-terminal transmembrane domain, the SNARE motif, or within the variable N-terminal cytoplasmic region [127, 134-139]. Vesicle-associated SNAREs, which cycle between consecutive intracellular compartments, presumably contain distinct signals for forward traffic to the target membrane and recycling to the donor compartment. Additionally, SNAREs that function in more than one trafficking pathway may contain separate signals for

targeting to the different transport routes. An important mechanism for SNARE protein targeting is their interaction with coat proteins [140, 141]. For example, interaction between the yeast ER-to-Golgi SNAREs Sed5p, Bet1p, and Sec22p with COPII and COPI coat proteins is required for their ER exit and recycling. These SNAREs bind to specific sites on the Sec24p subunit by using diverse sequence signals: Sed5/Syn5 utilizes a YNNSNPF signal for binding to the A site, the LXX (LM) E signal from Sed5p and Bet1p binds to the B site, and a conformation epitope on Sec22 binds to a large surface region of Sec23 and Sec24 to exit the ER [142-144]. SNAREs may also be delivered to their final destinations as part of a complex with accessory proteins or other SNARE molecules that contain the appropriate targeting signal [145, 146]. It is postulated in this study that the *Plasmodium falciparum* complement of SNARE proteins will exhibit atypical structural features required for targeting to the parasite-specific compartments and vesicle transport to the novel trafficking pathways in this intracellular parasite.

1.2.8. Protein targeting in P. falciparum

With exception of cytosolic proteins, which remain in the cytoplasm after translation on free ribosomes, eukaryotic proteins are generally targeted to specific cellular destinations via appropriate targeting signals. In addition to targeting proteins to common eukaryotic endomembrane compartments (ER, Golgi, mitochondria, plasma membrane), the malaria parasite has evolved unusual signals and mechanisms for protein targeting to several unique destinations. These include the apicoplast, digestive vacuole, micronemes, rhoptries, dense granules, and various membranous structures inside the host cell compartment [62, 64]. Protein targeting to these membrane-bound organelles may follow a direct post-translational insertion

process involving diverse cytosolic chaperones, or occur through a classical eukaryotic secretory pathway wherein an N-terminal hydrophobic signal sequence directs their co-translational passage into the ER and Golgi bodies. Further targeting of the proteins from the Golgi might involve various post-translational modification processes that include N- and/or O-glycosylation, and lipidation processes [147, 148]. O-glycosylation has been described as being the major form of protein glycosylation in intra-erythrocytic *P. falciparum*, whereas there is little or no N-glycosylation of the parasite proteins [149, 150]. In the absence of other targeting signals, the PV constitutes the default destination for all *P. falciparum* that enter the secretory system [15]. For most ER- and Golgi-resident proteins, various conserved signal motifs mediate their retention/retrieval from bulk flow. Many soluble ER resident proteins contain a C-terminus KDEL motif (HDEL in yeast or S(DE)EL in some *P. falciparum* proteins), which by interacting with the membrane receptor ERD2 results in their retrograde transport from the *cis*-Golgi into the ER [151-153]. ER transmembrane proteins, in contrast, posses either a C-terminal dy-lysine motif (KKXX) or an N-terminal di-arginine motif (XXRR), which signals their retrieval from the Golgi [154, 155]. Several *P. falciparum* homologues of ER marker proteins contain the classical –XDEL signal, suggesting that the mechanisms for ER protein retrieval might be conserved in malaria parasites. For example, PfERC contains a C-terminal –IDEL motif, whereas PfBip contains a –SDEL motif [156, 157]. The membrane-associated PfERD2 receptor contains a C-terminal KKXX motif, which is likely to mediate its retrieval from the Golgi.

Export of parasite proteins into the host cell compartment conceivably necessitates a second signal for translocation across the PVM, in addition to an N-terminal hydrophobic signal, which typically resembles a canonical ER-type signal peptide located close to the N-terminus, or

recessed at approximately 80 amino acids from the N-terminus [15, 62, 158, 159]. A majority of the exported proteins, but by far not all, contain a vacuolar translocation sequence (VTS) or *Plasmodium* export element (PEXEL motif) that seems to direct traffic of both soluble and membrane-bound proteins to the infected erythrocyte [160-162]. Although the VTS and PEXEL sequences, respectively identified by Hiller et al and Marti et al, differ slightly in their structures, they share the conserved five-residue core motif (R, K) x (L, I) x (E, D, Q) where x represents an aliphatic amino acid residue [15, 73, 163-165]. This PEXEL/VTS motif is preferably located 15-20 amino acids downstream of the N-terminal hydrophobic signal sequence in a majority of the exported proteins [160, 161]. Recent bioinformatics analyses have also identified three groups of PEXEL/VTS sequences with preferences around positions 20, 43, and 85 amino acids downstream the signal sequence [165]. Only 24% of the proteins, representing those with PEXEL/VTS preferences around position 20 and 43, actually possess a classical signal peptide. The group of proteins with PEXEL/VTS preferences around position 85 predominantly contains the recessed N-terminal hydrophobic segment, which has been shown to function as an ER targeting signal in *P. falciparum* [161, 166]. Some of the PEXEL/VTS-containing proteins, including all PfEMP1 proteins that are exported into the host erythrocyte, do not contain the canonical signal peptide. It is worth-noting that some of the exported proteins in *P. falciparum* lack both the PEXEL/VTS motif and the N-terminal signal sequence. These proteins include *P. falciparum* skeleton-binding protein (PfSBP), membrane-associated histidine-rich protein (MAHRP) and the coat protein (COP) II components PfSec31, PfSec23, and PfSar1, all of which seem to be vesicle associated [62, 64]. The lack of PEXEL/VTS motifs in some exported proteins indicates that more than one export mechanism must exist in malaria parasites.

By employing a pattern matching approach with SEED-TOP, Hiss et al identified a total of 1,557 (28%) polypeptides in *P. falciparum* with at least one PEXEL/VTS motif [165]. In a parallel analysis using a generalized Hidden-Markov-Model (false-positive rate: 5%), which requires a preceding hydrophobic region for prediction of exported proteins, it was found that only 7.4% of the *P. falciparum* may be exported into the host cell [163, 165]. This suggests that the presence of a PEXEL/VTS motif alone is not an absolute predictor for export. Additionally, a family-specific conservation of physicochemical residues seems to exist for some PEXEL/VTS-flanking regions, suggesting that the PEXEL-flanking sequences might influence regulated secretion of proteins, either temporally, or even in response to external stimuli [165]. This hints towards potential recognition of the PEXEL/VTS motif and flanking regions by yet an unknown interacting factor. It has been speculated that the posttranslational translocation of PEXEL/VTS-containing proteins across the PV membrane might rely on the combined effects of chaperones and protein modification enzymes that might unfold the higher-order organization of exported proteins, triggering a more efficient translocation through an unknown translocon [162, 167].

The signals and pathways responsible for nuclear protein targeting to the *P. falciparum* digestive vacuole remain poorly characterized. This novel lysosome-like organelle represents the site of haemoglobin degradation and heme detoxification in asexual forms of the parasite. Additionally, the digestive vacuole is a dynamic calcium store, containing several membrane transporters implicated in various mechanisms of anti-malarial drug resistance [168, 169]. Nuclear-encoded proteins that are targeted to the digestive vacuole include proteases and membrane transporters [170-175]. It has been suggested that some proteases (e.g. pro-plasmepsin) are transported in membrane-bound vesicles to cytostomal evaginations of the

parasite plasma/vacuolar membrane, from where they are directed to the food vacuole [176]. Recent studies by Dasaradhi et al revealed that the N-terminal sequence of the cysteine protease falcipain-2 might contain signals required for food vacuole targeting of the protein through the secretory pathway [173].

Similarly, there is currently very little data regarding the signals and mechanisms necessary for protein targeting to the apical organelles. Most proteins destined for the rhoptries, micronemes or dense granules carry either a canonical secretory signal sequence or an internal hydrophobic domain for entry into the secretory system [177-179]. A secondary targeting signal might then direct the proteins away from bulk flow into the different apical organelles. Consistent with microscopic observations that the apical organelles originate from Golgi-derived vesicles, protein sorting to these organelles is thought to occur within the Golgi, and might involve interactions between sequence motifs within their cytoplasmic tails and subunits of cytoplasmic adaptor protein complexes [180, 181]. Numerous *P. falciparum* rhoptry and microneme proteins contain a predicted tyrosine-sorting motif within their cytoplasmic tails that presumably target the proteins to the apical complex [177, 178, 182]. Mutation of a tyrosine motif within the cytoplasmic tail of the microneme protein thrombospondin-related anonymous protein (TRAP) results in mistargeting to the parasite surface[182]. Some apical complex proteins do not possess a cytoplasmic tail or transmembrane domain, thus might be targeted to these organelles via interaction with transmembrane escorter proteins containing the appropriate cytoplasmic tail signals [183, 184]. Correct timing of expression has been shown to be an important factor for targeting of some nuclear-encoded proteins to the apical organelles [185-188].

The great majority of mitochondrial proteins are nuclear encoded and have to be imported. Most mitochondrial targeting signals are located at the N-terminus of the nascent polypeptide chain, although examples of internal and C-terminal signals have been reported [189, 190]. In higher eukaryotes, the signals for mitochondrial import contain N-terminal pre-sequences, termed transfer peptides, of 25 to 125 amino acids in length, which are rich in hydroxylated and positively charged amino acids, but depleted of acidic residues. Mitochondrial transfer peptides interact with multiprotein translocase complexes at the outer and inner mitochondrial membranes, necessary for translocation into the matrix, where the pre-sequence is removed by a mitochondrial processing peptidase [191, 192]. Orthologs of several subunits of the translocase complex have been reported in *P. falciparum* and proteins eligibly targeted to the parasite mitochondria appear to contain N-terminal sequences with homologies to transfer peptides [193].

Studies on *P. falciparum* and its apicomplexan cousin *T. gondii* have shown that targeting to the apicoplast also requires an N-terminal signal sequence in addition to a recessed transit peptide [194, 195]. Comparative sequence analysis of apicoplast proteins have revealed that apicoplast transit peptides are enriched in lysine and asparagines, and depleted in glutamic and aspartic acid residues in the first 20 amino acids. According to recent models, the N-terminal signal sequence is responsible for co-translational import of apicoplast proteins to the ER, where it is cleaved in the ER lumen [196]. The transit peptide functions in diverting proteins away from the default secretory pathway into the apicoplast. Apparently, apicoplast proteins exit the secretory pathway before reaching the cis-Golgi. Recent evidence indicates that protein targeting to the apicoplast follows a brefeldin A-insensitive pathway, suggesting that vesicular transport

steps may not be required for targeting to this organelle [197]. An explanation for these findings is that the apicoplast presumably resides within or proximal to the ER, and its outer membrane may be continuous with the rough ER.

Following translation, some parasite proteins are trafficked independent of the ER into the nucleus. Experimental studies are yet to be undertaken to characterize signals involved in protein import into the *P. falciparum* nucleus. Analysis of nuclear localization signals of many eukaryotic proteins has revealed four main classes: P**KKKRK**V as found on SV40 large T antigen; **KK**PAATKKAGQA**KKKK**, a bipartite signal consisting of two clusters of basic amino acids separated by a 10 t0 14 spacer sequence; **PAAKRVKLD**, as found in c-Myc; and various other signals including ones that are associated with ribosomal proteins and hnRNPs [198-203]. Some nuclear proteins, however, do not appear to have a nuclear localization signal and seem to enter the nucleus via interactions with other nuclear-targeted proteins[199]. Sequence analysis of various nuclear located proteins in *P. falciparum* has revealed that some nuclear proteins contain one or more nuclear localization signals [204-206].

1.2.9. The P. falciparum proteome and sequence characteristics

P. falciparum contains three distinct genomes: nuclear, apicoplast and mitochondrial genomes. The AT-rich (80.6%) nuclear genome is composed of ~23 megabases distributed among 14 haploid chromosomes and encodes a total of 5,268 predicted proteins, about 60% of which have no homologues in higher eukaryotes [207-209]. The *P. falciparum* mitonchondrial genome consists of tandemly arrayed 6kb DNA, the smallest genomic content mtDNA known to

date encoding only 3 proteins (cytochrome c oxidase I, cytochrome c oxidase III, and cytochrome b). In contrast, the 35-kb apicoplast genome encodes 30 proteins [210, 211].

Of the 5,268 nuclear encoded proteins, about 350-450 (~8%) are predicted to be exported into the host cell compartment during asexual development in human erythrocytes. About 551 of these nuclear-encoded proteins are predicted to be targeted to the apicoplast, whereas 246 might take residence in the mitochondrion [163, 207]. Relatively little has been published on the expression profile, subcellular localization and role of the predicted *P. falciparum* proteins. Functional profiling of the proteome at four different developmental stages (sporozoite, merozoite, trophozoite, and gametocyte) suggests a tight stage-dependent regulation of gene expression in the malaria parasite [209]. Only 6% of the parasite proteins corresponding mostly to housekeeping proteins were present in all four stages (49% of the sporozoite proteins were unique to this stage, whereas 20-33% of trophozoite, merozoite and gametocyte proteins were unique to each of these stages) [209].

In addition to providing important clues to the parasite's cell biology, the identification and characterization of the parasite's unique proteomes provides the only promise to identify new and effective drug and vaccine targets against the infections.

1.2.10. Molecular genetics tools to study Plasmodium parasites

The release of the complete genome sequence of *P. falciparum* 3D7 strain has been very valuable in studying gene function and expression. However, such studies have been hindered by the lack of molecular genetics tools to manipulate this malaria parasite [212]. Forward genetic screens using RNAi does not appear to be feasible in *P. falciparum* as the parasite genome lacks

any discernable RNAi machinery [213, 214]. Additionally, plasmid DNA transfection of *P. falciparum* parasites remains very inefficient at between 10^{-5} and 10^{-6} [215, 216]. Because purified *P. falciparum* merozoites are not viable to allow for direct transfection procedures, the only strategy to transfect malaria parasites is by electroporation of RBCs that are infected with young ring-stage parasites [217-219]. Although DNA may be electroporated relatively efficiently into the RBC cytosol, only in rare instances does the DNA cross the PVM, parasite plasma membrane (PPM) and the nuclear membrane. Movement of DNA across the PVM, PPM and nuclear membranes appears to be spontaneous as parasites can be transfected with a marginally increased efficiency by infecting fresh RBCs preloaded with plasmid DNA [220]. The incorporation of Rep20 subtelomeric repeat elements into transfection vectors allows more rapid establishment of stably transformed lines. Rep20 promotes chromosomal tethering of the plasmids, allowing episomally replicating plasmids to segregate more evenly during mitosis [216]. This means that more parasites would receive the replicated DNA, hence are resistant.

Direct integration of transfected DNA is not possible and the existing strategies rely on a period of episomal plasmid replication and recombination before integrants may be obtained[221]. An integrase system and a random gene insertion piggyback transposon system have been developed for stable integration of plasmid DNA [222, 223]. Although gene knockout via homologous recombination is relatively straightforward in *P. falciparum* due to the haploid nature of its genome, genetic tools need to be developed for controlled mutagenesis or down-regulation of most essential genes.

CHAPTER 2:
THE PLASMODIUM FALCIPARUM COMPLEMENT OF SNARES

2.1. SUMMARY

P. falciparum inhabits terminally differentiated human erythrocytes, yet traffics several proteins into the host cell compartment that are critical for survival and virulence. To support these 'extraparasitic' protein transport processes, this malaria parasite extensively modifies the host cell compartment and induces the formation of various membrane-bound structures that serve as sorting stations for the exported proteins. Proteins destined for export into the infected erythrocyte enter the secretory system through the ER from where they are trafficked through an unstacked 'Golgi-like' structure, the parasite plasma membrane (PPM), the fluid-filled parasitophorous vacuole (PV) and parasitophorous vacuolar membrane (PVM) into the infected erythrocyte cytoplasm. Some of the exported proteins further associate with parasite-induced structures in the host cell cytoplasm called Maurer's cleft (MC) and tubovesicular network (TVN) before taking residence at the erythrocyte surface.

Vesicular transport processes have been proposed to mediate the unusual transport of lipids and proteins to various destinations in the infected host cell compartment. If this is correct then vesicle targeting and fusion at the parasite-specific organelles must involve novel SNARE complexes and trafficking processes. As a first step to understanding the role of SNARE proteins in malaria parasites, we have identified for the first time the *P. falciparum* complement of SNAREs (PfSNAREs). Bioinformatics analysis of the *P. falciparum* genome revealed 18 SNARE-like proteins that could be classified into five main phylogenetic groups; namely membrin-like, Bet1-like, VAMP-like, Syntaxin5-like subfamily, and a *P. falciparum*-specific

syntaxin-like subfamily. Expression of the PfSNAREs in *P. falciparum* was confirmed by reverse transcriptase PCR using gene-specific primers. Unique to the PfSNAREs was (1) presence of atypical zero-layer amino acids in some members (six PfSNAREs), (2) presence of up to two hydrophobic domain segments in three PfSNAREs, and (3) the occurrence of low-complexity regions in seven PfSNAREs. Additionally, the three PfSNAREs, PfSec22p, PfVti1p, and PfSyn13p, each contain a single insertion of the *Plasmodium* export element (PEXEL) within their N-terminal cytoplasmic tails which potentially might direct the export of these SNARE proteins into the host cell compartment.

As a model to study SNARE protein trafficking in malaria parasites, and to test our central hypothesis, we investigated the localization of the R-SNARE, PfSec22, which contains an unusual insertion of the PEXEL motif within its longin domain preceded by an atypical hydrophobic segment. We generated PfSec22-specific antibodies and GFP expressing cell lines for live cell imaging of N- or C-terminally tagged chimeras. Expression of both the GFP-tagged and untagged proteins in the malaria parasites was confirmed by immunofluorescence and Western blot assays using the peptide-derived PfSec22 antibodies. The data indicate that the Sec22 gene product in *P. falciparum* associates partially with mobile vesicular elements in the infected erythrocyte, and localizes predominantly to the parasite ER and Golgi interface. The association of PfSec22 with transport vesicles and the lipid bilayers was confirmed by immuno-electron microscopy examination of ultrathin sections, and by Western blot analyses of subcellular fractions. Our data supports a model in which the *Plasmodium* parasites export vesicle trafficking machineries into infected host cells, required for transport of virulence factors to the erythrocyte surface membrane.

2.2. MATERIALS AND METHODS

2.2.1. Database mining and identification of P. falciparum SNAREs

P. falciparum homologues of SNAREs were identified by independent NCBI PSI-BLAST and BLASTP searches of annotated proteins in the PlasmoDB Genome database (release 4.4). Query sequences were obtained either from previously published data (human SNAREs) [81] or extracted from known yeast and plant SNARE sequences available at http://www.yeastgenome.org/ and http://www.tigr.org/tdb/e2k1/ath1/ath1.shtml, respectively. All 56 hits resulting from the BLAST search were subsequently scanned for the occurrence of patterns, profiles and motifs stored in the PROSITE database (http://www.expasy.ch/prosite/) [224, 225]. Sequences were included as potential SNARE proteins if they contained one or more SNARE-motif structures. The identified PfSNARE motifs were again BLAST searched against the *P. falciparum* protein database (PlasmoDB) to detect orthologs with weak sequence homology to the human, yeast and plant SNAREs. The transmembrane regions of the PfSNARE proteins were identified using the ConPred II system (ConPred_elite and ConPred_all methods) available at http://bioinfo.si.hirosaki-u.ac.jp/~ConPred2/. ConPred II is a robust consensus prediction system that makes use of prediction results of several other methods including KKD, TMpred, TopPred II, DAS, TMAP, MEMSAT 1.8, SOSUI, TMHMM 2.0 and HMMTOP, and presents an accuracy level of 100% [226].

2.2.2. Sequence alignment and classification of PfSNARE proteins

To assign paralog names and classify the PfSNAREs following previously described criteria [81], the identified PfSNARE motif sequences were aligned by CLUSTALW

(DNASTAR MEGALIGN, slow/accurate/Blosum) against the complete set of human SNARE motifs. A name was assigned to each PfSNARE by adding the letters Pf to the human homologue to which it exhibited highest sequence identity. Full-length PfSNARE sequences were also aligned (CLUSTALW, slow/accurate/Blosum) and manually inspected for common structural features.

2.2.3. Parasite culture and RNA Isolation

The 3D7 strain *of P. falciparum* were grown in human A+ red blood cells at 5% hematocrit in RPMI 1640 supplemented with 0.5% Albumax (GibcoBRL) essentially as described [227]. Parasites were harvested from asynchronous cultures by treatment of the parasitized red blood cells with 0.05% saponin in PBS, pH 7.2 [228]. Total RNA was isolated from the parasite pellet using the RNAgents Total RNA Isolation System (Promega).

2.2.4. Expression analyses of PfSNAREs by RT-PCR

Based on the 5' and 3' nucleotide sequences of the identified PfSNARE genes, forward and reverse primers were designed to amplify each complete open reading frame (ORF). Restriction sites for *Bam*HI, *Eco*RI or *Xho*I, were incorporated at the 5'-end of each specific primer for subsequent cloning of the ORFs into an expression vector. The StrataScript™ one-tube RT-PCR system with Easy-A™ High-Fidelity PCR Cloning Enzyme was used to reverse transcribe and amplify individual ORFs using 200ng of total RNA and the respective gene-specific primers. A negative control containing all reagents except the reverse transcriptase was included. RT-PCR cycling conditions were as follows: 1 cycle of reverse transcription at 42ºC

for 30 minutes followed by transcriptase enzyme inactivation at 95ºC for 30 seconds; 5 cycles of denaturation at 95ºC for 30 seconds, annealing at 48-50ºC for 30 seconds and extension at 68ºC for 4 minutes; 35 cycles at 95ºC for 30 seconds, 58ºC for 30 seconds and 68ºC for 4 minutes and 1 cycle at 68ºC for 10 minutes. RT-PCR products were analyzed by electrophoresis on a 0.8% agarose gel in Tris-acetate EDTA buffer, pH 8.0.

2.2.5. Anti-peptide antibodies and expression analyses of PfSec22 proteins

To confirm the expression of the atypical PfSec22 protein in *P. falciparum*, we generated antipeptide antibodies for use in immunoblot and immunofluorescence microscopy analyses. The decapeptide 'YKDPRSNIAI', corresponding to residues 131-140 of PfSec22, was synthesized (Genscript) and conjugated to keyhole Limpet Hemacyanin (KLH) following the manufacturer's instructions (Pierce). Antisera were raised in rabbit against the conjugated peptide (Harlan Bioproducts for Science, Inc) and affinity purified by column chromatography using peptide-conjugated agarose beads (Pierce). The reactivity of these antibodies against the endogenous and/or GFP-tagged PfSec22 proteins was analyzed by standard Western blot techniques.

Briefly, parasites were released from the infected erythrocytes by treatment with 0.05% (w/v) saponin in PBS followed by three times PBS washes[228]. The obtained pellets were resuspended in M-Per mammalian protein extraction reagent (Pierce) containing a protease inhibitor cocktail (Roche Mini Complete EDTA-free) and benzonase (Novagen). Each suspension was incubated at 4ºC with agitation for 15 minutes, and then clarified by centrifugation at 20,800 x g for 5 minutes at 4°C. Protein concentrations in the supernatants were determined by Bradford analysis [229] using BioRad protein assay reagent. Sixty micrograms of each protein extract was resolved on a 10% SDS-PAGE followed by western blotting and

analysis using the purified antibodies at a 1:1000 dilution. Goat anti-rabbit HRP-conjugates, Pierce) were added at 1:5,000 dilutions, and the resulting complex was revealed by use of the Supersignal West Femto Chemiluminescence detection kit (Pierce).

2.2.6. Immunofluorescence Analysis of PfSec22 in Parasitized Erythrocytes

Immunofluorescence assays were performed in suspension as previously described by Tonkin *et al [215]*. Briefly, parasitized erythrocytes were washed once with phosphate-buffered saline (PBS) and subsequently fixed with a solution containing 4% paraformaldehyde + 0.0075% glutaraldehyde in PBS for 30 min at room temperature. Following one wash with PBS, the cells were permeabilized with 0.1% Triton X-100 for 10 min, followed by reduction of excess aldehydes with sodium borohydride at 0.1 mg/ml, and blockage of nonspecific binding sites with 3% BSA in PBS at room temperature for 1 h. For co-localization analyses, the cells were probed with appropriate antibodies (1° and 2°) in PBS containing 3% BSA at 4ºC overnight followed by three washes with PBS. The purified rabbit anti-PfSec22 antibodies were used at a 1 in 500 dilution whereas the primary antibodies against the ER marker PfBip were used at 1:1000 dilutions. The rat anti-PfBip (MRA-19) antibodies were obtained from the Malaria Research and Reference Resource Center (MR4). The secondary antibodies consisted of goat anti-rabbit Alexa-Fluor-555, or goat anti-rat Alexa Fluor-594 (Molecular Probes), each used at a dilution of 1 in 1,000 for 1 hour at room temperature. After washing three times with plain PBS, the cells were allowed to adhere to polyethyleneimine (PEI)-coated cover slips at room temperature for 15-20 minutes. The coverslips were rinsed with PBS and were mounted onto a glass slide with 50% glycerol containing 0.1 mg/ml of 1,4-diazabicyclo (2,2,2) octane (Sigma). Fluorescence signals from the secondary antibodies were captured using a laser scanning confocal microscope

(LSM 510, Carl Zeiss). The excitation/emission spectra settings were 543/555 for Alexa Fluor-555 conjugated antibodies and 543/594 nm for Alexa Fluor-594 conjugates.

2.2.7. Analysis of membrane-association properties of PfSec22

2.2.7.1. By freeze/thaw fractionation of soluble from membrane proteins

P. falciparum 3D7 parasites were purified by saponin treatment and resuspended in a TBS buffer (10 mM Tris-HCL, pH 7.4 + 150 mM NaCl), containing a cocktail of protease inhibitors (Roche). The cells were subjected to five cycles of freezing and thawing in liquid nitrogen followed by a brief sonication for 15 seconds to release both the cytosolic and the lumenal proteins. The disrupted cells were clarified by centrifugation at 100,000 x g for 1 h at 4ºC to separate the soluble proteins from the membrane-associated fractions. The pellet sample was then normalized with the TBS buffer to the volume of the supernatant and equivalent volumes analyzed by western blotting.

2.2.7.2. By alkaline extraction of peripheral from integral membrane proteins

Membrane pellets were prepared as described above and resuspended in 3 volumes of 0.1 M Na_2CO_3, pH 11. The suspension was mixed by rotation at 4^{o}C for 30 min, followed by centrifugation as above to separate the peripheral membrane proteins in the supernatant from the integral membrane protein in the pellet. The resulting pellet was normalized as described above and equal volumes analyzed by western blotting.

2.2.7.3. By phase separation of hydrophobic from hydrophilic membrane proteins

Integral membrane fractions were prepared by alkaline extraction as described above and solubilized using the Membrane Protein Extraction Reagent kit (Pierce). The solubilized fraction was clarified by centrifugation at 10, 000 X g for 3 minutes at 4^{o}C, and then clouded in a 37^{o}C water bath for 20 minutes. This was followed by centrifugation at 10,000 X g for 2 min at room temperature to remove the hydrophilic phase (top layer) from the hydrophobic protein phase (bottom layer). Equal volumes of the phase-separated samples were further diluted in Laemmli sample buffer and analyzed by western blotting.

2.2.8. Transfection and live cell imaging of GFP-tagged Chimeras

To determine the steady-state dynamics and subcellular localization of PfSec22, we generated transgenic parasites expressing the GFP-tagged proteins. cDNAs corresponding to the full-length ORF of PfSec22 was amplified by RT-PCR using gene-specific primer sets. The amplified cDNAs were cloned into the pGEM-T Easy vector (Promega) and sequence confirmed prior to subcloning into the AvrII/BglII (C-terminal GFP constructs) or BglII/XhoI (N-terminal GFP constructs) sites of a modified pDC *Plasmodium* expression vector [230, 231]. In this vector, a 5' *cam*oldulin (*cam*) promoter and a 3' hsp86 terminator element drives the expression of either an N-terminus or a C-terminus GFP- fused transgene. To modulate the expression levels of the transgenes, the corresponding 5'-UTR sequence (0.995kb segment) was amplified from genomic DNA by PCR and subcloned into the PsPOM I/AvrII sites, thus replacing the much stronger *cam* promoter sequence. *P. falciparum* 3D7 ring stage cultures (at 5% parasitemia) were transfected with Qiagen-purified plasmid DNA (100 µg) by electroporation using a Bio-Rad Gene pulser II (0.31 KV and 950 microfarads) essentially as described [230]. Forty-eight hours

after transfection, drug selection pressure was applied using the human DHFR inhibitor, WR99210 at a final concentration of 2.5 nM to select for transformed parasites[219]. Expression of GFP-tagged proteins in the transgenic parasites was analyzed by Western blotting using monoclonal GFP (B-2) antibodies (Santa Cruz Biotechnology) at a 1:500 dilution. The secondary antibodies were HRP-conjugated Goat anti-mouse used at a 1:20,000 dilution. For live cell imaging, the cells were mounted under a cover slip in 50% glycerol and observed within 15 minutes of removal from cultures by confocal microscopy. The GFP signals were captured at a spectra setting of 488/505 nm.

2.2.9. Immunolocalization of GFP-PfSec22 in transgenic parasites

The subcellular localization of PfSec22 was determined in transgenic parasites by immunofluorescence analyses using anti-PfErd2 (Golgi marker) and anti-PfBip (ER marker) antibodies. The rabbit anti-PfErd2 (MRA-1) and rat anti-PfBip (MRA-19) antibodies were obtained from the Malaria Research and Reference Reagent Resource (MR4) Center and used at a dilution of 1 in 1000. The secondary antibodies consisted of goat anti-rabbit Alexa-Fluor-555, or goat anti-rat Alexa Fluor-594 (Molecular Probes), each used at a dilution of 1 in 1,000 for 1 hour at room temperature. After washing three times with plain PBS, the cells were allowed to adhere to polyethyleneimine (PEI)-coated cover slips at room temperature for 15-20 minutes. The coverslips were rinsed with PBS and were mounted onto a glass slide with 50% glycerol containing 0.1 mg/ml of 1,4-diazabicyclo (2,2,2) octane (Sigma). Fluorescence signals from the secondary antibodies were captured using a laser scanning confocal microscope (LSM 510, Carl Zeiss). The excitation/emission spectra settings were 543/555 for Alexa Fluor-555 conjugated antibodies and 543/594 nm for Alexa Fluor-594 conjugates.

2.2.10. Cryo-electron microscopy

To determine the localization of PfSec22 at the ultra-structural level, the GFP-expressing cells were enriched by Percoll density centrifugation and fixed for 30 minutes at room temperature with 4% paraformaldehyde/0.1% glutaraldehyde (EMS) in 0.1M phosphate buffer, pH 7.2 (EMS). Upon three times wash with phosphate buffer, the cells were pelleted into 10% gelatin in phosphate buffer and infused with 2.3 M sucrose in phosphate buffer. The cryo-protected pellets were frozen in liquid nitrogen and cryo-transferred to a Leica EMFCS chamber. Ultrathin cryosections were obtained at -120^{o}C on a Leica Ultracut UCT using a Drukker ultramicrotome diamond knife. The resulting ribbons of frozen sections were collected onto carbon and formvar substrates mounted on 300 mesh nickel grids. The grids were floated on drops of BD JL8 anti-GFP (diluted 1:100 in 0.05 M phosphate buffer containing 1%BSA) at 5^{o}C overnight and then incubated at room temperature for 1 hour with a 1:50 dilution of 12nm colloidal gold-conjugated affinipure goat anti-mouse IgG/IgM (Jackson ImmunoResearch Laboratories) in 0.05M phosphate buffer containing 1% BSA. The grids were fixed with 1% gluteraldehyde and then embedded in 1% methylcellulose and 2.5% uranyl acetate prior to examination in a FEI Technai 12 TEM. The images were captured using a AMT XR111 digital camera.

2.2.11. Yeast complementation analyses

To test whether or not the atypical PfSec22 may complement a yeast *Sec22-3* temperature-sensitive allele, the PfSec22 open reading frame was amplified by RT-PCR and subcloned into the pMET25-HA vector using *Bgl*II/*Hind*III restriction sites. This vector allowed the constitutive expression of fusion proteins with a triple-HA tag to the N-terminus under

control of the MET25 promoter [232, 233]. Yeast cells (strain RSY279) were rendered competent by lithium chloride treatment, and separately transformed with 10µg of plasmid as described by Ito *et al* [234, 235]. The plasmids used in yeast transformation were the vector only, the PfSec22 recombinant vector, or the *Sacharomyces cerevisiae* Sec22 (YLR268W) plasmids. The transformants were streaked and selected on a synthetic met/his-free medium containing 0.67% yeast nitrogen base, 2% glucose and 0.1% 5-fluoroorotic acid.

For expression analyses, the transformed cells were grown in liquid media for 72 hours at the non-restrictive temperature (25^{o}C), and then harvested in 50mM Tris-HCl, pH 8.0 containing 1% Triton X-100 and 62.5 mM EDTA. Thirty five micrograms of proteins from each clarified lysate was resolved by SDS-PAGE and immunoblotted using rabbit anti-HA antibodies (Zymed labs) at 0.5µg/ml.

2.3. RESULTS

2.3.1. P. falciparum encodes 18 putative SNARE proteins

In an effort to identify and characterize PfSNARE proteins, first we used a PSI-BLAST approach to search the completed *P. falciparum* genome database (PlasmoDB) using human SNARE motifs as queries. This approach resulted in the identification of 15 SNARE domain-containing proteins from the parasite genome. Next, we undertook an extensive search of the PlasmoDB by direct BLASTP analysis using 116 different SNARE motifs derived from the human, yeast, and *Arabidopsis* genome databases. This broadened approach yielded 3 additional PfSNARE homologues, resulting in a total of 18 identified SNARE genes (table 2). By comparison, 27 SNARE domain-containing proteins were recently identified in the genome of a

closely related protozoan parasite *L. major* using a direct BLASTP search approach [236]. The human and yeast genomes each encodes 36 and 24 SNARE proteins, respectively [81, 124]. A second BLAST search of the *P. falciparum* genome database using the PfSNARE motifs as query sequences did not identify any recognizable SNARE polypeptides, which might have been distantly related to our initial query sequences. Furthermore, none of the SNARE families alone was able to detect all 18 PfSNAREs. For example, the PfSNARE MAL8P1.21 was detected only by one query from the yeast SNAREs, seven queries from plant and none of the 36 queries from the set of human SNAREs. Similarly, PF14_0535 was detected by 2 queries from the human SNAREs and none of the yeast or plant SNARE sequences. Because human and yeast SNAREs are the most extensively characterized, and because all members of the yeast SNAREome also have homologues in humans, PfSNAREs were named on the basis of their sequence identities with the human SNAREs (Table 1). Names were assigned to the parasite proteins by adding the prefix Pf to the name of the corresponding human SNARE homologue. Thus, the name PfSyn5p was assigned to MAL13P1.169 based on the fact that human Syntaxin5 presented the highest sequence identity (35.2%) to this PfSNARE. Similarly, MAL8P1.21 was named as PfVAMP7p despite not being detected by any of the human query sequences. On the other hand, PF14_0500 that showed highest identity (25.9%) against human SNAP29c was assigned the name PfBet1p. Our rationale for this is that PF14_0500 has only one SNARE motif unlike SNAP29c with two motifs, and because human Bet1 was the next SNARE with highest sequence identity (24.1%) to PF14_0500. Because PFI0515w and MAL13P1.135 exhibit highest sequence identity with Ykt6 and because both PfSNAREs display similar structural patterns that include an N-terminal longin domain and a C-terminal CAAX prenylation motif, they are herein considered as isoforms and are named PfYkt6.1p and PfYkt6.2p, respectively. However, these two proteins are only 27.8%

identical in their SNARE domain and 25.6% identical when full-length sequences were aligned. Functional studies, however, need to be undertaken to confirm the above designations and to determine the role of SNARE proteins in the *P.falciparum* trafficking pathways.

2.3.2. All 18 PfSNAREs are expressed in blood stages of P. falciparum.

To verify the transcriptional expression of the PfSNARE in asexual blood stage of *P. falciparum* parasites, we synthesized the corresponding cDNAs by RT-PCR using gene-specific primers. As shown in Fig. 6, cDNAs with the correct sequence sizes were obtained by this procedure, establishing that all 18 PfSNAREs are expressed in *P. falciparum*. Further studies, however, will have to be undertaken to confirm the full-length sizes of these genes given that our RT-PCR primers were designed based on the predicted ORFs as published in PlasmoDB, which may be incomplete. For example, annotation of PfYkt6.2 (MAL13P1.135) incorrectly overlooked the short 3' exon containing the C-terminal prenylation motif of this putative SNARE. Therefore, the 3' region of the alternate predicted ORF, chr13.glimmerm_638, was considered for amplification in our expression analysis. Our expression analysis supports previous micro-array results that include data for 16 of the PfSNAREs, available at http://www.sciencemag.org/cgi/data/1087025/DC1/2 [186]. As shown by the micro-array data, the expression levels of most PfSNARE transcripts varied with the parasite developmental stages, some (PfYkt6.2, PfSyn3, PfSyn6, PfSNAP23, and PfSyn5) of which are expressed exclusively in the blood stages. PfSyn17 is expressed only in the gametocyte stage.

2.3.3. In silico analyses reveal atypical structural features in some PfSNAREs

Because of the uniqueness of *P. falciparum* protein-trafficking pathways and the surprisingly low number of expressed SNARE genes, we analyzed full-length sequences of the PfSNAREs to detect any inter-species differences that might be required for the parasite-specific functions. Interestingly, some *Plasmodium* homologues of human SNAREs contained up to two hydrophobic segments each flanking the SNARE core motif. These PfSNAREs include: PfSec22p, PfVAMP7p and PfSyn13p. Five of the PfSNAREs contain no hydrophobic segments. Additionally, the three PfSNAREs PfSec22, PfSyn13p and PfVti1p contain sequence motifs that were predicted using MalSig to correspond to the host cell targeting PEXEL/VTS motif. However, the functional significance of these sequence features will have to be determined experimentally.

Compared to all known eukaryotic SNAREs, the putative PfSyn3p is the largest SNARE so far identified. This PfSNARE has a protein sequence of 967 amino acids and is structurally composed of a single internal SNARE motif flanked on both sides by an asparagine-rich region. As revealed by RT-PCR (Fig. 6), the PfSyn3 gene was transcribed giving an amplification product of approximately 2900bp. Other unusually large PfSNAREs include PfSyn18p (441aa), PfSyn11p (442aa) and PfSyn13p (336aa). In human, syntaxin18 is the largest SNARE protein comprising 335 amino acid residues [237]. The core SNARE motif of PfSNAREs is confined within a minimum sequence length of 54 residues. As indicated in Fig. 3, six of the PfSNAREs exhibit neither the conserved arginine (R) of neuronal VAMPs nor the glutamine (Q) of non-VAMPs at the zero layer position. Present at this position are atypical amino acid residues that include asparagines (N) in two PfSNAREs, Isoleucine (I) in two PfSNAREs, serine (S) in one PfSNARE and histidine (H) in one PfSNARE (Fig 7). The presence of isoleucine at the ‘0’ layer

position of some syntaxins (PfSyn3p and PfSyn13p), and of an arginine residue in place of glutamine at the zero layer position of PfSyn11p are novel findings amongst all known SNARE families Other structural domains found within PfSNARE proteins include a profilin-like longin domain (4 PfSNAREs), a CAAX motif (2 PfSNAREs) and an asparagine-rich low complexity region (8 PfSNAREs).

2.3.4. Phylogenetic analysis reveals a putative syntaxin subfamily of PfSNARE

We analyzed the phylogenetic relationship between PfSNARE motifs with a representative set of mammalian SNARE protein sequences. As shown in Fig. 8, phylogenetic analysis of the PfSNAREs resulted in their classification into five subfamilies: membrin-like PfSNAREs (4 members), Bet1-like PfSNAREs (3 members), VAMP-like PfSNAREs (6 members), Syntaxin5-like PfSNAREs (3 members), and a putative Pf-specific syntaxin-like subfamily (4 PfSNAREs). The existence of a *P. falciparum*-specific syntaxin sub-family is consistent with the presence of unique trafficking pathways in this organism. A unique feature of this subfamily is the occurrence of atypical zero layer amino acid residues that include arginine, isoleucine, or asparagines. This subfamily seems to have diverged from the syntaxin (Qa) family of PfSNARE and supports previous observations that the syntaxin family of protozoa constitutes a highly divergent group [238].

2.3.5. Partial export of endogenous PfSec22 in P. falciparum-infected host cells

In an attempt to determine the functional role of PfSec22, we tested the ability of the HA-tagged protein to complement a Sec22-3 temperature-sensitive allele in transformed yeast cells.

As shown in Fig. 9, the yeast cells that were transformed with the HA-PfSec22 or HA only constructs were inviable when cultured at the restrictive temperature (37^{o}C). Immunoblot analyses of lysates from the HA-ScSec22 transformed cells in comparison to the HA-PfSec22 or HA only cells suggest that the yeast cells were unable to express the full-length PfSec22 protein. Unlike the ScSec22 protein, which migrated at the expected band size (~28kDa), three closely migrating antigen fragments of low molecular weights (<15kDa) were detected in the HA-PfSec22 lysates. The expected band sizes of the HA-PfSec22 and 3xHA (vector only) proteins were 29kDa and 3kDa, respectively. This failure of the yeast cells to express the full-length malaria gene might be attributable to an inability of the yeast translation machinery to recognize the AT-rich PfSec22 nucleotide sequence (76% AT-rich), or due to a rapid turn-over of the heterologous protein.

We therefore generated anti-peptide antibodies that were used to analyse the expression profile of PfSec22 in cultured malaria parasites by immunofluorescence detection of the endogenous proteins in fixed cells and Western blot analyses of various subcellular fractions. The peptide antigen was derived from the inter-domain region located between the longin domain and the SNARE motif, which showed high sequence specificity to the PfSec22 protein when compared to other parasite proteins. As shown in Fig. 10, the affinity purified antibodies specifically recognized a 26-kDa protein in cell-free extracts from ring, trophozoite, and schizont stage parasites, corresponding to the predicted molecular mass of the full-length PfSec22 protein. Expression of PfSec22 protein in all asexual life-cycle stages of the parasite is consistent with the gene transcription profile (available at www.PlasmoDB.org).

By immunofluorescence analyses, we observed that the majority of the PfSec22 antigen localized to membrane-like compartments inside the parasite cytoplasm (Fig. 11A). We

investigated the membrane-association properties of PfSec22 by (i) freeze-thaw separation of membrane proteins from soluble fractions, (ii) alkaline extraction of peripheral membrane proteins from integral membrane proteins, and (iii) Triton X-114 solubilization of integral membrane proteins followed by immunodetection. The ER-restricted lumenal chaperone PfBip was used as a marker for the soluble non-membrane-associated proteins, whereas the presence of the KDEL receptor PfErd2 in the fractions marked the membrane-associated proteins. As shown in Fig. 11B, the endogenous PfSec22 protein partitioned alongside PfErd2 in the membrane fractions and was efficiently solubilized into the hydrophilic phase after detergent extraction using Triton X-114. PfErd2 was only partly solubilized by this detergent, consistent with its topological function as a multi-pass membrane protein containing up to seven transmembrane domains [66]. These results suggest that PfSec22 is an integral membrane protein, consistent with a requirement in vesicle trafficking.

To determine whether PfSec22 associates with the parasite ER/Golgi interface, as has been reported for other Sec22 orthologs [239-242], we investigated its co-localization with the ER marker PfBip. A similar co-localization experiment using the Golgi marker PfErd2 was precluded because both the anti-PfSec22 and available anti-PfErd2 antibodies originated from the same host species. As shown in Fig. 11C, PfSec22 localized predominantly to the ER, consistent with a potential role in ER-to-Golgi transport in the malaria parasite. Surprisingly, albeit only in trophozoite-infected cells, we detected a small proportion of the PfSec22 antigen in isolated vesicular structures inside the host cell cytoplasm, suggesting that PfSec22 might transiently participate in vesicle traffic within the host cell compartment.

2.3.6. Partial export of GFP-tagged PfSec22 proteins in transgenic parasites

To better understand the steady-state dynamics of PfSec22 in *P. falciparum* parasites, we generated a transgenic cell line expressing the GFP-tagged proteins under control of the endogenous *PfSec22* promoter sequence. Additionally, to ensure that a suitable tagging approach was being employed, we first investigated the effect of the GFP tag. Transgenic parasites were developed that expressed the PfSec22 protein with GFP appended either to its C-terminus (PfSec22-GFP) or to the N-terminus (GFP-PfSec22). We confirmed the expression of both fusion proteins by immunoblot analyses using either anti-PfSec22 or anti-GFP antibodies. As shown in Fig. 12A, two protein bands corresponding to the expected sizes of the GFP-tagged proteins (~54 kDa) and the endogenous protein (26 kDa) were detected in each transgenic cell lysate using the anti-PfSec22 antibodies. In contrast, only the 54-kDa bands were detected in these extracts using the anti-GFP antibodies (Fig. 12A). These data established that full-length proteins were expressed in the respective cell lines, and that PfSec22 is not processed at the N-terminus as has been reported for most PEXEL-containing proteins [243].

Live cell imaging of GFP fluorescence revealed significant differences in the distribution of the PfSec22-GFP and GFP-PfSec22 chimeras (Fig. 12B and 12C, respectively). In transgenic parasites expressing the C-terminally tagged protein, the GFP fluorescence was observed predominantly in the parasite cytosol (Fig. 12B). In some trophozoite-infected cells, representing about 10 % of the trophozoite-infected erythrocytes in culture, the GFP fluorescence was also detected inside the erythrocyte cytosol (Fig. 12B). In comparison, the N-terminally tagged protein (GFP-PfSec22) localized predominantly to ER-like structures in the parasite cytoplasm. Consistent with our immunofluorescence data, the GFP-PfSec22 also associated with TVN-like extensions and mobile vesicular elements inside the infected host cytoplasm (Fig. 12C and D).

We confirmed the identity of the PfSec22-associated structures by immunoelectron microscopy using gold-labeled anti-GFP antibodies. As shown in Fig. 13, the GFP-tagged protein was predominantly associated to the crescent-shaped ER in ring-stage parasites (Fig. 13A), and to the perinuclear ER in early trophozoite cells. Development of the parasites through the late-trophozoite stage was accompanied by the generation of a complex network of vesicular elements at the parasite periphery, a subset of which was detected in the erythrocyte cytosol (Fig. 13B and C). As indicated with the dotted arrow in Fig. 13C, the exported PfSec22-associated structures appeared to enter the erythrocyte cytosol via TVN-like protrusion of the vacuolar membrane. PfSec22-stained vesicles were also detected within the vacuolar space (Fig 13B), suggesting a two-step transport process for this tail-anchored membrane protein into the infected erythrocyte.

Consistent with other previous EM studies, the unstacked *Plasmodium* Golgi was not obvious by our transmission electron microscopy analysis. To determine whether GFP-PfSec22 also associates with the parasite Golgi, we investigated its co-localization with either PfErd2 (*cis*-Golgi marker) or PfBip (ER marker). Immunofluorescence experiments were also undertaken using the anti-PfSec22 antibodies to validate the use of the GFP-tagged proteins in our study. As shown in Fig. 14, the GFP-PfSec22 chimera co-localized significantly with PfErd2 and PfBip, suggesting that PfSec22 presumably cycles between the parasite ER and Golgi. The GFP-PfSec22 fluorescence also overlapped with the anti-PfSec22 antibody signal (Fig. 14), suggesting that both the tagged and untagged proteins were similarly targeted within the parasite. Taken together, our findings suggest that PfSec22 is predominantly a v-SNARE of the parasite ER/Golgi interface but which may play an additional role in vesicle traffic inside the infected

erythrocyte cytosol. These findings are consistent with presence of atypical sequence features in PfSec22, notably the recessed N-terminal hydrophobic signal and the PEXEL-like motif.

2.4. DISCUSSIONS

Until now, little is known about the protein trafficking machineries that mediate the vectorial transport and fusion of transport vesicles in *P.falciparum*-infected cells. Moreover, no studies have been undertaken to identify and characterize the role of SNARE proteins in the unique protein trafficking pathways of this important human parasite. Exhaustive analyses of the *P. falciparum* genome database using various bioinformatics approaches have enabled us to identify 18 putative SNARE proteins that presumably represent a subset of SNARE-like proteins in the malaria parasite, when considering the multitude of trafficking pathways in *P. falciparum*-infected cells. Asexual forms of this malaria parasites target nuclear-encoded proteins to several unique destinations within its cytoplasm that include the digestive food vacuole, micronemes, rhoptries and dense granules, and to parasite-induced compartments of the infected host cell that include the TVN, Maurer's clefts and knob structures. To compensate for the multiplicity of transport pathways in this organism, members of the PfSNARE family presumably might participate in more than one transport route and might form novel SNARE complexes at the parasite-specific pathways. Alternatively, the malaria parasite might have evolved other proteins with SNARE-like activities to compensate for its unique transport pathways. This argument is supported by observations in both yeast and mammals that the 'SNAREs', use1 and Sec20, are two unconventional fusogens that assemble into SNARE complexes with Sec22p and Syn18 but which contain no defined SNARE motifs structure. In spite of the conserved organization of the

SNARE motifs in *P. falciparum*, a significant degree of sequence divergence was observed in the PfSNARE family when compared with their human orthologs (table 1). This is consistent with the general observation that SNARE proteins from distantly related organisms share little sequence identity. For instance, yeast and human Bet1p share only 20.6% identity in their respective SNARE motifs. Similarly, yeast and human Sec22 are only 32.8% identical. It thus appears that the SNARE activity of a protein is conferred by structural organization of the SNARE motif rather than the amino acid composition.

Members of the PfSNARE family also exhibit novel features that include 1) the presence of atypical amino acid residues at the zero layer position of some proteins, 2) the unusual presence of two hydrophobic domains and PEXEL-like sequences in some proteins, 3) the occurrence of low-complexity regions in some members, and 4) the occurrence of unusually large-size proteins in the PfSNARE family. Atypical zero layer amino acids have been reported in some members of both yeast and human SNAREs and include aspartate residues in human Vti1 and Slt1[81, 237], and serine in yeast Bet1p [244]. Asparagine and histidine residues have also been reported among syntaxin subfamily members in some protozoa, and in some synaptobrevins of the ciliate *Paramecium tetraurelia* [238, 245].

Prediction of transmembrane (TM) domains revealed that 13 of the 18 PfSNAREs might be ‘tail-anchored in *P. falciparum*, consistent with a requirement as membrane fusion proteins. We employed the ConPred II system to locate the putative TM domains in each PfSNARE. ConPred II is a consensus prediction system that utilizes 9 different prediction algorithms (see methods section) to locate TM domains of proteins with 100% accuracy [226]. Most SNAREs contain a C-terminal hydrophobic segment, which is thought to serve as a membrane anchor and signal for entry of the protein into the secretory system [132, 246, 247]. Surprisingly, 3

PfSNAREs (PfSec22p, PfVamp7p, and PfSyn13p) were predicted to contain a second TM domain that could be found at variable distances upstream of the SNARE motif sequence. To our knowledge, no SNARE proteins have yet been identified that contain more than one TM domain. Detailed studies are needed to understand the functional significance of these unique structural features and to determine whether or not they can be exploited for drug discovery.

A few localization studies have revealed that some components (COPII and NSF proteins) of the *P. falciparum* ER-to-Golgi vesicle trafficking machinery also associate with membrane-bound structures in the infected host cell compartment [62, 248]. To determine whether *P. falciparum* homologues of ER/Golgi SNARE also exhibit unusual localization patterns in the infected erythrocytes, we investigated the distribution pattern of the atypical PfSec22 protein in both wild-type and transgenic parasites. In mammals, Sec22b localizes to the ER, the intermediate compartment, and to the *cis*-Golgi interface where it participates in two distinct SNARE complexes involved in anterograde ER-to-Golgi traffic (Sec22b, Syn5, Bet1 and GS27) and retrograde transport from *cis*-Golgi back to the ER (Sec22b, Use1, Sec20 and Syn18). In these complexes Sec22b functions as a t-SNARE for the COPII-derived vesicles and as a v-SNARE for the retrograde COPI-derived vesicles [84]. In yeast, Sec22p functions as the v-SNARE in both the anterograde and retrograde transport pathways. Our data revealed that PfSec22 is a v-SNARE that presumably cycles between the ER and *cis*-Golgi, and associates partially with mobile vesicles in the host cell compartment. The association of PfSec22 with membrane-bound vesicles was confirmed by transmission electron microscopy using monoclonal anti-GFP antibodies. PfSec22-containing vesicles were detected within the parasitophorous vacuolar space, suggesting a two-step model for export of the tail-anchored SNARE protein in the intracellular malaria parasite.

Although the significance of PfSec22 export in *P. falciparum* has not yet been investigated in this study, it is conceivable that this v-SNARE might play a role in regulated export of parasite components into the infected host cell, presumably, by interacting with other exported t-SNAREs. Our study is the first report of an exported SNARE protein in *Plasmodium* parasites, leading the way for identification of novel eukaryotic SNARE functions in the malaria parasite.

Table 1: Nomenclature and sequence features of PfSNAREs

Names were assigned to the PfSNAREs based on their sequence identities with individual human SNARE protein motifs, determined by MegALIGN (DNASTAR) ClustalW multiple sequence alignment analyses. The SNARE motifs and hydrophobic (transmembrane) domains were identified on each PfSNARE using ScanProsite and ConPred_all consensus prediction methods, respectively. The PEXEL and recessed signal sequences were located using the MALSig malaria signal prediction algorithm. Absence of each of the analyzed sequence features, or disagreement between more than 50% of the prediction algorithms employed is indicated “none”.

Table 1: Nomenclature and sequence features of PfSNARE

PfSNARE	Gene ID	Accession no.	Size (aa)	SNARE motif	TMDs	PEXEL motifs	% identity with human
PfBet1	PF14_0500	DQ649415	163	104-157	None	none	Bet1 (24.1%)
PfGS27	PF11_0119	DQ649430	289	205-258	265-285	none	GS27 (33.3%)
PfSec22	PFC0890W	DQ649420	221	139-192	58-78 & 198-218	RSIIE	Sec22b (35.2%)
PfSNAP23	MAL13P1.113	DQ649423	198	28-81 & 142-195	none	none	SNAP23 (29.6%)
PfSyn2	PFL0505C	DQ649429	310	221-274	283-303	none	Syn2 (27.8%)
PfSyn3	PF14_0535	DQ649414	967	535-588	none	none	Syn3 (18.5%)
PfSyn5	MAL13P1.169	DQ649424	281	199-252	259-279	none	Syn5 (35.2%)
PfSyn6	PFE1505W	DQ649418	225	145-198	203-223	none	Syn6 (25.9%)
PfSyn11	PF14_0300	DQ649427	442	353-406	417-437	none	Syn11 (31.5%)
PfSyn13	PF11_0052	DQ649428	336	240-293	4-24, 303-323	RNITE	Syn13 (24.1%)
PfSyn16	PFL2070W	DQ649425	302	216-269	279-299	none	Syn16 (40.7%)
PfSyn17	PFB0480W	DQ649426	314	227-280	289-309	none	Syn17 (35.2%)
PfSyn18	MAL13P1.365	DQ649416	441	360-413	418-438	none	Syn18 (20.4%)
PfVti1	PF14_0464	DQ649417	253	135-188	199-219	RNLSE	Vti1b (22.2%)
PfVAMP7	MAL8P1.21	DQ649422	276	194-247	110-130, 253-273	none	VAMP7 (16.7%)
PfVAMP8	MAL13P1.16	DQ649421	208	123-176	186-206	none	VAMP8 (31.5%)
PfYkt6.1	PFI0515W	DQ649419	199	137-190	none	none	Ykt6 (29.6%)
PfYkt6.2	MAL13P1.135	DQ649413	221	161-214	none	none	Ykt6 (46.3%)

Fig 6: Expression analysis of PfSNAREs by RT-PCR

Complimentary DNAs (cDNAs) were amplified from asexual parasite mixed-stage total RNA using gene-specific primers and a single-tube RT-PCR approach as described under "Materials and Methods". In the 'control' reaction, the StrataScript Reverse Transcriptase enzyme was replaced with an equal volume of RNase-free water in the presence of the PfSec22 primer sets. Molecular size standards (MW in kilobase pairs) are indicated on both sides of the gel.

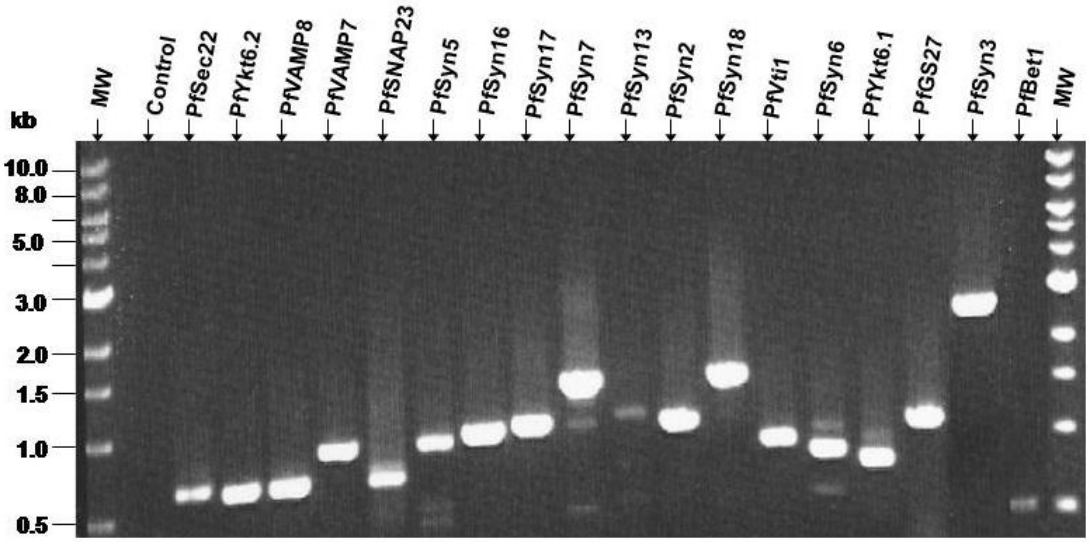

Figure 6: Expression analysis of PfSNAREs by RT-PCR

Fig 7: Sequence alignment of PfSNARE core motifs

The various conserved layers were numbered according to Fasshauer *et al* [104]. The different colors represent 1) the hydrophobic heptad repeats (orange color), 2) the conserved arginine residue of R-SNAREs (pink), 3) the conserved glutamine residue of Q-SNAREs (green), and 4) the atypical zero layer residues (blue). PfSNAP23p-n refers to the N-terminus SNARE motif of PfSNAP23p while PfSNAP23p-c refers to its C-terminus motif

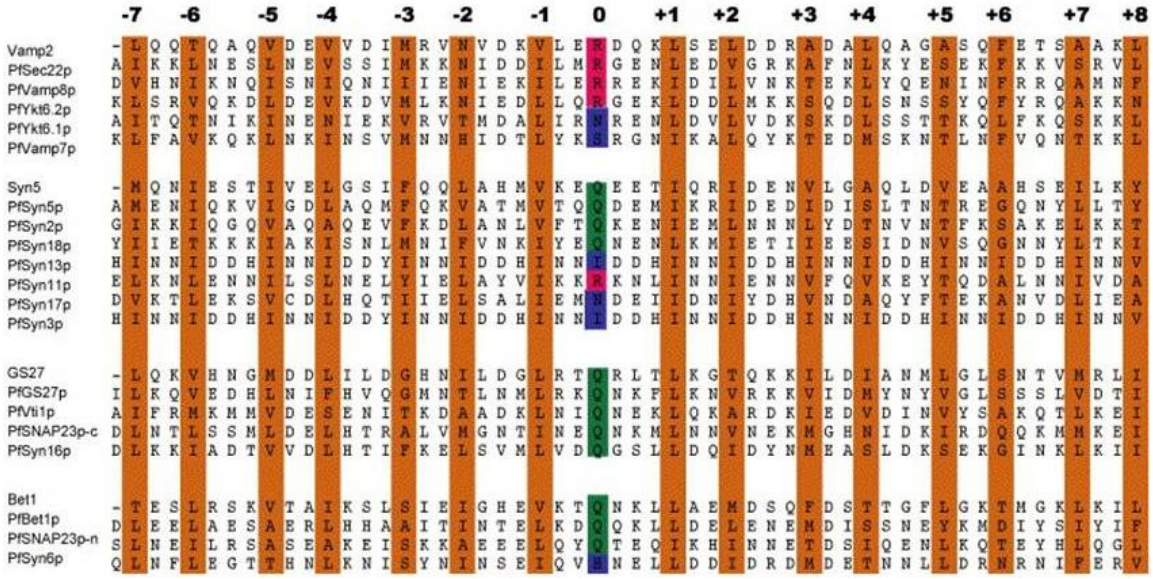

Figure 7: Sequence alignment of PfSNARE core motifs

Fig 8: Phylogenetic analysis of PfSNARE subfamilies

The phylogenetic tree was constructed using DNASTAR MegAlign program (ClustalW, slow/accurate/Blosum). Branch lengths represent the evolutionary distance.

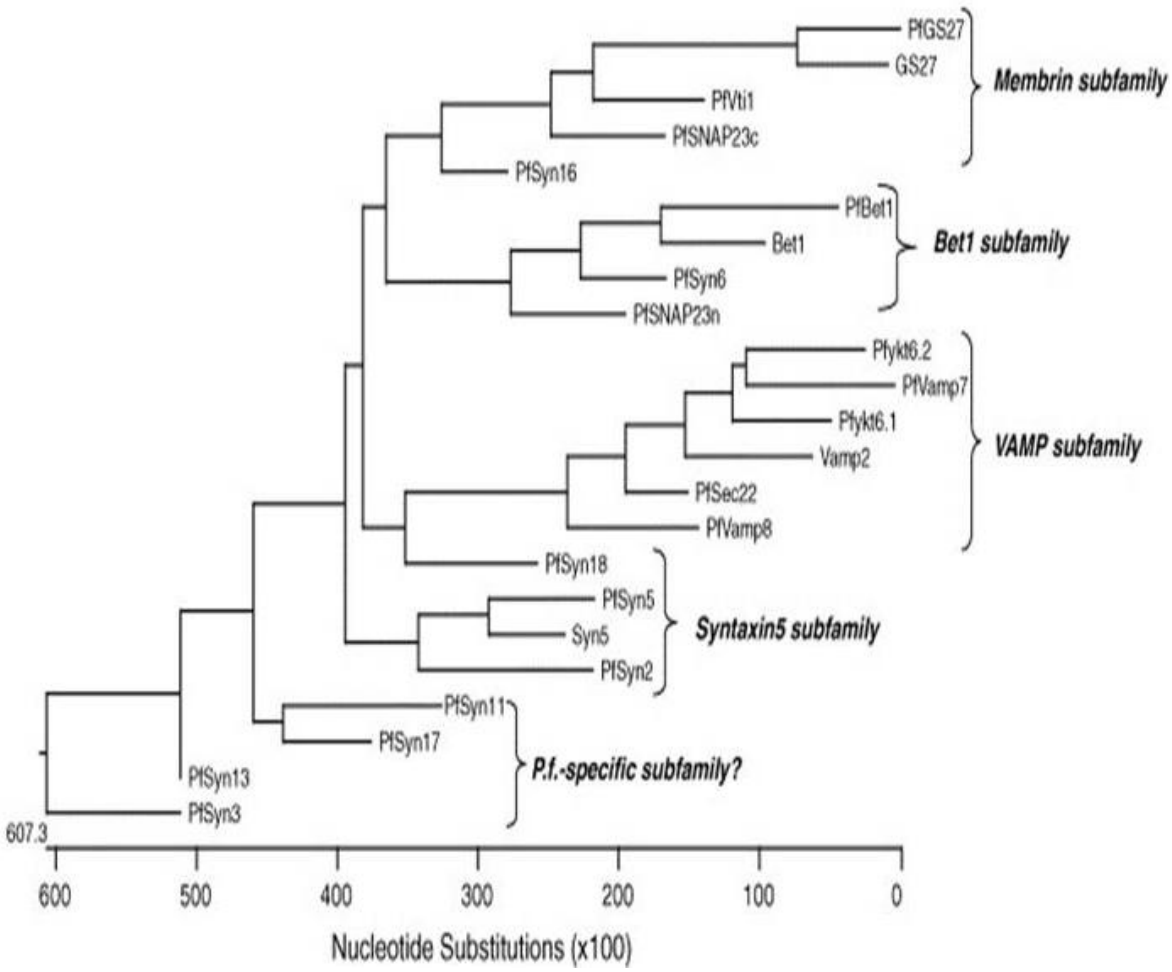

Figure 8: Phylogenetic analysis of PfSNARE subfamilies

Fig. 9: Yeast expression of PfSec22 and complementation analysis

A temperature-sensitive sec22-3 strain was transformed with either empty pMET25-3xHA plasmid (3xHA), wild-type epitope-tagged Sec22 (HA-ScSec22), or HA-tagged PfSec22 cDNA (HA-PfSec22). Growth was tested at the permissive temperatures 25^{o}C (**A**) and 30^{o}C (**B**), or at the restrictive temperature 37^{o}C (**C**) for up to 72 hours following transformation. Expression of the triple-HA tag in each cell line was verified by Western blot analyses using polyclonal anti-HA antibodies (**D**). Unlike the yeast Sec22p protein (HA-ScSec22), which conferred complementation of the Sec22-3 allele at the restrictive temperature, the HA-PfSec22 yeast cells were inviable at this temperature presumably due to failure of these cells to express the AT-rich (76% AT) PfSec22 gene construct.

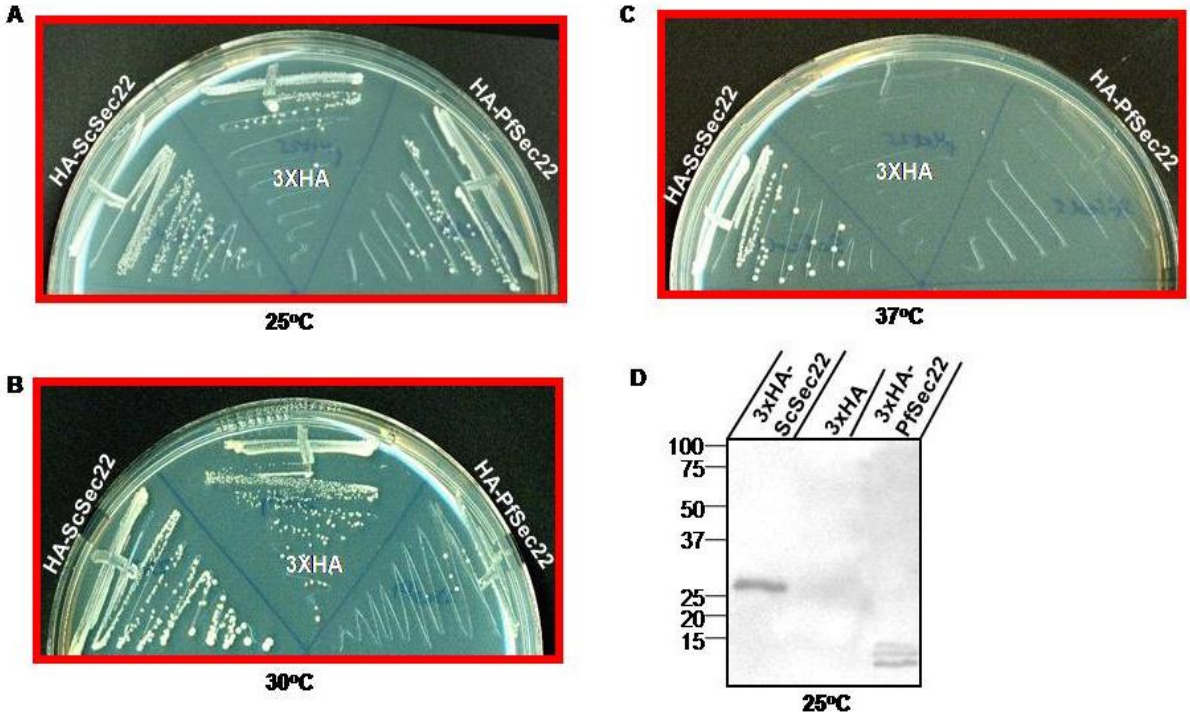

Figure 9: Yeast expression of PfSec22 and complementation analyses

Figure 10: Western blot analysis of PfSec22 expression in P. falciparum asexual stages

Antibodies were generated against a peptide sequence located within the non-conserved region of PfSec22 and affinity purified as described in the 'Materials and Methods' section. Immunoblot analysis of parasite extracts shows expression of the endogenous PfSec22 protein in ring (R), trophozoite (T), and schizont (S) stage parasites. Absence of antibody reaction with the uninfected erythrocyte lysate (UE) indicates high specificity of the antibodies to PfSec22 proteins.

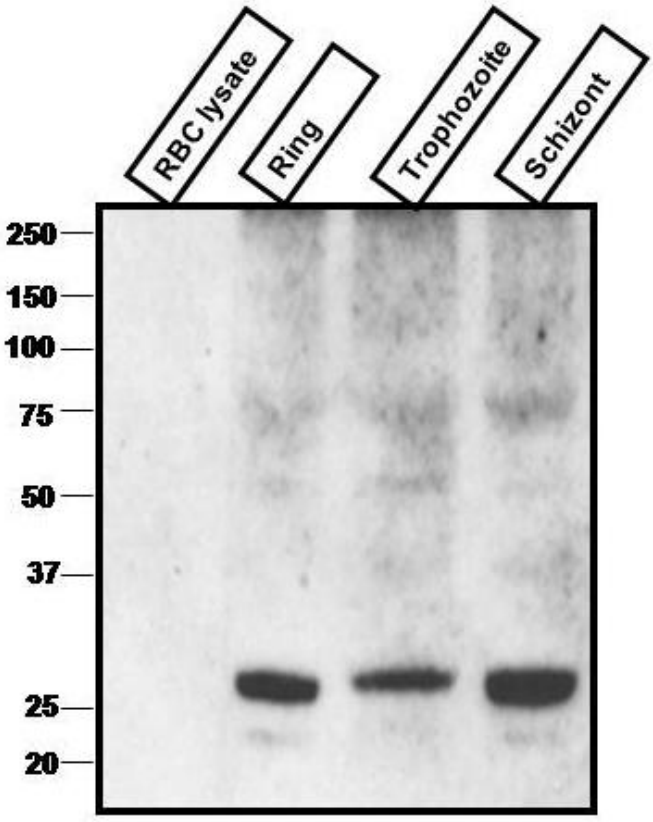

Figure 10: Western blot analysis of PfSec22 expression in *P. falciparum* asexual stages

Figure 11: Immunolocalization and membrane-association of PfSec22

(A) Immunofluorescence analyses of *P. falciparum*-infected erythrocytes using anti-PfSec22 antibodies and goat anti-rabbit Alexa Fluor-555 secondary antibodies. An intense ring of PfSec22 fluorescence is visible in ring and trophozoite infected cells. Isolated foci of PfSec22 fluorescence (black arrow) are also detected in the host cell compartment in trophozoite-infected cells suggesting export of PfSec22 into the erythrocyte cytosol. **(B)** Membrane association of PfSec22. Saponin-purified parasites were lysed by freeze–thaw/sonication, and then centrifuged to separate the membrane-anchored proteins (P1) from the soluble cytosolic and lumenal proteins (S1). Integral membrane proteins (P2) were separated from the peripheral membrane proteins (S2) by alkaline extraction with 0.1 M Na_2CO_3 solution at pH 11. The solubility profiles of the integral membrane proteins were further analyzed by Triton-X114 extraction to separate the hydrophilic proteins in the aqueous (aq) phase from the hydrophobic proteins (hy) in the detergent phase. Normalized volumes of the samples pairs were loaded into each well and immunoblotted with antibodies against the PfSec22 protein, the soluble protein PfBip, or the integral membrane protein marker PfErd2. Thirty-five micrograms of the freeze-thaw lysate were loaded in the lane denoted L. **(C)** The association of PfSec22 with the parasite ER was investigated by co-immunofluorescence analysis using rabbit anti-PfSec22 and rat anti-PfBip antibodies as indicated. Both proteins co-localized significantly to membrane profiles inside the parasite cytoplasm.Scale bars, 2μm

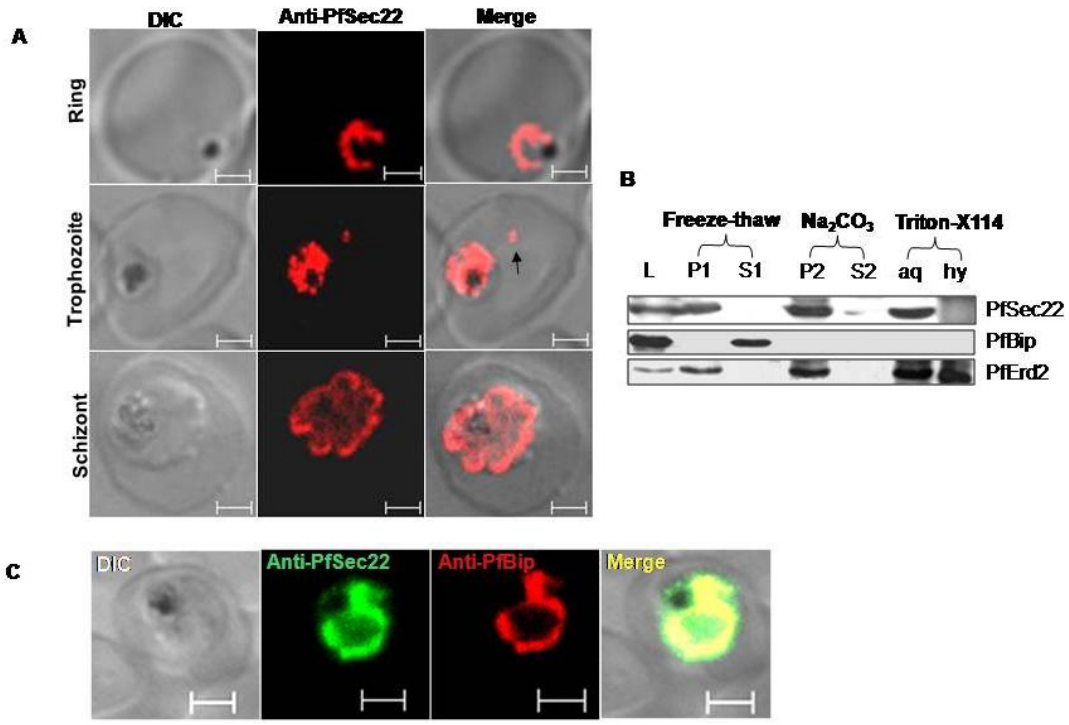

Figure 11: Immunolocalization and membrane-association of PfSec22

Figure 12: Transgene expression and live cell imaging of GFP-tagged PfSec22 proteins

(A) Immunoblot analyses using anti-PfSec22 antibodies (*left* blot) or monoclonal anti-GFP antibodies (*right* blot) confirms expression of the N-terminal GFP-tagged PfSec22 (N-GFP) and the C-terminal GFP-tagged PfSec22 (C-GFP) proteins (~54 kDa) in the respective transgenic cell lines but not in untransfected parasites (3D7). The anti-PfSec22 antibodies also detected a ~26 kDa protein in whole cell extracts from all three cell lines that corresponds to the untagged PfSec22 protein. **(B)** Live cell imaging of parasites expressing the C-terminal GFP-tagged PfSec22 (PfSec22-GFP), showing diffuse localization of the protein throughout the parasite cytoplasm, and export in trophozoite-infected cells. **(C)** Confocal micrographs showing localization of the N-terminal GFP-tagged protein (GFP-PfSec22) in early- (*first* row) and mid-trophozoite (*second* row) stage parasites. In addition to the ER-like profiles, GFP-PfSec22 associates with tubovesicular elements in the infected host cell. The micrographs represent differential interference contrast (DIC), GFP fluorescence, and a merge between the two. **(D)** Association of GFP-PfSec22 with mobile extraparasitic vesicles. Images were captured at regular time intervals as indicated on each micrograph. Scale bars, 2μm.

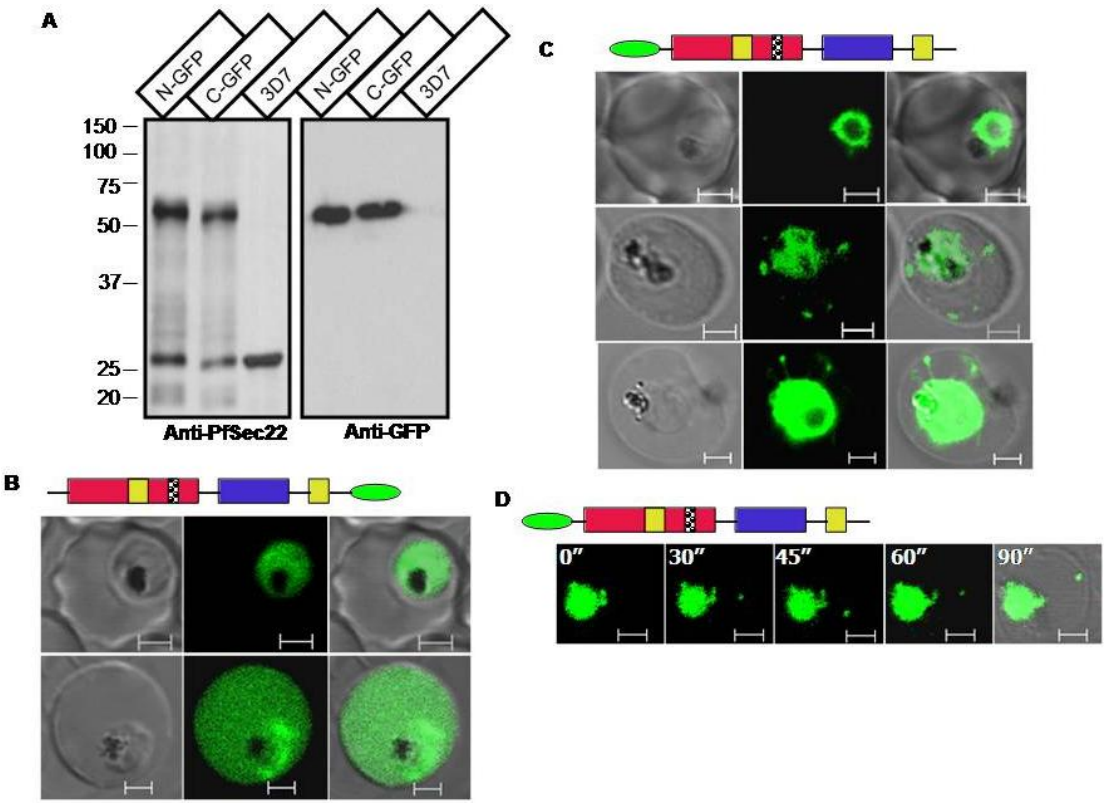

Figure 12: Transgene expression and live cell imaging of PfSec22 proteins

Figure 13: Cryo-immunoelectron microscopy of GFP-PfSec22

Ultrathin cryosections of the GFP-PfSec22 expressing cells were probed with monoclonal anti-GFP antibodies followed by immunogold detection using gold (12nm)-labeled anti-mouse secondary antibodies. **(A)** Association of GFP-PfSec22 with ER-derived transition vesicles (black arrowhead). **(B)** Association of GFP-PfSec22 with membrane-limited vesicles (white arrowheads) in the host cell compartment. **(C)** Association of GFP-PfSec22 with the TVN-like extension (dotted arrow) and membrane-bound vesicles (white arrowhead) in the infected erythrocyte cytosol. N: nucleus, MC: Maurer's cleft, RBC: red blood cell cytosol. Scale bars are 500 nm in (A) and 100 nm in (B) and (C).

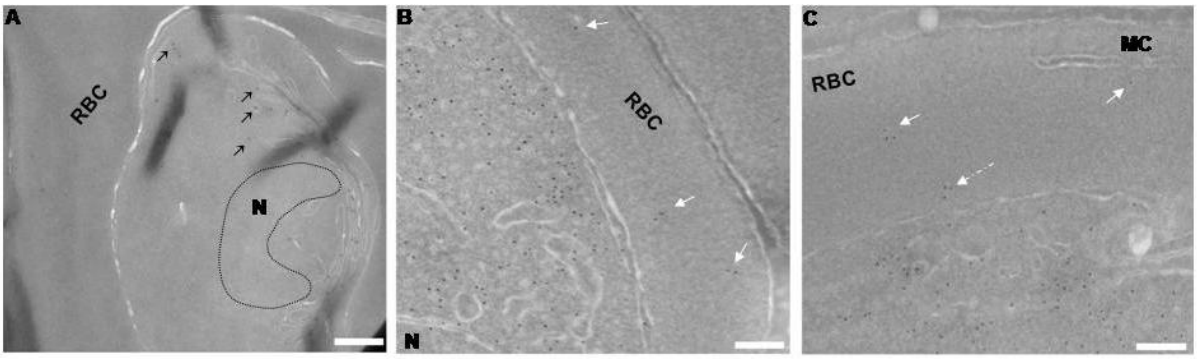

Figure 13: Cryo-immunoelectron microscopy of GFP-PfSec22

Figure 14: Co-immunofluorescence analysis of GFP-PfSec22

Immunoflorescence micrographs showing co-localization of GFP-PfSec22 with PfErd2 (top row) and PfBip (ER marker, middle row). The untagged and GFP-tagged PfSec22 both co-localize significantly within the parasite cytoplasm as determined by labeling with the anti-PfSec22 antibodies. Scale bars, 2µm.

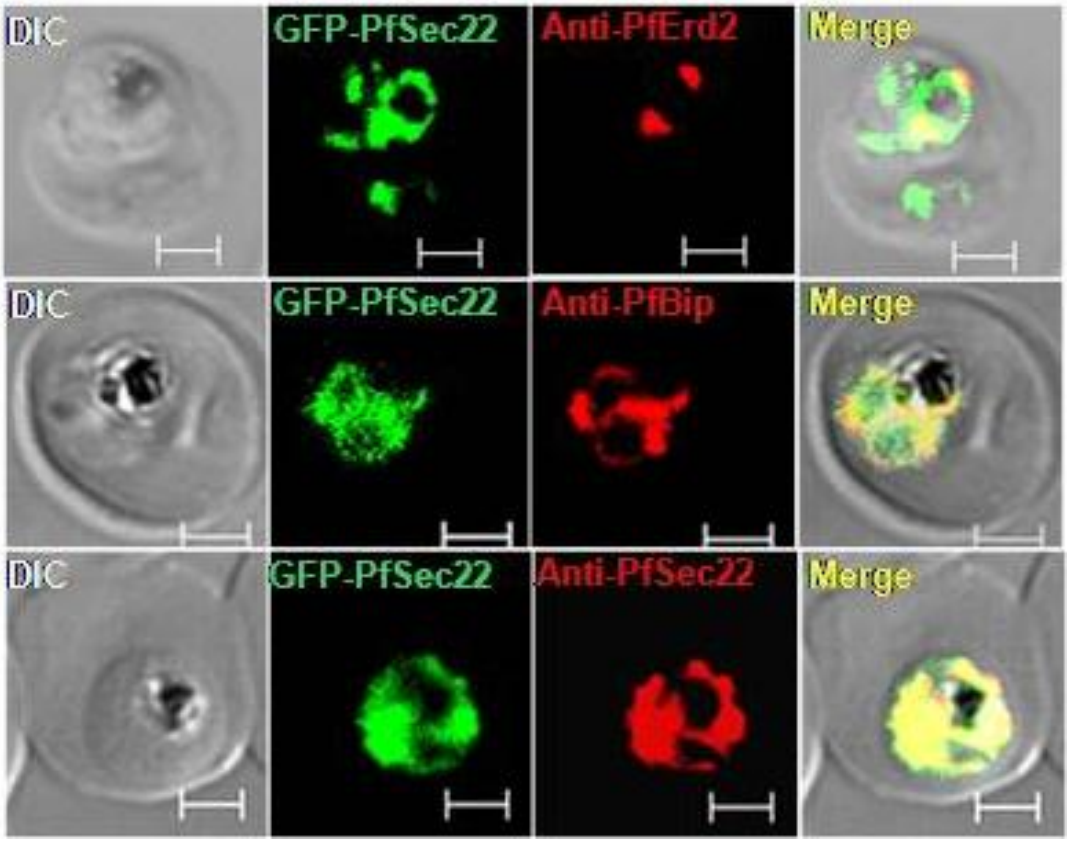

Figure 14: Co-immunofluorescence analysis of GFP-PfSec22

CHAPTER 3:
DETERMINANTS OF SEC22 TRAFFICKING IN P. FALCIPARUM

3.1. SUMMARY

In this study, we identified a Sec22 ortholog in *Plasmodium falciparum* (PfSec22) that contains an atypical insertion of the *Plasmodium* export element within the longin domain preceded by an N-terminal hydrophobic segment. We also showed that PfSec22 cycles predominantly between the ER and Golgi compartments in the malaria parasite, and partially associates with mobile vesicular elements in the infected host cell. Here, we have investigated the role of (1) the C-terminal hydrophobic domain, (2) the PEXEL motif, (3) the atypical longin domain, and (4) the N-terminal hydrophobic segment in PfSec22 trafficking in asexual forms of the malaria parasite. Transgenic parasites were developed that expressed N-terminally tagged GFP-PfSec22 mutants and examined by live confocal microscopy. Our data suggest that ER exit of PfSec22 is regulated by motifs within the α3 segment of the longin domain, deletion of which resulted in ER retention of the protein. The data further suggest that export of PfSec22 beyond the parasite ER/Golgi interface occurs independent of its membrane insertion and that the PEXEL-like motif is non-essential in the putative export process. Additionally, we showed that the N-terminal hydrophobic segment that is located within the β3 segment of the longin domain plays a crucial role in export of PfSec22 to the host cell and in retrograde transport from the Golgi back to the ER. Deletion of this region resulted in retention of the protein in the Golgi. The association of the N-terminal hydrophobic domain mutant with Golgi was analyzed by brefeldin A treatment and by sucrose density gradient fractionation of organellar compartments. Our study is the first report of the involvement of the longin domain in retrograde transport of Sec22 v-

SNARE to the ER, and provides new insights in protein targeting along the secretory system in malaria parasites. The data however suggest major differences between the PfSec22 longin domain and orthologues in yeast and humans, perhaps indicative of novel Sec22 trafficking mechanisms in *Plasmodium* parasites.

3.2. MATERIALS AND METHODS

3.2.1. Sequence analysis and homology modeling of PfSec22 longin domain

Multiple sequence alignments were performed by CLUSTALW (Megalign DNASTAR) using the PfSec22, human Sec22b and yeast Sec22p polypeptide sequences to identify structural features that are unique to the *P. falciparum* Sec22 protein. To highlight the unique structural differences, and potential role of the PfSec22-specific structures, the protein was modeled by SWISS-MODEL 8.05 using the crystal structure of Sec22b as template [138, 249].

3.2.2. Deletion constructs and site-directed mutagenesis

Transfection plasmids were designed to express green fluorescent protein (GFP)-tagged Sec22 mutant proteins under the control of the endogenous promoter sequence. The primer set 5'-GGAAGATCTATGTGCGATGTAGTATTACTT-3' and 5'-CCGCTCGAGTTATTTTAGATTTAATACCCTTGA-3' was used to generated the C-terminal hydrophobic domain mutant GFP-PfSec22Δ198-221 by PCR using the wild type pDC-*GFP-PfSec22* plasmid as template. Similarly, the primer set 5'-GGATCCAGCTTTTTTATTTTTAAACGAT-3' and 5'-

CCGCTCGAGTTAAAAATAATTTTTAAAAATTATAATT-3' was used to construct the GFP-PfSec22Δ1-78 fusion genes from the wild type plasmid. DNA encoding amino acids 1-58 of the full length Sec22 protein was also amplified by PCR using primers 5'-GGAAGATCTATGTGCGATGTAGTATTACTT-3' and 5'-GGATCCAAAATGGTAATTAAAATTGTTAG-3' and subsequently ligated via the *Bam*HI site at the 5'-terminus of PfSec22Δ1-78, cloned in a pGEMT-Easy vector. The resulting PfSec22Δ58-78 fusion construct was then subcloned into pDC2-0.995 vector to obtain the GFP-PfSec22Δ58-78 mutant construct. Deletion of the entire longin domain sequence was achieved by PCR using the primer set …., and the resulting fragment was subcloned at the BglII/XhoI site of pDC2-0.995 vector. The GFP-PfSec22Δ198-221.PEXEL(R>A) construct was generated from the GFP-PfSec22Δ198-221 mutant plasmid by site-directed mutagenesis of the PEXEL motif-specific arginine, replacing it with an alanine codon. All constructs were confirmed by sequencing prior to transfection of *P. falciparum* 3D7 parasites. Ring stage parasites were transfected by electroporation (Biorad Gene pulser II at 0.31kV, 950μF, maximum capacitance) using 100μg of purified plasmid (Qiagen Maxiprep kit). Positive selection for transfected parasites was achieved using 2.5 nM WR99210 as previously described [250, 251].

3.2.3. Live cell imaging and immunofluorescence analyses of PfSec22 mutants

Both live and fixed cells were examined using a laser scanning confocal microscope (LSM 510, Carl Zeiss). The excitation/emission spectra settings were 488/505 nm for GFP, 543/555 for Alexa Fluor-555 conjugated antibodies, or 543/594 nm for Alexa Fluor-594 conjugates. To image live parasites, the cells were mounted under a cover slip in 50% glycerol and observed within 15 minutes of removal from cultures. Immunofluorescence assays were

performed in suspension as previously described by Tonkin *et al* [215]. Briefly, the cells were washed once with phosphate-buffered saline (PBS) and subsequently fixed with a solution containing 4% paraformaldehyde + 0.0075% glutaraldehyde in PBS for 30 min at room temperature. Following one wash with PBS, the cells were permeabilized with 0.1% Triton X-100 for 10 min, followed by reduction of excess aldehydes with sodium borohydride at 0.1 mg/ml, and blockage of nonspecific binding sites with 3% BSA in PBS at room temperature for 1 h. For co-localization analyses, the cells were probed with appropriate antibodies (1° and 2°) in PBS containing 3% BSA at 4ºC overnight followed by three washes with PBS. Rabbit anti-PfErd2 (MRA-1) and rat anti-PfBip (MRA-19) antibodies were obtained from the Malaria Research and Reference Resource Center (MR4) and were each used at a dilution of 1 in 1,000. The secondary antibodies were goat anti-rabbit Alexa-Fluor-555, or goat anti-rat Alexa Fluor-594 (Molecular Probes), each used at a dilution of 1 in 1,000 for 1 hour at room temperature. After washing three times with plain PBS, the cells were allowed to adhere to polyethyleneimine (PEI)-coated cover slips at room temperature for 15-20 minutes. The coverslips were rinsed with PBS and were mounted onto a glass slide with 50% glycerol containing 0.1 mg/ml of 1,4-diazabicyclo (2,2,2) octane (Sigma).

3.2.4. Sucrose density gradient centrifugation and immunoblot analyses

250 mg of saponin-isolated parasites were resuspended in ice-cold TBS buffer, containing protease inhibitor cocktail (Roche) in the presence of 2 mM EDTA or 5 mM $MgCl_2$ and incubated on ice for 30 minutes. Cells were disrupted by 5 freeze-thaw cycles and then cleared at 10,000 X g for 5 minutes at 4^oC. The suspension was then adjusted to 47% sucrose and deposited (1.5 ml final volume) at the bottom of a discontinuous sucrose gradient comprising 1

ml of 40% sucrose, 1 ml of 35% sucrose, 0.75 ml of 25% sucrose, and 0.75 ml of 20% sucrose. The gradient was centrifuged at 100, 000 X g for 16 hours at 4^{o}C in a Beckman SW50.1 rotor, and fractionated into 0.5 ml aliquots by piercing the bottom of the tube using a fraction recovery system (Beckman). Equal volumes of fractions were analyzed by immunoblotting using either the anti-PfSec22, or anti-PfErd2, or anti-PfBip antibodies, each at a concentration of 1 in 1000.

3.2.5. Effect of Brefeldin A

To confirm the association of the GFP-tagged proteins with the Golgi and transitional vesicles, we investigated the effect of the vesicle transport inhibitor brefeldin A on their steady-state dynamics [252-254]. GFP-expressing cells were cultured in the presence of BFA (5µg/ml) for one hour at 37^{o}C and examined by live confocal microscopy or by immunofluorescence analysis using antibodies to the Golgi-resident protein PfErd2. Control experiments consisted of the same cultures prepared in equivalent amounts of the drug solvent.

3.3. RESULTS

3.3.1. The P. falciparum Sec22 homologue exhibits novel features

Multiple sequence alignment and homology modeling of the PfSec22 protein revealed major structural differences when compared to the human and yeast orthologues. As shown in Fig. 15 A and B, the N-terminal longin domain of PfSec22 contains a decapeptide sequence insertion, located at an unusual loop-like region between the α2 and α3 segments, that contains the PEXEL-like motif (^{105}RSIIE^{109}). This motif is preceded by a stretch of hydrophobic residues

located within the β5 segment of the longin domain (Fig. 15A). Prediction analyses using the Malaria Signal prediction algorithm (MalSig) suggested that the N-terminal hydrophobic segment might function as a recessed transport signal for PfSec22 targeting into the parasite's default export pathway (prediction probability = 0.8192).

PfSec22 also contains a C-terminal hydrophobic segment that presumably serves as a membrane anchor, and might also double as a targeting signal. In this study, we investigated the role of the C-terminal hydrophobic domain, the atypical longin domain, the N-terminal hydrophobic domain, and the PEXEL motif in PfSec22 trafficking in transgenic malaria parasites.

3.3.2. The C-terminal hydrophobic domain is required for membrane insertion of PfSec22

To investigate whether or not the putative C-terminal transmembrane domain is a determinant for PfSec22 targeting in the malaria parasite, we developed a transgenic cell line expressing the deletion mutant GFP-PfSec22Δ198-221 (see schematic diagram in Fig. 16). As shown in Fig. 16, deletion of this C-terminus hydrophobic segment (amino acids 198 to 221) resulted in a cytosolic protein that was also released into the erythrocyte cytosol in a pattern similar to the C-terminally tagged full-length protein (compare Fig.12B and Fig. 16). These results suggest that the C-terminal hydrophobic segment is required for PfSec22 targeting to the parasite ER/Golgi interface and membrane-integration of the protein. The data further suggest that the occasional export of PfSec22 into the infected erythrocyte may involve processes independent of its membrane integration.

3.3.3. PfSec22 export into host cells occurs independently of the PEXEL motif

To investigate the role of the PEXEL-like sequence (RSIIE), we mutated the PEXEL arginine residue using the GFP-PfSec22Δ198-221 construct. This mutant construct was selected over the wild type construct because the expressed GFP-PfSec22Δ198-221 protein was relatively more predominant in the host cell (~10% of trophozoite-infected cells) than the wild type protein (~5% of infected erythrocytes cells). The critical role of the PEXEL arginine in N-terminal processing and translocation of canonical PEXEL motif-containing proteins across the PVM has previously been demonstrated [164, 243, 255]. Replacement of this conserved residue in the exported proteins GBP130, KAHRP, or in STEVOR inhibits transport to the erythrocyte cytosol, and accumulation at the ER. Additionally, such mutations ablate the proteolytic cleavage of the proteins at the PEXEL motif [164]. In our study, replacement of the PEXEL-like arginine in PfSec22 with alanine (GFP- PfSec22Δ198-221.PEXEL(R>A)) did not inhibit export of the cytosolic protein to the host cell cytoplasm (Fig. 17). These findings suggest that the PfSec22 PEXEL-like sequence is inactive in the protein export processes. Alternatively, this motif plays a non-essential role in PfSec22 export to the host cell cytoplasm.

3.3.4. The longin domain is critical for ER/Golgi recycling and partial export of PfSec22

To determine the role of the longin domain in PfSec22, we generated transgenic parasites expressing GFP-tagged mutants, lacking either the first 78 amino acid residues of the protein (GFP-PfSec22Δ1-78 mutant) or the entire longin domain (GFP-PfSec22Δ1-124). As shown in Fig. 18A, truncation of the longin domain at position 78 dramatically shifted the steady-state accumulation of the v-SNARE from the ER to the Golgi. These findings suggest that GFP-

PfSec22Δ1-78 presumably has a preference for the parasite Golgi and that residues 1-78 might encode signals required for ER retrieval of PfSec22. Interestingly, deletion of the entire longin domain at position 124 resulted in retention of the GFP-PfSec22Δ1-124 protein in the ER (Fig. 19). Together, these results suggest that the C-terminal end of the longin domain (residues 78 to 124), corresponding to the α3 segment, is critical for ER exit of the PfSec22. Both the GFP-PfSec22Δ1-78 and GFP-PfSec22Δ1-124 deletion mutants did not traffic into the host erythrocyte cytosol as observed with the wild-type protein and the C-terminal hydrophobic domain mutants. These results suggest that the PfSec22 longin plays a critical role in ER/Golgi recycling of the protein as well as export to the host erythrocyte cytoplasm.

3.3.5. The N-terminal hydrophobic domain is required for PfSec22 exit from the Golgi

Our findings that N-terminus sequence from amino acids 1 to 78 was required for Golgi-to-ER recycling of PfSec22 suggested that the retrieval signal is located in this region. Additionally, domain mapping and prediction analyses also suggested that the N-terminal hydrophobic segment might potentially serve as a recessed export motif for PfSec22 in malaria parasites. To investigate the role of this domain in PfSec22 trafficking, we developed minimized deletion mutant lacking only the N-terminal hydrophobic segment (GFP-PfSec22Δ58-78 mutant). As shown in Fig 20, the Δ58-78 deletion resulted in a Golgi localization of PfSec22, similarly to the GFP-PfSec22Δ1-78 mutant.

The Golgi targeting of the GFP-PfSec22Δ58-78 mutant was further investigated by sucrose density gradient fractionation of organellar compartments, and by brefeldin A (BFA) inhibition assays. To overcome common difficulties in resolving the parasite ER from other

membrane-bound compartments, the co-fractionation experiments were done in the presence of the chelating agent EDTA, or in the presence of the rough ER stabilizing agent $MgCl_2$ [256, 257]. By this approach, a redistribution of the PfSec22 proteins alongside the ER marker PfBip, from a low-density fraction (in the presence of EDTA) to a high-density fraction (in the presence of $MgCl_2$), suggested its association with the rough ER. To validate our ER-redistribution assay, we used the wild-type GFP-PfSec22 expressing cell line. Samples from equal volumes of the sucrose gradient fractions were analyzed by Western blot using the anti-PfSec22, anti-PfBip (ER marker), or anti-PfErd2 (Golgi marker) antibodies. As shown in Fig. 21A, treatment of the wild-type parasites with EDTA resulted in enrichment of both the endogenous (PfSec22) and GFP-tagged (GFP-PfSec22) proteins at two different zones: a low-density zone (fraction 6 and 7) and a high-density zone (fraction 2, 3 and 4). Both zones were also detected using the anti-PfBip antibodies but not the anti-PfErd2 antibodies, suggesting that these zones represent the ER-containing fractions. In contrast with PfBip that completely redistributed to the high-density zone upon $MgCl_2$ treatment, both the endogenous (PfSec22) and GFP-tagged (GFP-PfSec22) proteins only partially redistributed from the low-density zone (Fig. 21B). The remaining PfSec22 signals at the low-density zone presumably represent transport vesicles, or lipid-rich containers.

Unlike the wild-type PfSec22 proteins from the GFP-PfSec22 expressing parasites, the buoyant density of the GFP-PfSec22Δ58-78-associated compartments in the mutant cell line did not change in the presence of EDTA or $MgCl_2$ (Fig. 21C and D). This mutant protein consistently was enriched in the high-density (low lipid content) fractions, similarly to the Golgi protein PfErd2. The results strongly support our immunofluorescence data, indicating that the N-terminal hydrophobic segment resides predominantly in the Golgi. A small proportion of the mutant protein also remained in the low-density zone, consistent with an association with

transport vesicles or other lipid-rich structures. In support of the Golgi retention of the hydrophobic domain mutant, treatment of the parasites with brefeldin A (BFA) for 1 hr resulted in partial redistribution of the protein back to the ER (Fig. 22), a phenomenon typical of most Golgi-localized proteins including the *cis*-Golgi marker PfErd2 [253].

Together, the above data suggest that the ER exit of PfSec22 occurs independently of residues 1 to 78 of the longin domain and that the N-terminal hydrophobic segment (amino acid 58-78) is required for Golgi-to-ER recycling of the v-SNARE and export to the host erythrocyte cytoplasm.

3.5. DISCUSSIONS

Our findings that the longin domain of PfSec22 contains atypical features and associates with vesicular structures within the infected erythrocytes have led us to investigate the trafficking determinants of this v-SNARE. Our data strongly suggest that export of PfSec22 into the infected host cell is independent of its membrane-insertion, and N-terminal processing of the PEXEL/VTS sequence. Presumably, export of PfSec22 might involve processes similar to those that are utilized by several non-PEXEL/VTS motif-containing proteins that also lack the functional N-terminal signal sequence. These exported proteins include the Maurer's cleft-associated proteins PfSBP1 and PfMAHRP-1, and the ring-exported proteins PfREX-1 and 2. The trafficking pathways and signals that are involved in export of these non-PEXEL/VTS containing proteins to the host cells are poorly understood. It has been suggested that the transmembrane domain and second half of the N-terminus of PfMAHRP-1 contain the putative targeting signals [258]. For PfREX-1, a stretch of hydrophobic amino acids and an additional 10

amino acid residue seem to be important for export [259]. Unlike PfMAHRP-1, PfREX-1 appears to cross the secretory pathway in a soluble state and only after delivery into the erythrocyte cytosol does it associate with the MC via a coiled-coil motif [259]. PfSBP1 contains a transmembrane domain which is thought to be required for entry into the parasite's secretory pathway. It is also believed that additional domains in the PfSBP1 polypeptide that affect the net charge distribution, the solubility profile, and membrane topology of the protein also play a role in sorting beyond the parasite plasma membrane [260].

In an attempt to decipher the trafficking determinants of PfSec22, we investigated the role of the N-terminal longin domain and N-terminal hydrophobic segment. Truncation of the N-terminal longin domain at position 78 or 124 of the polypeptide chain, or deletion of the N-terminal hydrophobic segment resulted in inhibition of PfSec22 export into the infected host cell, suggesting that the N-terminal segment is required for export beyond the RG/Golgi interface. Additionally, deletion of the entire longin domain, but not the N-terminal truncation, resulted in retention of the protein in the ER. In yeast and mammals, ER exit of Sec22 is believed to involve a conformational epitope formed by interaction of motifs within the second half of the longin domain and the SNARE motif [137, 138, 261]. Deletion of the entire longin domain or mutation of the conserved residues in yeast and mammalian Sec22 proteins results in retention of the protein at the ER. This putative ER export motif is located within the α3 segment of the PfSec22 longin domain and is characterized by the conserved amino acids I118 and D121.

Truncation of the N-terminal longin domain at position 78 of the protein (GFP-PfSec22Δ1-78) resulted in export from the ER and retention in the Golgi. We interpreted this data as evidence for a defective recycling of the mutant proteins from the Golgi back to the ER. In yeast, recycling of Sec22p requires interactions with the COPI budding complex and with the

SNARE proteins Ufe1 and Sec20 [242]. Until now, no studies have identified the retrieval signal of the Sec22 gene products. Expression of yeast Sec22p in sec20-1 or ufe1-1 deficient cells, or in the COPI (sec21-1 and sec27-1) deficient cells, results in accumulation of the protein in the Golgi and a lack of ER staining by anti-Sec22 antibodies [242]. It is, therefore, likely that recycling of PfSec22 may involve interactions between sequence motifs in the N-terminal region and *Plasmodium* homologues of the COPI complex and the SNARE proteins.

Deletion of the N-terminal hydrophobic domain alone similarly prevented PfSec22 recycling to the ER, suggesting that the retrieval signal for PfSec22 in located within the N-terminal hydrophobic segment. To our knowledge, this study provides the first experimental evidence for the role of the Sec22 longin domain in retrograde transport of the v-SNARE, and is the first detailed analysis of SNARE protein targeting in malaria parasites. It is however not clear whether this N-terminal hydrophobic segment (amino acids 58-78) directly functions as a retrieval signal for PfSec22, or whether this region indirectly contributes to an overall structure that is required for the recycling and export processes.

Figure 15: Sequence analyses and homology modeling of PfSec22 longin domain

(A) Sequence alignment of PfSec22 with its homologues in humans and yeast. Identical amino acids are highlighted in yellow while the PEXEL-like motif is shaded in red. The five beta strands (β1-5) and three alpha helix (α1-3) structures of the longin domain are indicated. Black boxes indicate the predicted hydrophobic segments (N-terminal hydrophobic and C-terminal hydrophobic segments). PfSec22 and human Sec22b are 30.9% identical; PfSec22 and yeast Sec22p are 26.2% identical. In comparison, the human and yeast Sec22 polypeptides are 37.2% identical. **(B)** Ribbon structures of human Sec22b and PfSec22 longin domains showing the location of the PEXEL-like motif (RSIIE). The PfSec22 structure was modeled via SWISS-MODEL 8.05 using the human Sec22b sequence as template.

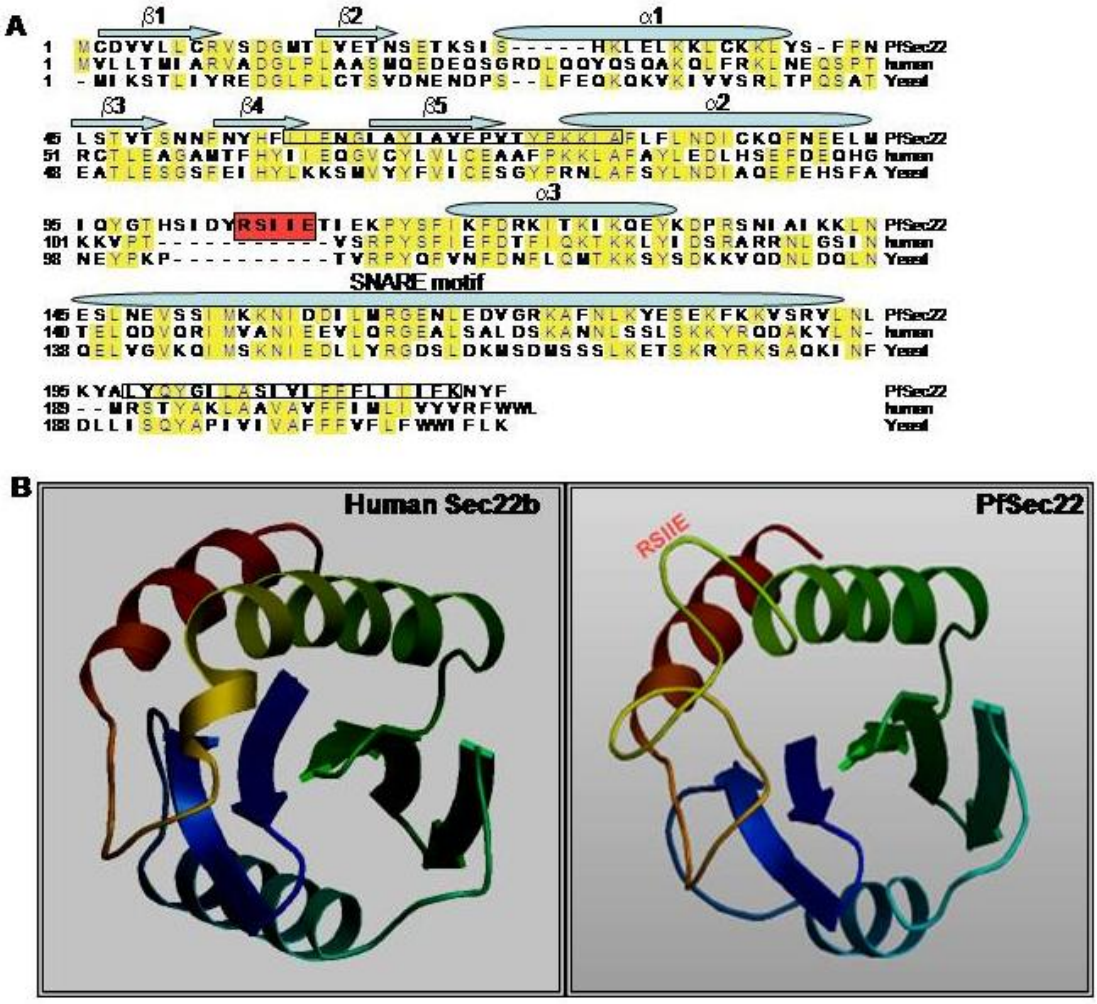

Figure 15: Sequence analysis and homology modeling of PfSec22 longin domain

Figure 16: Role of the C-terminal hydrophobic domain in PfSec22 trafficking

Deletion of the C-terminal hydrophobic domain (GFP-PfSec22Δ198-221) resulted in a diffuse localization within the parasite cytoplasm and in the infected host cell in a pattern similar to that of the C-terminally tagged full-length protein (see Fig. 12). These results suggest that the C-terminal hydrophobic domain plays an essential role in ER targeting and membrane-integration of PfSec22. Scale bars, 2μm.

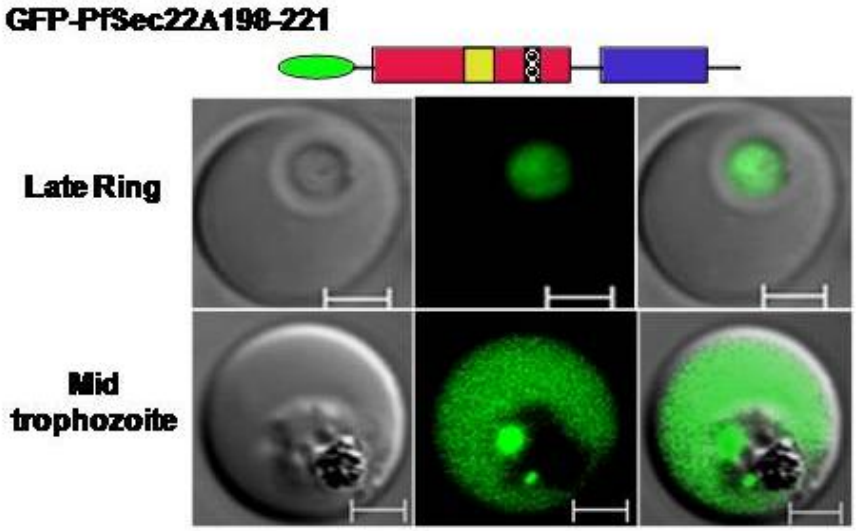

Figure 16: Role of the C-terminal hydrophobic domain in PfSec22 trafficking

Figure 17: Export of PfSec22 PEXEL motif mutant into infected host cells

Replacement of the PEXEL arginine with alanine (i.e RSIIE to ASIIE) did not inhibit export of the soluble GFP-PfSec22Δ198-221 protein to the erythrocyte cytoplasm at trophozoite stages, suggesting that the PEXEL-like motif might play a nonessential role in PfSec22 export into the infected host cells. Scale bars, 2μm.

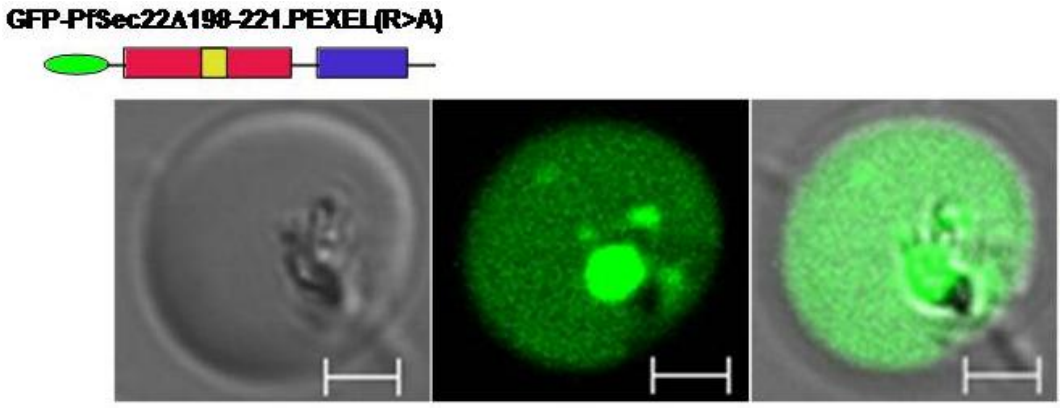

Figure 17: Export of PfSec22 PEXEL motif mutant into infected host cells

Figure 18: Retention of the PfSec22Δ1-78 deletion mutant in the Golgi

Transgenic parasites were generated expressing a truncated PfSec22 mutant (GFP-PfSec22Δ1-78) that lacks the N-terminal amino acid residues from position 1 to 78. Live imaging (top panel) and localization analyses using anti-PfErd2 antibodies confirm retention of the GFP-PfSec22Δ1-78 protein in the Golgi. Scale bars, 2μm.

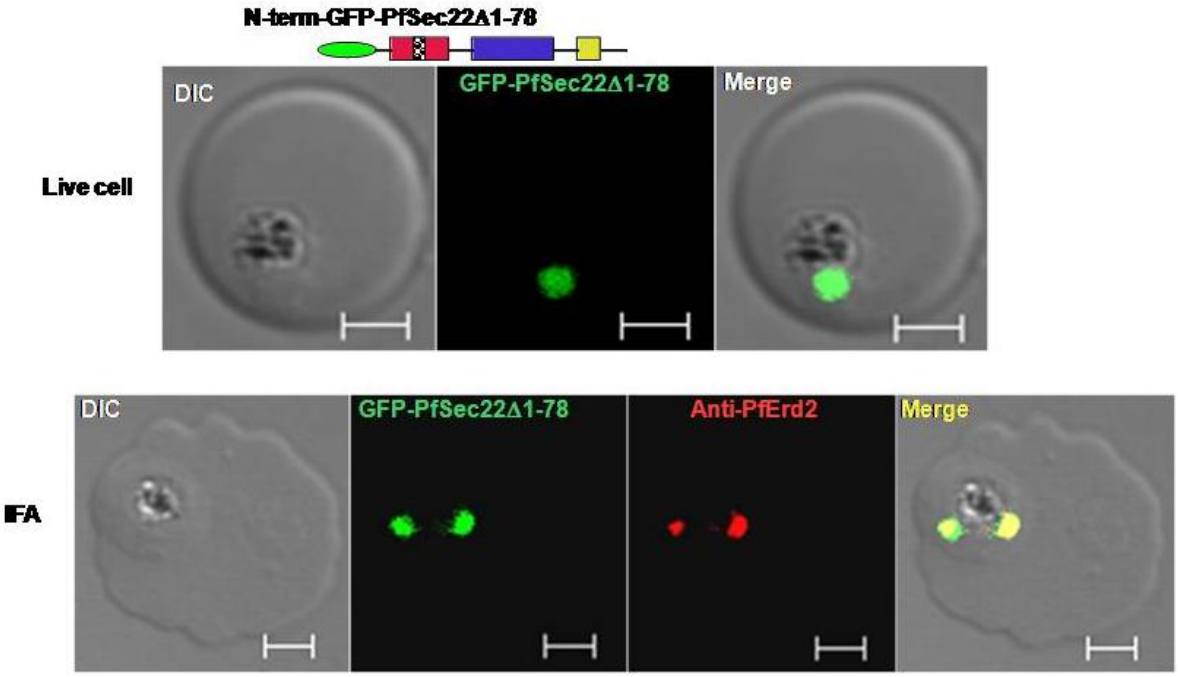

Figure 18: Retention of the PfSec22Δ1-78 deletion mutant in the Golgi

Figure 19: Retention of the PfSec22Δ1-124 deletion mutant in the ER

Transgenic parasites were generated that express a deletion mutant of PfSec22 (GFP-PfSec22Δ1-124) lacking the entire longin domain. This deletion mutant accumulated in the ER and was not export into the host cell. Scale bars, 2µm.

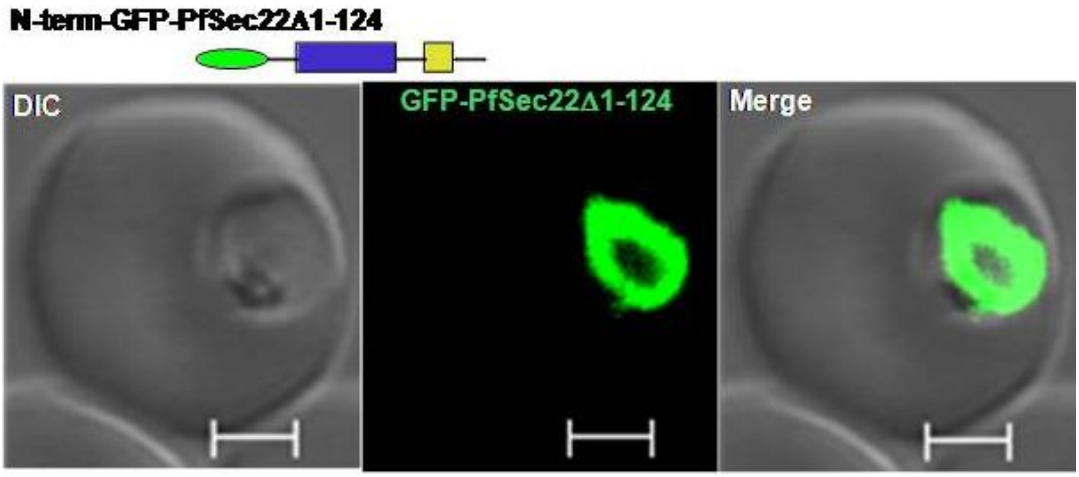

Figure 19: Retention of the GFP-PfSec22Δ1-124 mutant in the ER

Figure 20: Retention of the N-terminal hydrophobic domain mutant in the Golgi

Deletion of the N-terminal hydrophobic segment (amino acids 58 to 78) resulted in a Golgi localization of the the mutant protein (GFP-PfSec22Δ58-78). The confocal micrographs represent the steady-state localization of the mutant protein in live parasites (top panel), co-localization with the Golgi marker PfErd2 (middle panel) and co-staining with the ER marker PfBip (bottom panel). Scale bars, 2µm.

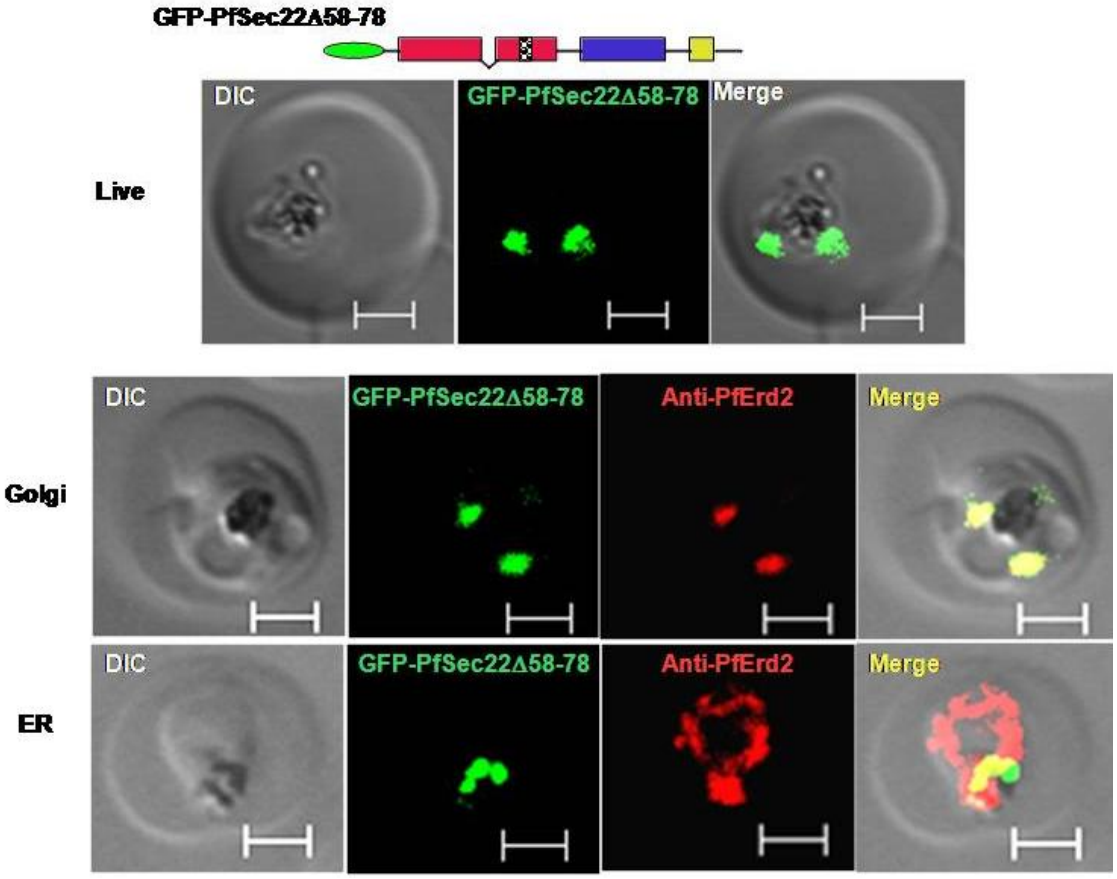

Figure 20: Retention of the N-terminal hydrophobic domain mutant in the Golgi

Figure 21: Differential fractionation of PfSec22 and PfSec22Δ58-78 mutant

Western blots showing co-fractionation of the endogenous PfSec22 protein with GFP-PfSec22 **(A and B)**, but not with the PfSec22Δ58-78 mutant **(C and D)** in identical sucrose density gradients. Parasites were lysed in the presence of 2 mM EDTA **(A and C)**, or in the presence of 5 mM $MgCl_2$ **(B and D)**, and the effect of each reagent on the buoyant density of the proteins was detected by Western blot analyses of the density fractions. Numbers represent the fraction numbers, collected from bottom (fraction 1) to top (fraction 10) of a discontinuous sucrose density gradient consisting of 1.5 ml of 47%, 1 ml of 40%, 1 ml of 35%, 0.75 ml of 25%, and 0.75 ml of 20% sucrose. GFP-PfSec22 and the untagged protein both partially redistributed to the high-density fractions (fractions 1-4) alongside PfBip in the presence of $MgCl_2$ **(B)** suggestive of PfSec22 association with the ER. Compared to the untagged wild-type protein (PfSec22), which redistributed alongside PfBip in the presence of $MgCl_2$, the GFP-PfSec22Δ58-78 mutant was consistently detected in the high-density fractions in the presence of EDTA **(C)** or $MgCl_2$ **(D)**, suugesting its association with the Golgi. A small amount of PfSec22 proteins also associated with the low-density fractions (fractions 5-7) in both the EDTA and $MgCl_2$-treated samples, suggesting an association with lipid-rich structures that presumably represent transport vesicles.

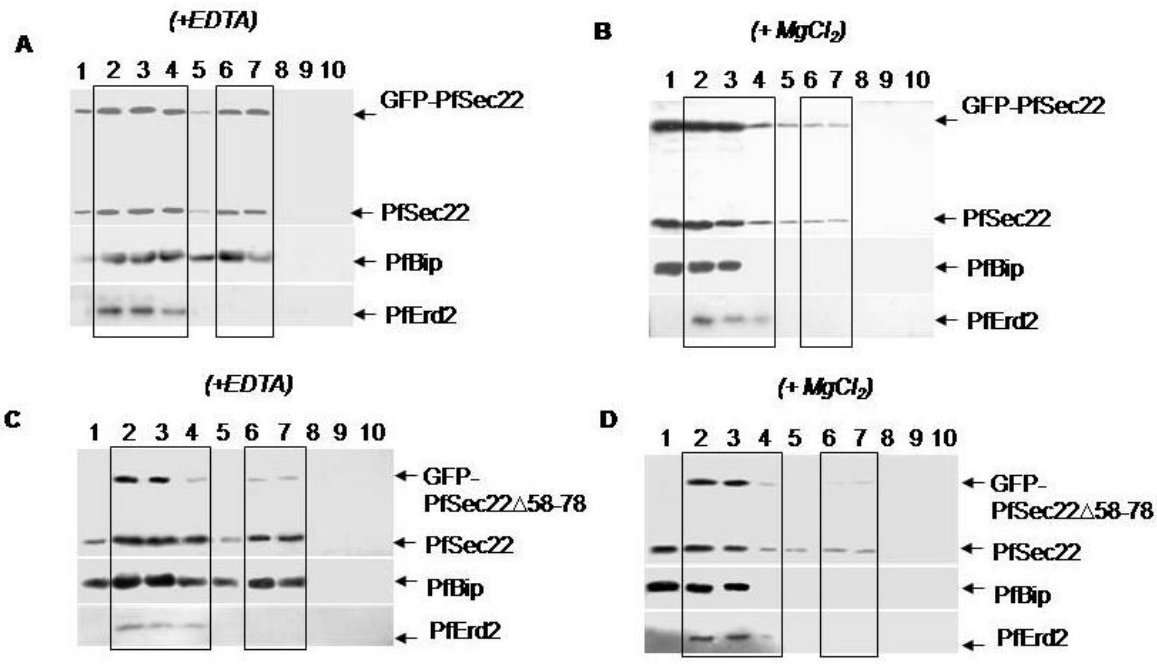

Figure 21: Differential fractionation of PfSec22 and PfSec22Δ58-78 mutant

Figure 22: Effect of BFA on Golgi localization of the PfSec22Δ58-78 deletion mutant

Treatment of the GFP-PfSec22Δ58-78 expressing parasites with brefeldin A (BFA) resulted in partial redistribution of the mutant protein to the ER (top row), similarly to the Golgi-localized PfErd2 protein (bottom row). Treatment of the parasites with the drug solvent (0.5% methanol in RPMI medium) did not inhibit GFP-PfSec22Δ58-78 transport to the Golgi (data not shown). Scale bars, 2µm.

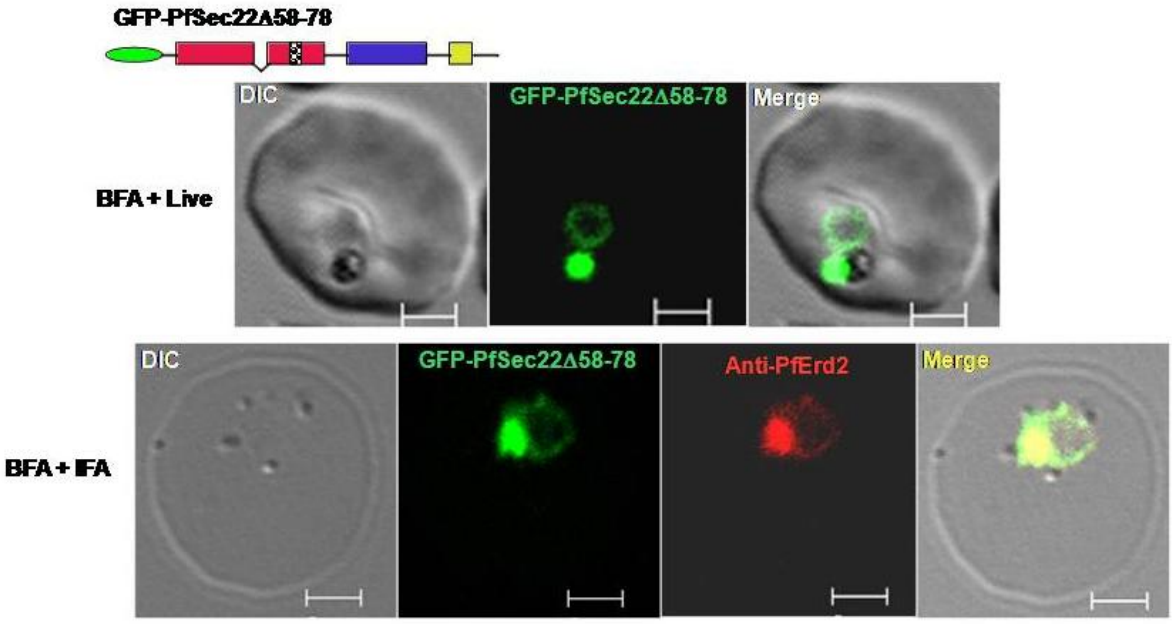

Figure 22: Effect of BFA on Golgi localization of PfSec22Δ58-78 deletion mutant

CHAPTER 4:
CHARACTERIZATION OF PFSEC22 INTERACTING PFSNARES

4.1. SUMMARY

SNARE proteins function in intracellular membrane traffic by selectively assembling into complexes that bridge vesicle and target membranes prior to fusion. In this study we identified a novel Sec22 gene product (PfSec22) that associates partially with mobile vesicular elements in *P. falciparum*-infected erythrocytes. Export of the v-SNARE in malaria parasites is unusual, suggesting a similar export of the PfSec22-interacting t-SNAREs into the infected host cell. In an effort to characterize the subunit components of the putative PfSec22 complexes, we investigated the interacting PfSNAREs by Far-Western analyses and surface Plasmon resonance spectroscopy using the purified recombinant proteins. We then generated transgenic parasites expressing the GFP-tagged PfSec22-interacting SNAREs for live cell imaging and localization analyses. Additionally, we investigated the *in vivo* binding potentials of the Q-SNAREs against the endogenously expressed PfSec22 protein by immunoprecipitation studies using anti-GFP antibodies. We found that the R-SNARE PfSec22 exhibits strong binding interactions with PfSyn5 (K_D: 0.5µM), PfBet1 (K_D: 1.6µM), PfSyn16 (K_D: 2.3µM), PfSyn18 (K_D: 3.4µM), PfSyn6 (K_D: 3.8µM) and PfGS27 (K_D: 4.1µM). Interaction of PfSec22 with the Syn16 and Syn6 gene products is atypical. Our initial attempts to develop transgenic parasites expressing the GFP-tagged PfSyn16 and PfSyn6 proteins have been unsuccessful. Meanwhile, transgene expression of PfSyn5, PfGS27 and PfBet1 revealed Golgi localization of these three Q-SNAREs, consistent with a role in ER/Golgi transport. Treatment of the transgenic parasites with the vesicle traffic inhibit Brefeldin A resulted in partial re-distribution into the ER, suggestive of

their association with the early secretory pathway. Compared to GFP only controls, immunoprecipitation of the GFP-tagged chimeras resulted in PfSec22 pull-down in cell extracts from the PfSyn5, PfBet1 and PfGS27 expressing parasites, validating the interaction of these different PfSNAREs *in vivo*. Our data indicate a conserved ER-to-Golgi SNARE complex assembly in *P. falciparum*, and suggest that PfSec22 might form novel SNARE complexes in malaria parasites.

4.2. MATERIALS AND METHODS

4.2.1. cDNA cloning and expression of recombinant proteins

cDNA encoding various PfSNAREs were obtained by reverse transcriptase PCR using the StrataScript Easy A one-tube RT-PCR system (Stratagene) and gene specific primers. For His-tagged proteins, the amplified open reading frames were cloned by ligation independent cloning (LIC) into either pET43.1EKLIC or pET50.1EKLIC vectors following the manufacturer's instructions (Novagen). GST-tagged gene constructs were generated by ligation of the amplified cDNA first into pGEMT Easy vector followed by subcloning into the *Bam* HI and *Xho* I sites of pGEX6P.1 vector. The recombinant plasmid DNAs were amplified in XL10Gold or Novablue *E. coli* cells and purified using the Qiagen Miniprep Plasmid Kit (Qiagen).

The recombinant proteins were over-produced in BL21 (DE3) CodonPlus-RIPL E. coli cells using various optimum conditions. Briefly, overnight cultures of the recombinant bacteria were subcultured in 600ml of Luria Bertani (LB) media containing 100µg/ml ampicillin, 34µg/ml chloramphenicol and 75µg/ml streptomycin at 37^{o}C to an OD_{600} between 0.4 and 0.5.

Bacteria growth was continued for an additional 1 hr either at 37^{o}C or 30^{o}C or 20^{o}C depending on pre-determined induction conditions followed by addition of isopropyl-thio-β-galactoside (IPTG) to a final concentration of 0.1mM (pGEX vectors) or 1mM for the pET vectors. The bacterial cells were harvested after 4hrs by centrifugation at 6,000rpm for 15 min at 4^{o}C and resuspended in 30 ml of lysis buffer as described below.

4.2.2. Affinity purification of fusion proteins

For the His-tagged proteins, bacteria pellets in 50 mM Sodium phosphate, pH 7.6 containing 300mM NaCl, 50U Benzonase, 0.1mg/ml lysozyme and Complete EDTA-free protease inhibitors (Roche) were lysed by French press (3 times at 1500 psi) and clarified by centrifugation at 10, 000rpm for 10 min at 4^{o}C. The supernant was added to 2ml bed volume of pre-washed Talon Super-flow resin (Novagen) and incubated with gentle mixing at 4^{o}C for 2 hrs. The unbound sample was removed by three washes at 10 minutes intervals in lysis buffer without Benzonase or lysozyme, and the resin was then transferred to a gravity flow column. The resin was again washed with 20 bed volumes of lysis buffer and eluted with a step-wise gradient of imidazole (10, 25, 50, 80, 100, 150, 250, and 500mM) in lysis buffer without the enzymes. The partially purified fractions were pooled and further purified by size exclusion chromatography on a HiLoad Superdex-75 column using 10mM HEPES, pH 7.4 plus 150mM NaCl as column buffer. One milliliter fractions were collected and the protein-containing fractions were pooled and concentrated by Vivaspin centrifugation.

GST-tagged PfSec22 proteins were purified using a Glutathione Sepharose 4B column as described in the above batch and gravity flow procedures. The bacteria pellets were lysed in 1XPBS, pH 7.6 containing 50U Benzonase, 0.1mg/ml lysozyme, 0.1% Triton X-100 and 1XHalt

protease inhibitors (Thermo Scientific), and the bound proteins were eluted with 20mM reduced glutathione in 50mM Tris-HCl, pH 8.0. Fractions containing the pure proteins were pooled and concentrated by Vivaspin centrifugation. The concentration of proteins in each sample was determined using a Bradford reagent kit (Biorad).

4.2.3. Biotinylation of recombinant PfSec22 and Far-Western analyses

Two hundred and forty micrograms of recombinant PfSec22 proteins were labeled with an 80-fold molar excess of N-hydroxysuccinimide-LC-Biotin (Pierce) for 18hrs at 4^{o}C. The biotinylated sample was then dialyzed against two buffer changes (2 litres each) of PBS, pH 7.6 for 3hrs at 4^{o}C.

For Far-Western analysis, 20µg of the recombinant Q-SNAREs were resolved by SDS-PAGE and electrophoretically transferred onto Polyvinylidene fluoride (PVDF) membrane (Millipore). After blocking in 5% skim milk in PBS, pH 7.2 containing 0.1% Tween 20 for 1 hr at room temperature, the membranes were transferred into a fresh solution containing the biotinylated PfSec22 protein at a final concentration of 5µg/ml and incubated with gentle mixing for 36hrs at 4^{o}C. The membranes were subsequently washed three times at 5 minutes each in blocking solution and incubated with avidin peroxidase conjugate (Thermo Scientific) solution at a final concentration of 2µg/ml for 2hrs at room temperature. After washing 3 times at 10 minutes intervals, the membranes were developed using the Supersignal West Femto substrate kit (Pierce).

4.2.4. Surface plasmon resonance spectroscopy

Surface Plasmon resonance (SPR) spectroscopy analyses were performed using the SensiQ SPR system and HisCap Sensor chips (ICX Technologies). The chips were sensitized by injecting 50µl of 50mM Nickel chloride at a flow-rate of 25µl/min and then purged with 500µl of air and water. To immobilize the His-tagged Q-SNAREs, 200µl of sample at 20µg/ml in 10mM HEPES, pH7.4 containing 150mM NaCl were passed over the chip at a flow-rate of 25µl/min. After washing the chips three times with 500µl of buffer, 80µl of GST-tagged PfSec22 (30µg/ml in 50mM Tris-HCL, pH 8.0) were passed at a flow-rate of 10µl/min. Binding of R-SNARE to the Q-SNARE was measured as an increase in SPR and recorded in response units (RU). Once sample injection was complete, the surface was regenerated by two 75-µl washes with 200mM EDTA, followed by three times washes with 500µl air and water. The obtained data was then analyzed using the QDAT^{TM} analysis software (Biological Software, Ltd).

4.2.5. Plasmids and transfection

To investigate the subcellular localization of the PfSec22-interacting Q-SNAREs, we generated transgenic parasites expressing the GFP-tagged proteins. Complementary DNAs corresponding to the full-length ORF of each Q-SNARE homologue was amplified by RT-PCR using gene-specific primer sets. The amplified cDNAs were cloned into the pGEM-T Easy vector (Promega) and sequence confirmed prior to subcloning into the BglII/XhoI sites of the modified pDC vector. *P. falciparum* 3D7 ring stage cultures (at 5-8% parasitemia) were transfected with Qiagen-purified plasmid DNA (100 µg) by electroporation using a Bio-Rad Gene pulser II (0.31 KV and 950 microfarads). Forty-eight hours after transfection, drug selection pressure was applied using the human DHFR inhibitor, WR99210 at a final

concentration of 2.5 nM to select for transformed parasites. Expression of GFP-tagged proteins in the transgenic parasites was analyzed by Western blotting using monoclonal GFP (B-2) antibodies (Santa Cruz Biotechnology) at a 1:500 dilution. The secondary antibodies were HRP-conjugated Goat anti-mouse used at a 1:20,000 dilution. For live cell imaging, the cells were mounted under a cover slip in 50% glycerol and observed within 15 minutes of removal from cultures by confocal microscopy. The GFP signals were captured at a spectra setting of 488/505 nm.

4.2.6. Brefeldin A treatment

To confirm the association of the GFP-tagged SNAREs with the secretory pathway, we investigated the effect of the vesicle transport inhibitor brefeldin A on their steady-state dynamics. GFP-expressing cells were cultured in the presence of BFA (5µg/ml) for one hour at 37^{o}C and examined by live confocal microscopy. Control experiments consisted of the same cultures prepared in equivalent amounts of the drug solvent.

4.2.7. Co-immunoprecipitation and immunoblot Analysis

To confirm the *in vivo* interaction of PfSec22 with the Q-SNAREs, whole cell lysates were obtained from parasites expressing the GFP-tagged PfSyn5, PfGS27 or PfBet1 proteins for co-immunoprecipitation analyses. Parasites were isolated by saponin treatment and solubilized in 1XPBS plus 2% Triton X-100, pH 7.4 containing 50U/ml Benzonase and a protease inhibitor cocktail (Roche) for 20 minutes at 4^{o}C. Cleared lysates were obtained by centrifugation at 10.000rpm for 5 minutes at 4^{o}C.

For each co-immunoprecipitation experiment, 500µg of parasite lysate were added to 2µg of monoclonal GFP (B-2) antibodies (Santa Cruz Biotechnology, Inc) and incubated with end-over-end inversion for 16hrs at 4^{o}C. Forty microlitres of protein A agarose beads (Invitrogen) were added to each sample and incubated for an additional 3hrs at 4^{o}C. The beads were washed (5 minutes inversion at 4^{o}C followed by centrifugation at 4,000rpm) three times with PBS to remove unbound proteins. The collected beads were boiled for 3 minutes in 50µl of 2XLaemnli sample buffer and 20µl resolved by SDS-PAGE. The separated proteins were blotted onto PVDF membranes and probed with either PfSec22 antibodies or rabbit anti-GFP antibodies (GenScript) at 1 in 1000 or 1 in 500 dilutions, respectively. Detection of the antigen signals was by use of the Supersignal West Femto chemiluminescence kit (Pierce).

4.3. RESULTS

4.3.1. PfSec22 exhibits direct binding interactions with six distinct PfSNAREs in vitro

Our findings that PfSec22 associates with mobile vesicular elements in the parasitized erythrocytes suggested that this PfSNARE might participate in vesicle transport and fusion within the host cell cytoplasm. If true, then malaria parasites might export a subset of the PfSec22-interacting SNAREs into the host cell required for fusogenic SNARE assemblies. The Sec22 gene products in yeast and mammals mediate vesicle fusion by interacting with the ER-to-Golgi SNARE proteins Syn5, Bet1 and GS27 (anterograde traffic) or the Golgi-to-ER SNARE proteins Syn18, Sec20 and Use1 (retrograde traffic). Binary interactions between cognate SNARE proteins are expected to nucleate the formation of fusion-competent ternary and quaternary complexes *in vivo* and *in vitro*. However, inhibitory and non-fusogenic Sec22

SNARE complexes have been reported in *in vitro* binding and fusion experiments involving the yeast Q-SNAREs Vti1, Gos1 and Sft1 [96, 262].

To identify and to characterize all PfSec22 interacting PfSNAREs, first we examined the binding capability of 12 recombinant PfSNAREs (non-R-SNAREs) with PfSec22 *in vitro*. Full-length PfSNAREs were expressed using the *E. coli* BL21 (DE3)codonplus strain as either His-tagged proteins (PfSec22 and the non-R-SNAREs) or GST-tagged proteins (PfSec22 only), and then purified by a combination of gel filtration and affinity (metal or glutathione) chromatography. As shown in Fig 23A (SDS-PAGE) and Fig. 23B (far-Western blot), PfSec22 specifically interacted with PfBet1, PfGS27, PfSyn5, PfSyn16, and PfSyn18 when compared to the BSA signal (background control). No positive signals were detected in the lanes containing PfSNAP23, PfSyn2, PfSyn3, PfSyn6, PfSyn11 and PfSyn17, suggesting that these PfSNAREs do not form binary complexes with PfSec22 *in vitro*. Alternatively, binding of PfSec22 to these PfSNAREs might require the presence of both SNARE proteins in solution.

As an alternative approach to identify the PfSec22-interacting PfSNAREs, we investigated the binding capability of the His-tagged PfSNAREs by SPR spectroscopy using a GST-tagged PfSec22 protein as analyte. Consistent with our far-western data, PfSec22 formed stable binary complexes with PfBet1, PfGS27, PfSyn5, PfSyn16, PfSyn18, and also with PfSyn6 (Fig. 24). These results are summarized in Table 3 alongside the far-Western data. The direct binding of PfSec22 to PfSyn6 and PfSyn16 is atypical, as these two Q-SNAREs are expected on the basis of the functional locations of the yeast and mammalian homologues to function within the post-Golgi environment. Compared to PfSyn16, and to the classical PfSec22-interacting Q-SNAREs, PfBet1, PfSyn5, PfGS27 and PfSyn18, the PfSyn6 protein did not interact with PfSec22 when immobilized on a solid phase prior to addition of the R-SNARE. Presumably, this

might occur as a result of an irreversible destabilization of the PfSyn6 SNARE helix following denaturation with sample buffer during gel electrophoresis. Additionally, PfSyn6 contains a positively charged and bulky histidine residue in place of glutamine at the zero layer position, which might interfere with binding of this protein to the R-SNARE PfSec22 under solid phase conditions.

4.3.2. Localization of PfBet1, PfSyn5 and PfGS27 to the ER/Golgi interface

To establish whether the PfSec22-interacting PfSNAREs also associate with noncanonical destinations within *P. falciparum*-infected erythrocytes, we generated transgenic parasites expressing the GFP-tagged proteins. In this present study, GFP-expressing parasites were successfully obtained following transfection with PfBet1, PfSyn5 and PfGS27 plasmids but not with the PfSyn6 and PfSyn16 constructs. Our failure to obtain transgenic parasites with the PfSyn6 and PfSyn16 constructs might have resulted from toxicity of the over-expressed proteins during during drug selection. It would be necessary to use the respective endogenous promoter elements for a controlled expression of these PfSNAREs in transgenic parasites. Alternatively, the localization of these PfSNAREs may be achieved by immunofluorescence studies requiring highly specific antibodies.

Compared to the GFP-tagged PfSec22 protein (Fig. 27A), which localizes predominantly to both the ER and Golgi compartments, the Q-SNARE chimeras PfSyn5, PfBet1 and PfGS27 each localized to the parasite Golgi at steady-state (Fig. 27B, C and D, respectively). The association of these PfSNAREs with the Golgi membranes was confirmed by brefeldin A (BFA)-treatment. BFA is a fungal metabolite that inhibits vesicular transport along the ER/Golgi pathway resulting in the redistribution of Golgi-membrane proteins back into the ER and

accumulation of exported malaria proteins at the ER/Golgi interface [263, 264]. As shown in Fig. 27 (see second row of each panel), treatment with BFA resulted in partial redistribution of the PfSNAREs back to the ER, and induction of a perinuclear compartment (red arrowheads) that also accumulated the PfSNAREs. These compartments presumably represent a chimeric structure formed by fusion of the enlarged Golgi with the parasite transitional ER.

The observed effect of BFA on the Golgi-targeting of these PfSNAREs is suggestive of their intracellular trafficking via the parasite ER compartment. We confirmed the Golgi localization of PfSyn5, PfBet1 and PfGS27 by immunofluorescence analyses using specific antibodies against the Golgi marker PfErd2 and ER marker (PfBip). As shown in Fig. 28, the GFP fluorescence in all three cell lines significantly overlapped the PfErd2 signals when compared to their co-localization with PfBip (Fig. 28A, B and C). In contrast, the GFP-PfSec22 fluorescence overlapped significantly with the antibody signals from both the Golgi and ER marker (Fig. 28D). The localization of PfSyn5, PfSyn5, PfBet1 and PfSec22 to the ER/Golgi interface is consistent with the intracellular locations of their human and yeast homologues. The restricted steady-state localization of PfSyn5, PfBet1 and PfGS27 to the Golgi compartment is indicative of a potential role as the t-SNARE component involved in anterograde ER-to-Golgi vesicle transport in *P. falciparum*. Consistent with our EM studies, PfSec22 localizes to both ER and Golgi presumably acting as the corresponding v-SNARE. Together, our data suggest a conserved ER-to-*cis*-Golgi transport process in the malaria parasite, *P. falciparum*.

4.3.3. PfSec22 forms SNARE complexes with PfBet1, PfGS27and PfSyn5 in vivo

To confirm the *in vivo* binding of PfSec22 to the Golgi-localized Q-SNAREs PfBet1, PfGS27 and PfSyn5, we immunoprecipitated the fusion proteins from each transgenic cell line

using monoclonal anti-GFP antibodies. The experimental controls consisted of cell lysates from the double GFP (GFP-GFP)-expressing parasites (negative control) and the GFP-PfSec22-expressing cells (positive control). The immunoprecipitates were then analyzed by Western blotting using PfSec22 anti-peptide antibodies, or polyclonal anti-GFP antibodies. As shown in Fig. 29, immunoprecipitation of the GFP-tagged PfBet1, PfGS27 and PfSyn5 proteins resulted in co-precipitation of endogenous PfSec22. No PfSec22 signal was detected in the negative control precipitate, indicating that binding of PfSec22 to the GFP chimeras was specific to the Q-SNARE protein. Immunoprecipitation of the GFP-tagged PfSec22 chimera also resulted in precipitation of a relatively small amount of the endogenous PfSec22 protein. Presumably, this finding is suggestive of a homo-polymerization of the PfSec22 protein *in vivo* or indicative of the co-assembly of both protein species into the same SNARE complexes.

Taken together, our data strongly suggest that PfSec22, PfSyn5, PfBet1 and PfGS27 assemble into a SNARE complex presumably involved in ER-to-Golgi trafficking in malaria parasites.

4.4. DISCUSSIONS

In this study, we undertook a comprehensive examination of direct pair-wise interactions between recombinant PfSNAREs in the hopes of identifying all PfSec22 complexes that might nucleate the higher order SNARE complexes *in vivo*. Compared to *in vitro* findings with some yeast and mammalian SNARE proteins showing promiscuity of some SNARE-SNARE interactions [262, 265, 266], we observed a significantly high level of selectivity of the PfSec22 interactions *in vitro*. This vesicle-associated R-SNARE (PfSec22) selectively formed binary

SNARE complexes with PfSyn5 (Qa), PfSyn18 (Qa), PfBet1 (Qb), PfSyn6 (Qb), PfGS27 (Qc), and PfSyn16 (Qc), but not with PfSyn2, PfSyn3, PfSyn11, PfSyn17 and PfVti1 as determined by surface plasmon resonance spectroscopy and far-western analyses. In yeast, Sec22 assembles into fusogenic SNARE complexes with Sed5 (Syn5), Bet1, Bos1 (GS27), Sec20, Syn18 and Use1, and also form atypical binding interactions with Ykt6, Gos1, and Sft1 [262]. Whereas homologues of the yeast SNAREs Sec20, Use1, Gos1 and Sft1 were not detected in the *P. falciparum* genome database, previous studies by us failed to detect any binary interactions between PfSec22 and PfYkt6.1 suggesting a stringent selective binding interaction between PfSec22 and the PfSNAREs. Meanwhile, although PfSec22 did not directly interact with six of the twelve PfSNAREs *in vitro*, we cannot rule out the possibility that some of these PfSNAREs may participate in a higher order ternary or quaternary SNARE complex requiring a preformed binary complex between PfSec22 and some of the complex components. In mammals, for example, binding of the Golgi-to-ER recycling SNARE proteins Use1 (p31) and Sec20 (BNIP1) to Sec22b requires a pre-formed complex between Sec22b and Syn18, suggesting a sequential-ordered mechanism for some fusogenic SNARE protein assemblies [267]. Studies are yet to be undertaken to investigate the possibility of ordered SNARE assemblies in *P. falciparum*.

In an effort to confirm the PfSec22 complexes *in vivo*, and to determine the subcellular locations of the interacting partners, we generated transfection plasmids for each cognate SNARE gene that were used to express the GFP-tagged chimeras in transgenic parasites. In this study, we successfully developed transgenic parasites expressing the PfSyn5, PfBet1 and PfGS27 gene products, but not the PfSyn6 and PfSyn16 proteins. Because the transcription patterns of PfSyn5, PfBet1 and PfGS27 were similar to that of the *camoldulin* gene product in *P. falciparum*, we expressed these constructs under control of the *camoldulin* promoter element.

Compared to the GFP-PfSec22 cell lines, which emerged in culture after 3 weeks of continuous drug pressure, transgene expression of the PfSyn5, PfGS27, and PfBet1 chimeras appeared to delay the parasite growth in culture. The selection periods for these cell lines were ~8 weeks for PfSyn5 and PfGS27, and ~6 weeks for PfBet1. Failure to obtain GFP expressing cell lines with the PfSyn6 and PfSyn16 constructs presumably could be attributable to inability of malaria parasites to tolerate multiple copies of these genes during development or, alternatively, due to a miss-timing of the gene expression levels using the heterologous *P. falciparum camoldulin* promoter element. The endogenous gene transcription patterns for these two PfSNAREs are not yet known.

Consistent with the intracellular locations of the yeast and mammalian homologues [81], the PfSyn5, PfBet1 and PfGS27 gene products each localized to the parasite Golgi at steady-state as determined by co-immunofluorescence and live confocal microscopy studies. Unlike the PfSec22 proteins, which partially localized to the infected erythrocyte cytoplasm at trophozoite stages, the *in vitro* binding partners PfSyn5, PfBet1 and PfGS27 were not exported beyond the Golgi structure in all stages, suggesting that the partial export of PfSec22 into the host cell might involve processes that are both selective and highly regulated during parasite development. As revealed by our immunoprecipitation experiments, these three PfSNAREs presumably participate in SNARE complex formation with the vesicle-associated PfSec22 protein *in vivo*. Together, the data presented in this study strongly suggest a conserved SNARE-mediated ER-to-Golgi vesicle transport mechanism in *P. falciparum*. However, only PfSec22 localized significantly to both the ER and Golgi suggesting that, in *P. falciparum* parasites, PfSec22 presumably functions as the v-SNARE in both the anterograde and retrograde transport pathways.

Additionally, our data suggest that PfSec22 might form novel SNARE complexes required for a potential role in vesicle traffic and fusion within the erythrocyte cytoplasm. According to the SNARE hypothesis, each fusogenic SNARE complex comprises at least one representative of the SNARE sub-families R, Qa, Qb, and Qc, resulting in a quaternary QabcR SNARE complex. The PfSec22-interacting SNAREs that we identified presumably can form a maximum of eight distinct quaternary complexes on the basis of the "1R:3Q" rule. These possibilities include (1) PfSec22/PfSyn5/PfBet1/PfGS27, (2) PfSec22/PfSyn5/PfBet1/PfSyn16, (3) PfSec22/PfSyn5/PfSyn6/PfGS27, (4) PfSec22/PfSyn5/PfSyn6/PfSyn16, (5) PfSec22/PfSyn18/PfBet1/PfGS27, (6) PfSec22/PfSyn18/PfBet1/PfSyn16, (7) PfSec22/PfSyn18/PfSyn6/PfGS27, and (8) PfSec22/PfSyn18/PfSyn6/PfSyn16. As the SNARE proteins PfSyn5, PfBet1 and PfGS27 are less likely to participate in transport beyond the ER/Golgi interface, it would be of interest to characterize the steady-state locations of PfSyn6, PfSyn16 and PfSyn18, and to confirm or rule out the existence of the PfSec22/PfSyn18/PfSyn6/PfSyn16 SNARE complex *in vivo*.

Figure 23: Far-Western analysis of PfSec22-interacting PfSNAREs

(A) SDS-PAGE gel of purified recombinant PfSNARE proteins stained with Coomassie Brilliant blue. The PfSNAREs were expressed as His_6/NusA/S.taggged proteins and purified by a combination of metal affinity and gel permeation chromatography. 20µg of proteins were analyzed for each sample. MK: prestained molecular weight standards, BSA (5µg): bovine serum albumin used as background control in far-Western experiments, B-PfSec22 (5µg): biotin-conjugated PfSec22 proteins used as positive control in far-Western. Two major breakdown products are present in the PfSyn3, PfSyn11 and PfSyn18 lanes. **(B)** 20µg of each SNARE sample was subjected to SDS-PAGE using a 10% resolving gel and transferred to PVDF membranes. The membranes were then incubated with 5µg/ml of biotinylated PfSec22 protein and the labeled bands were identified by blotting with an avidin-peroxidase conjugate.

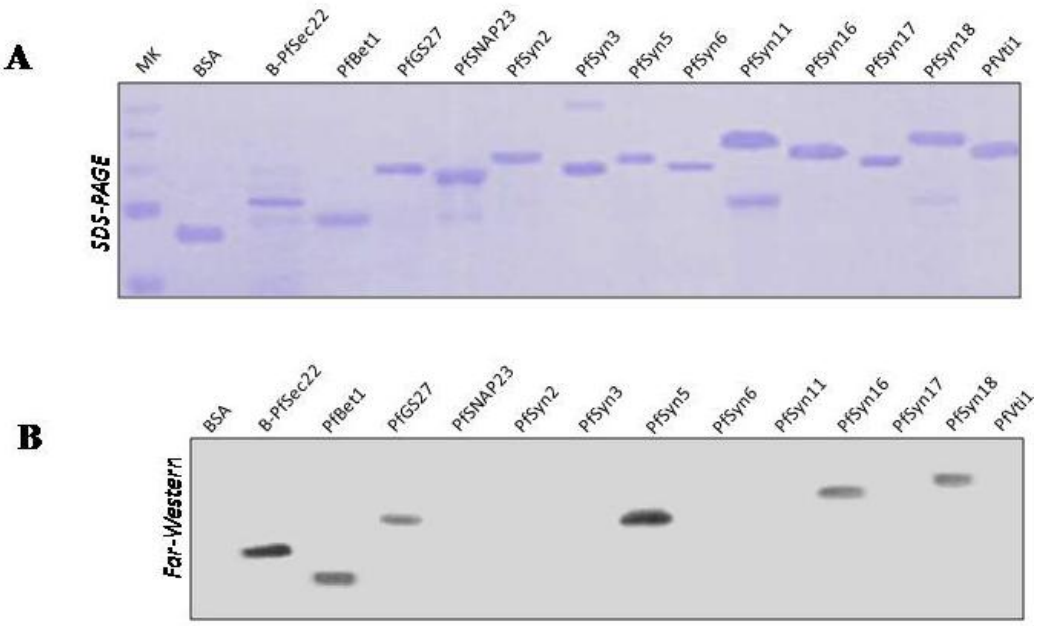

Figure 23: Far-Western analyses of PfSec22 interacting PfSNAREs

Figure 24: SPR analyses of PfSec22-interactions with purified PfSNAREs

Individual His_6-tagged PfSNARE were immobilized onto a nickel charged Hiscap chip and their binding with the GST-tagged PfSec22 was measured as time course (in seconds) increase in SPR response units. Strong binding of the PfSec22 protein to each of the PfSNARE was determined by its resistance to elution with the run buffer (50 mM Tris-HCL, pH 8.0). The arrows denote the start of each wash with the run buffer. Dissociation constants (K_D) were calculated using the QDAT^{TM} analysis software.

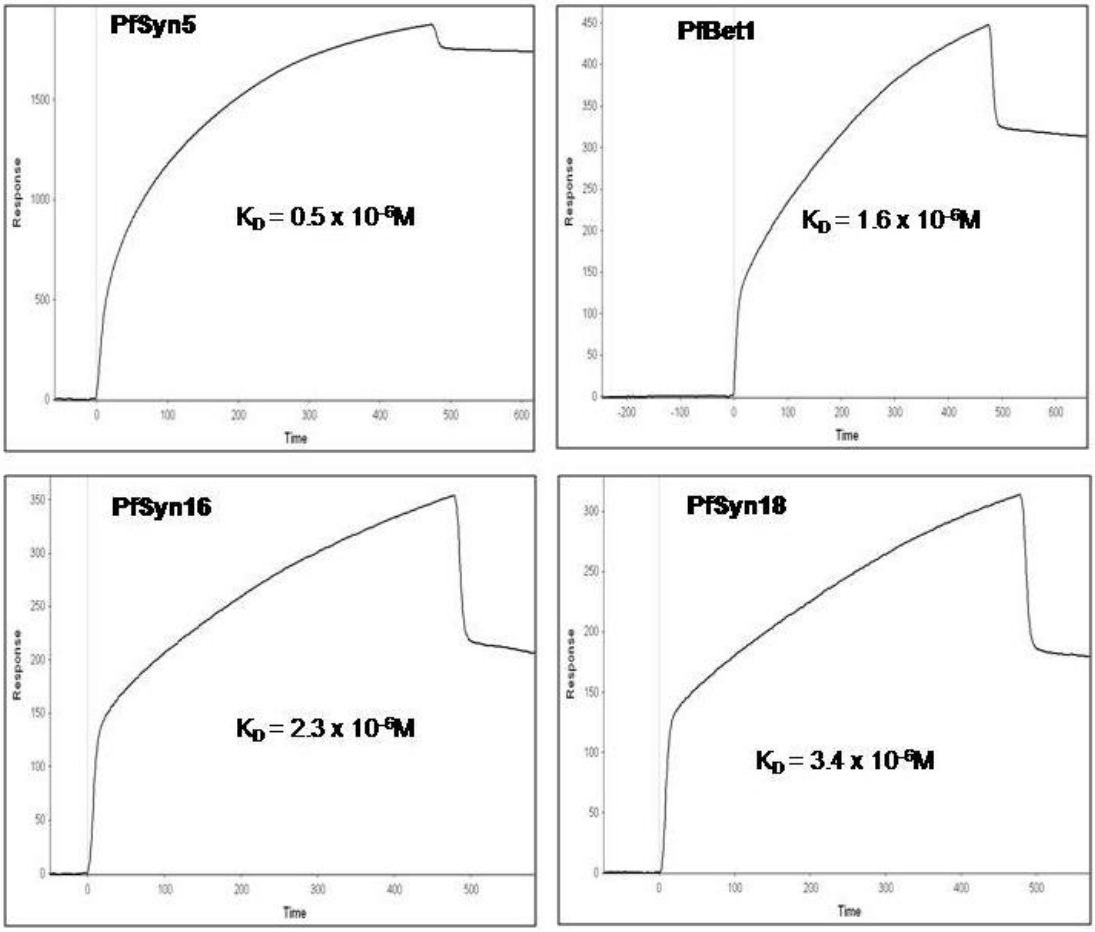

Figure 24: SPR analysis of PfSec22 binding to PfSyn5, PfBet1, PfSyn16 and PfSyn18

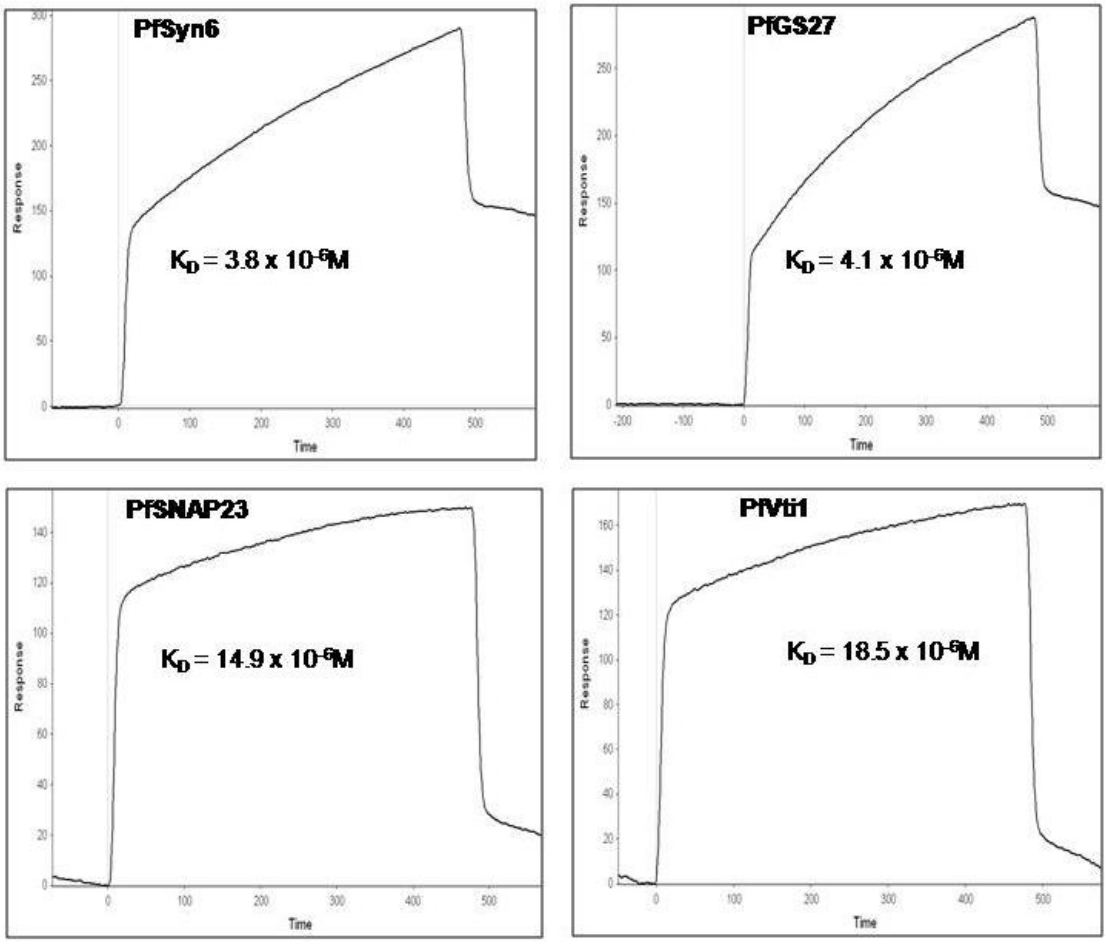

Figure 25: SPR analysis of PfSec22 binding to PfSyn6, PfGS27, PfSNAP23 and PfVti1

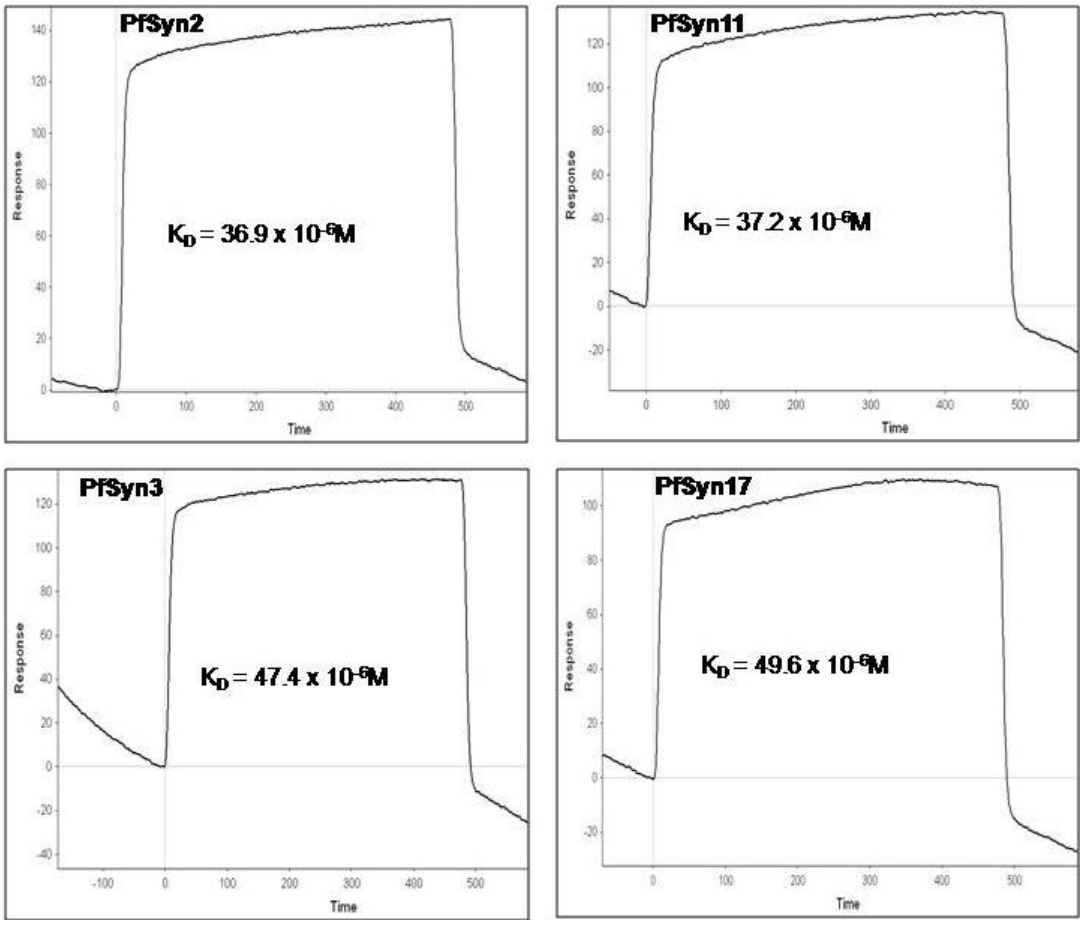

Figure 26: SPR analysis of PfSec22 binding to PfSyn2, PfSyn11, PfSyn3 and PfSyn17

Table 2: *In vitro* binding interactions involving PfSec22 R-SNARE

PfSNARE	Zero layer residue	Mammalian Orthologue	Far-Western	SPR	K_D (μM)
PfBet1	Q	IC, *cis*-Golgi	+	+	1.6
PfGS27	Q	IC, *cis*-Golgi	+	+	4.1
PfSNAP23	Q	PM	-	-	14.9
PfSyn2	Q	PM	-	-	36.9
PfSyn3	I	PM	-	-	47.4
PfSyn5	Q	Golgi	+	+	0.5
PfSyn6	H	TGN, endo	-	+	3.8
PfSyn11	R	TGN, late endo	-	-	37.2
PfSyn16	Q	TGN	+	+	2.3
PfSyn17	N	ER	-	-	49.6
PfSyn18	Q	ER	+	+	3.4
PfVti1a	Q	*trans*-Golgi	-	-	18.5

Figure 27: Steady-state location and effect of BFA on PfSyn5, PfBet1 and PfGS27 proteins

Transgenic parasites expressing each of the indicated GFP-tagged PfSNARE were incubated under normal culture conditions in the absence or presence of brefeldin A (5µg/ml) for 1hr, and examined by live confocal microscopy. Compared to the GFP-PfSec22 protein, which localizes predominantly to both the ER and Golgi structures, the Q-SNAREs PfSyn5, PfBet1 and PfGS27 localized exclusively to the Golgi bodies at steady state. BFA treatment resulted in a partial redistribution of each of the four proteins to the ER suggesting their association with the early endomembrane system. Arrows indicate BFA-induced bodies that presumably results from fusion of the dissociating Golgi bodies with the ER. Scale bars, 2µm.

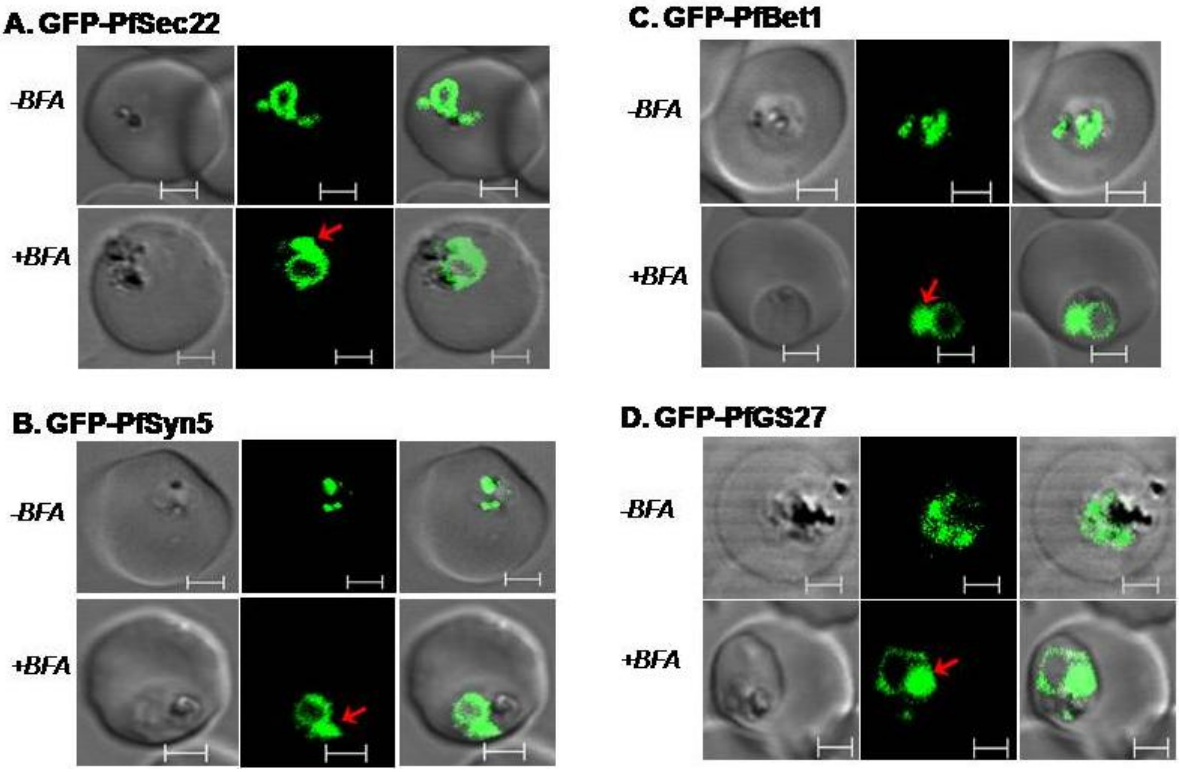

Figure 27: Steady-state location and effect of BFA on PfSyn5, PfBet1 and PfGS27 targeting

Figure 28: Differential localization of PfSyn5, PfBet1, PfGS27 and PfSec22 to ER and Golgi

Immunoflorescence micrographs highlighting a tight association of the GFP-tagged PfPfSyn5 (A), PfBet1 (B) and PfGS27 (C) proteins with Golgi, as determined by co-staining with antibodies against PfErd2. In contrast, the GFP-PfSec22 protein (D) co-localized significantly with both the PfErd2 and PfBip proteins at the Golgi and ER compartments, respectively. The GFP-PfSec22 signal is also apparent within the infected host cell cytoplasm in trophozoite parasites. Scale bars, 2µm.

A. GFP-PfSyn5

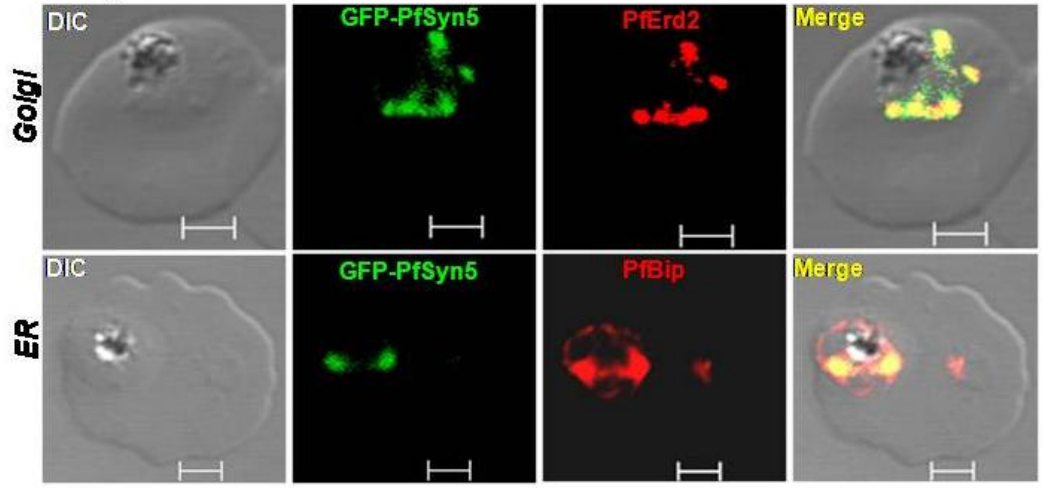

B. GFP-PfBet1

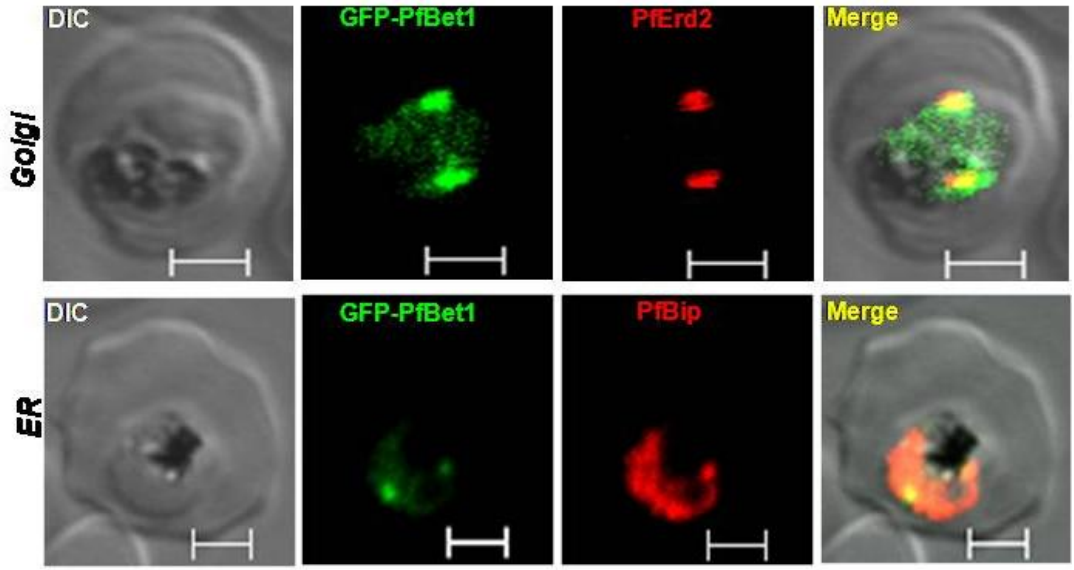

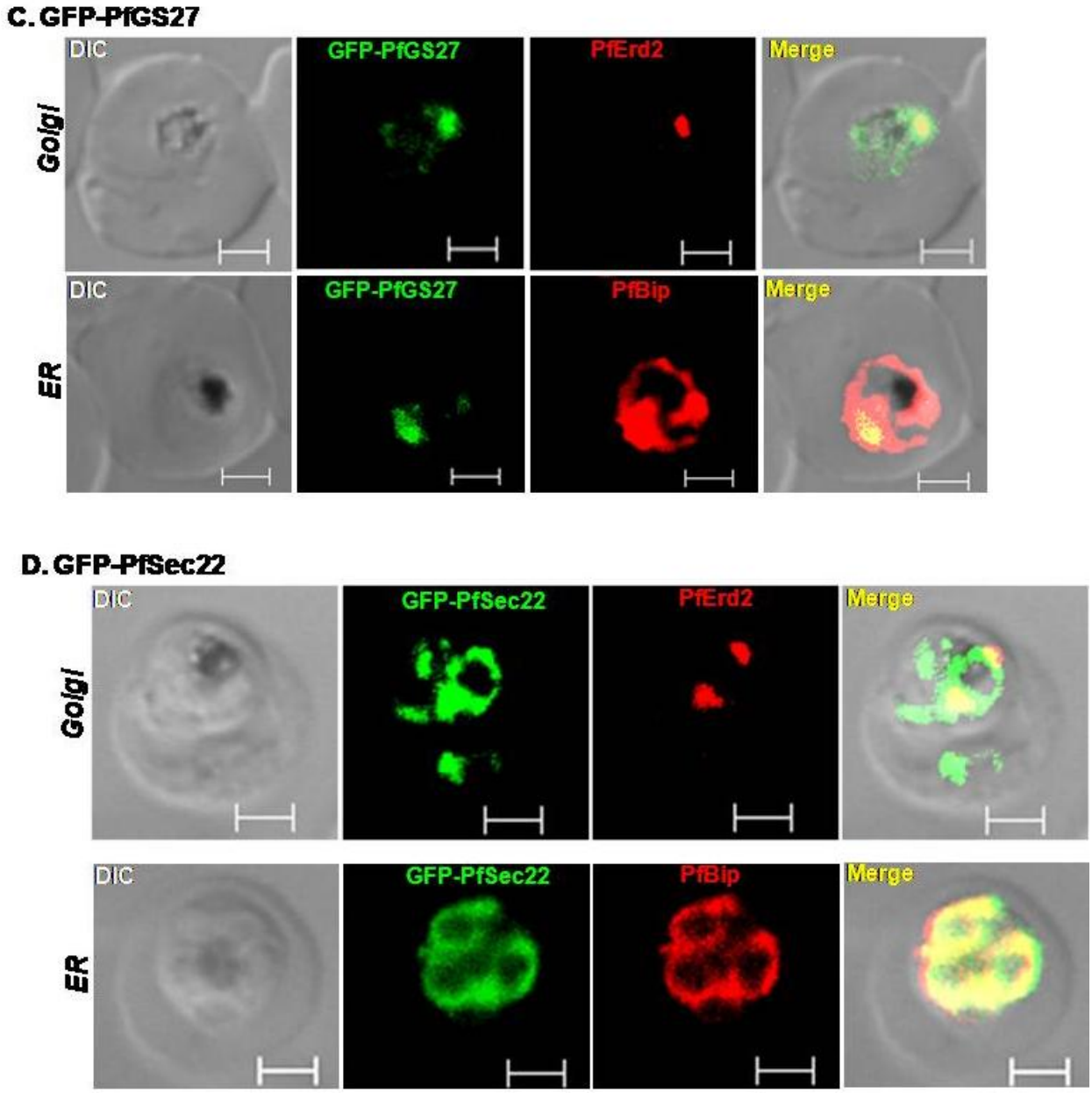

Figure 28: Differential localization of PfSec22, PfSyn5, PfBet1 and PfGS27 to ER and Golgi

Figure 29: Interaction of PfSec22 with PfBet1, PfGS27 and PfSyn5 in vivo

The GFP-tagged PfBet1, PfGS27 and PfSyn5 proteins were immunoprecipitated from each cell lysate using monoclonal anti-GFP antibodies and then immunoblotted by using polyclonal anti-PfSec22 or anti-GFP antibodies, as indicated to the left of each blot.

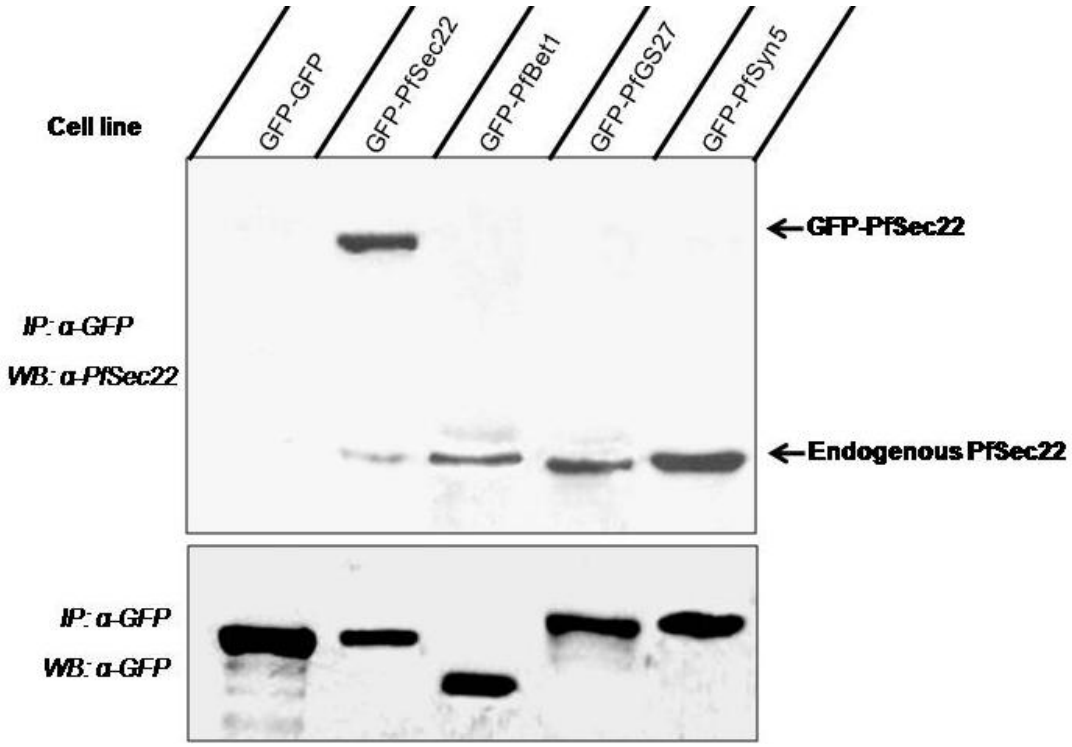

Figure 29: Interaction of PfSec22 with PfBet1, PfGS27 and PfSyn5 *in vivo*

CHAPTER 5
GENERAL DISCUSSIONS AND CONCLUSIONS

The aim of this dissertation was to investigate the potential role of SNARE proteins in vesicle traffic in *P. falciparum*, with focus on the molecular characterization of atypical PfSNAREs. We identified 18 SNARE domain-containing gene products in *P. falciparum* that presumably represent a subset of all PfSNAREs. By comparative analysis with homologues in yeast, plants and humans, we identified species-specific features in 10 of the PfSNAREs. These atypical features include the 1) presence of putative *P. falciparum*-specific export motifs, 2) presence of atypical amino acid residues at the zero layer position, and 3) frequent occurrence of low-complexity regions within the polypeptide chains. We showed that the *Sec22* gene product in *P. falciparum* (PfSec22) exhibits unusual structural characteristics and associates with a novel transport pathway involved with vesicle targeting in *P. falciparum*-infected host cells. PfSec22 also associates significantly with the parasite ER and Golgi compartments suggesting that this SNARE protein might function in multiple membrane trafficking pathways in *P. falciparum*. We determined that the atypical N-terminal hydrophobic domain performs a dual role, mediating the Golgi-to-ER recycling of PfSec22 and export of the v-SNARE to the infected host cell.

Although PfSec22 forms direct binding interactions with known Sec22 cognate SNARE proteins *in vitro* and *in vivo*, the interacting PfSNAREs that we investigated localized exclusively to the parasite ER/Golgi interface. We propose that PfSec22 might participate in a novel fusogenic SNARE complex required for vesicle targeting in *P. falciparum*-infected erythrocytes. A summation of our findings is discussed below in the context of their relevance and significance to our understanding of the molecular cell biology of malaria parasites.

5.1. THE P. FALCIPARUM SNAREOME

P. falciparum exhibits an unusual endomembrane system that is characterized by multiple membrane trafficking pathways and unique intracellular organelles. Our data suggest that vesicle targeting through the parasite endomembrane organelles might depend on the participation of only 18 SNARE core motif-containing proteins. Remarkably, several isoforms of mammalian syntaxins and VAMP family members were absent in the *P. falciparum* genome. This finding may be explained by the evolutionary distance of the human malaria parasite relative to higher eukaryotes, in which recent genome duplication events might have resulted in increase in the number of SNARE isoforms [268]. Although the number of SNARE-encoding genes that we identified in *P. falciparum* is consistent with the SNAREomes of other closely related unicellular eukaryotes including *Giardia* (17 SNAREs), *Leshmania major* (27 SNAREs) and *Entamoeba histolytica* (31 SNAREs), the PfSNAREome is unexpectedly small in relation to the number of possible vesicle transport pathways in this intracellular parasite [236, 269-271]. The *Saccharomyces cerevisiae* genome encodes 24 SNARE proteins, the human 36 SNAREs, and *Arabidopsis thaliana* 54 SNAREs [81, 124, 241]. The small number of PfSNAREs may be explained in part by limitations in the existing genome-based algorithms, and by the divergent nature of the putative PfSNARE motifs when compared with the query SNARE sequences. We believe that *P. falciparum* presumably expresses species-specific proteins with SNARE-like activities in order to compensate for the multiplicity of trafficking pathways in this organism. Such parasite-specific proteins presumably could be identified through *in vivo* binding experiments or via genetic manipulation of the parasite genome. Alternatively, members of the identified PfSNARE family might form novel fusogenic SNARE complexes at multiple intracellular locations. This is true for some yeast and mammalian SNARE proteins which form

distinct SNARE complexes at different intracellular trafficking pathways. In mammals, for example, syntaxin 5(Syn5) participates in three distinct complexes required for 1) homotypic fusion of ER-derived vesicles (Syn5/GS27/Bet1/Sec22b) into vesicular tubular clusters (VTC), also known as ER-Golgi transport container (EGTC) or ER-Golgi intermediate compartment (ERGIC), 2) fusion of VTC with cis-Golgi (Syn5/GS28/Bet1/Ykt6), and intra-Golgi traffic (Syn5/GS28/GS15/Ykt6) [81].

5.2. PARTIAL EXPORT OF PFSEC22 INTO P. FALCIPARUM-INFECTED ERYTHROCYTES

We showed for the first time that *P. falciparum* parasites partially export the *P. falciparum* Sec22 protein (PfSec22) into the host cell cytoplasm where it associates with TVN-like structures and with mobile vesicular elements in trophozoite-infected cells. The PfSec22-associated vesicles were also detected within the parasitophorous vacuole suggesting that export of this SNARE protein might occur via a two-step model that involves vesicle budding at the parasite plasma membrane (negative curvature) and fusion with the TVN/PVM membranes.

The exported PfSec22 protein was observed only in trophozoite-infected cells, suggesting that the involved processes might be subject to regulation by yet unidentified factors. Regulated export of proteins into *P. falciparum*-infected erythrocytes has previously been reported [272, 273]. The Golgi-resident protein sphingomyelin synthase, for example, localizes partially to subdomains of the PPM/PVM junction in trophozoite-infected cells that presumably serve as budding sites for nascent TVN and transport vesicles [272]. This regulated export of sphingomyelin synthase might induce local changes in TVN membrane lipid compositions resulting in membrane deformation and budding. For example, the dynamic and asymmetrical distribution of various phospholipids (outer leaflet) and sphingomyelin (inner leaflet) on nascent

TVN subdomains has been proposed to modulate growth of the TVN structure into the infected erythrocyte cytoplasm and extraparasitic vesicle budding, independent of coat formation [48, 272]. It is likely that the developmental export of sphingomyelin synthase, coupled with local changes in the PVM/TVN membranes might regulate vesicle formation and export of various membrane-associated proteins across the PV interface into the erythrocyte cytoplasm [274].

The export of PfSec22 into the infected host cell appeared to be specific when compared to other PfSNAREs that have been investigated in this study. This suggests that the export mechanism might involve a signal-mediated process. Signal-mediated export of most malaria involves the *Plasmodium*-specific export motif (PEXEL motif), which is thought to interact with a putative translocon complex at the PV/PVM interface [15, 62, 275, 276]. However, a subset of the *Plasmodium* exported proteins does not contain the PEXEL motif, thus may utilize other putative signals and mechanisms for traffic across the PVM. We showed in this study that export of PfSec22 was independent of the PEXEL-like motif using targeted gene mutations, supported by the lack of N-terminal processing of the GFP-tagged protein as has been reported for many PEXEL-dependent malaria proteins [243]. By generating various N-terminus deletion mutant proteins, we demonstrated that export of PfSec22 into the host cells requires an intact longin domain sequence for both ER export and Golgi exit of the protein. It is not yet understood whether further transport of this PfSNARE across the PPM and PVM compartments requires additional sorting signals. Future studies will examine the role of sequence regions upstream the N-terminal hydrophobic domain in export across the PV membranes. We have also shown in this study that the N-terminal hydrophobic domain also plays a critical role in ER recycling of the v-SNARE, thus in retrograde transport of Golgi-derived vesicles back into the ER. Our finding is the first to implicate the longin domain in ER/Golgi recycling of Sec22 gene products. Further

studies will determine whether or not similar sequence regions in other eukarotic Sec22 protein perform similar functions.

5.3. ORGANIZATION OF THE P. FALCIPARUM ER-GOLGI INTERFACE

Although *P. falciparum* parasites are believed to contain a functional ER-Golgi transport system, the organization of this important trafficking route in malaria parasites is poorly understood. We revealed in this study that PfSec22 is a vesicle-associated protein, which predominantly cycles between the ER and Golgi structures following a brefeldin A-dependent process. In an effort to characterize the steady-state locations of all PfSec22-interacting PfSNAREs, we found that the ER-to-Golgi SNARE orthologues PfSyn5, PfBet1 and PfGS27 also localized to the ER-Golgi interface in *P. falciparum*. Unlike the PfSec22 protein, these SNARE proteins were not exported to the erythrocyte cytoplasm suggesting a selective sorting process for the exported PfSec22 protein. Within the parasite, the PfSyn5, PfBet1 and PfGS27 proteins localized exclusively to the Golgi structure, and formed direct *in vivo* binding interactions with the PfSec22 protein. Our data suggest a conserved SNARE complex assembly involving the v-SNARE PfSec22, and the t-SNAREs PfSyn5, PfBet1 and PfGS27 that presumably mediate ER-to-Golgi vesicle trafficking in *P. falciparum*. BFA-treatment resulted in the redistribution of all four PfSNAREs to the ER compartment supporting their direct association with the early secretory system. The data also suggest the existence of various sorting machineries at the ER-Golgi interface that might be involved in ER-to-Golgi sorting or Golgi-to-ER recycling of the malaria proteins. This argument is supported by our studies with the PfSec22 longin domain mutants, which differentially localized to either the Golgi bodies or to the ER compartment. In most model system, protein sorting at the ER membrane is mediated by the coat

protein complex Sec23/Sec24, which together with the Sec13/Sec31 dimer and Sar1-GTPase play a crucial role in vesicle budding from the ER [114]. Homologues of these coat proteins have been identified in *P. falciparum* and their intracellular locations determined. Whereas PfSec24 exclusively localizes to the *Plasmodium* ER exit sites, PfSar1, PfSec23 and PfSec31 localize partially to the infected host erythrocyte cytoplasm [231, 277-279]. Our findings with PfSec22 are in agreement with export of some ER-to-Golgi trafficking machineries, including the SNARE complex disassembly factor PfNSF, into *P. falciparum* infected host cells [248].

In conclusion, the data presented in this dissertation provide the first detailed study of SNARE protein expression, sorting and complex assembly in malaria parasites. Our data also provide the first experimental evidence for SNARE protein export to the novel vesicle transport pathways in *P. falciparum*-infected erythrocytes. This present study sets the stage for the characterization of other PfSNAREs and, perhaps, the identification of new drug targets against malaria parasites.

REFERENCES

1 Perkins, S. L. and Austin, C. (2008) Four New Species of Plasmodium from New Guinea Lizards: Integrating Morphology and Molecules. J Parasitol, 1

2 Rogerson, S. J., Mwapasa, V. and Meshnick, S. R. (2007) Malaria in pregnancy: linking immunity and pathogenesis to prevention. Am J Trop Med Hyg. **77**, 14-22

3 Hartl, D. L. (2004) The origin of malaria: mixed messages from genetic diversity. Nat Rev Microbiol. **2**, 15-22

4 Lopez, A. D., Mathers, C. D., Ezzati, M., Jamison, D. T. and Murray, C. J. (2006) Global and regional burden of disease and risk factors, 2001: systematic analysis of population health data. Lancet. **367**, 1747-1757

5 Snow, R. W., Guerra, C. A., Noor, A. M., Myint, H. Y. and Hay, S. I. (2005) The global distribution of clinical episodes of Plasmodium falciparum malaria. Nature. **434**, 214-217

6 Snow, R. W., Guerra, C. A., Mutheu, J. J. and Hay, S. I. (2008) International funding for malaria control in relation to populations at risk of stable Plasmodium falciparum transmission. PLoS Med. **5**, e142

7 Thwing, J., Skarbinski, J., Newman, R. D., Barber, A. M., Mali, S., Roberts, J. M., Slutsker, L. and Arguin, P. M. (2007) Malaria surveillance - United States, 2005. MMWR Surveill Summ. **56**, 23-40

8 Breman, J. G., Alilio, M. S. and Mills, A. (2004) Conquering the intolerable burden of malaria: what's new, what's needed: a summary. Am J Trop Med Hyg. **71**, 1-15

9 Holding, P. A. and Snow, R. W. (2001) Impact of Plasmodium falciparum malaria on performance and learning: review of the evidence. Am J Trop Med Hyg. **64**, 68-75

10 Chima, R. I., Goodman, C. A. and Mills, A. (2003) The economic impact of malaria in Africa: a critical review of the evidence. Health Policy. **63**, 17-36

11 Deressa, W., Hailemariam, D. and Ali, A. (2007) Economic costs of epidemic malaria to households in rural Ethiopia. Trop Med Int Health. **12**, 1148-1156

12 Greenwood, B. M., Fidock, D. A., Kyle, D. E., Kappe, S. H., Alonso, P. L., Collins, F. H. and Duffy, P. E. (2008) Malaria: progress, perils, and prospects for eradication. J Clin Invest. **118**, 1266-1276

13 Sturm, A., Amino, R., van de Sand, C., Regen, T., Retzlaff, S., Rennenberg, A., Krueger, A., Pollok, J. M., Menard, R. and Heussler, V. T. (2006) Manipulation of host hepatocytes by the malaria parasite for delivery into liver sinusoids. Science. **313**, 1287-1290

14 Maier, A. G., Cooke, B. M., Cowman, A. F. and Tilley, L. (2009) Malaria parasite proteins that remodel the host erythrocyte. Nat Rev Microbiol. **7**, 341-354

15 Marti, M., Baum, J., Rug, M., Tilley, L. and Cowman, A. F. (2005) Signal-mediated export of proteins from the malaria parasite to the host erythrocyte. J Cell Biol. **171**, 587-592

16 Ben Mamoun, C., Gluzman, I. Y., Hott, C., MacMillan, S. K., Amarakone, A. S., Anderson, D. L., Carlton, J. M., Dame, J. B., Chakrabarti, D., Martin, R. K., Brownstein, B. H. and Goldberg, D. E. (2001) Co-ordinated programme of gene expression during asexual intraerythrocytic development of the human malaria parasite Plasmodium falciparum revealed by microarray analysis. Mol Microbiol. **39**, 26-36

17 Bannister, L. H., Hopkins, J. M., Margos, G., Dluzewski, A. R. and Mitchell, G. H. (2004) Three-dimensional ultrastructure of the ring stage of Plasmodium falciparum: evidence for export pathways. Microsc Microanal. **10**, 551-562

18 Bannister, L. H., Hopkins, J. M., Fowler, R. E., Krishna, S. and Mitchell, G. H. (2000) A brief illustrated guide to the ultrastructure of Plasmodium falciparum asexual blood stages. Parasitol Today. **16**, 427-433

19 Garcia, C. R., de Azevedo, M. F., Wunderlich, G., Budu, A., Young, J. A. and Bannister, L. (2008) Plasmodium in the postgenomic era: new insights into the molecular cell biology of malaria parasites. Int Rev Cell Mol Biol. **266**, 85-156

20 Beier, J. C. (1998) Malaria parasite development in mosquitoes. Annu Rev Entomol. **43**, 519-543

21 Waller, R. F., Keeling, P. J., van Dooren, G. G. and McFadden, G. I. (2003) Comment on "A green algal apicoplast ancestor". Science. **301**, 49; author reply 49

22 Roos, D. S., Crawford, M. J., Donald, R. G., Fraunholz, M., Harb, O. S., He, C. Y., Kissinger, J. C., Shaw, M. K. and Striepen, B. (2002) Mining the Plasmodium genome database to define organellar function: what does the apicoplast do? Philos Trans R Soc Lond B Biol Sci. **357**, 35-46

23 Kohler, S., Delwiche, C. F., Denny, P. W., Tilney, L. G., Webster, P., Wilson, R. J., Palmer, J. D. and Roos, D. S. (1997) A plastid of probable green algal origin in Apicomplexan parasites. Science. **275**, 1485-1489

24 Blackman, M. J. and Bannister, L. H. (2001) Apical organelles of Apicomplexa: biology and isolation by subcellular fractionation. Mol Biochem Parasitol. **117**, 11-25

25 Dluzewski, A. R., Mitchell, G. H., Fryer, P. R., Griffiths, S., Wilson, R. J. and Gratzer, W. B. (1992) Origins of the parasitophorous vacuole membrane of the malaria parasite, Plasmodium falciparum, in human red blood cells. J Cell Sci. **102 (Pt 3)**, 527-532

26 Langreth, S. G., Jensen, J. B., Reese, R. T. and Trager, W. (1978) Fine structure of human malaria in vitro. J Protozool. **25**, 443-452

27 Atkinson, C. T. and Aikawa, M. (1990) Ultrastructure of malaria-infected erythrocytes. Blood Cells. **16**, 351-368

28 Bannister, L. H., Hopkins, J. M., Fowler, R. E., Krishna, S. and Mitchell, G. H. (2000) Ultrastructure of rhoptry development in Plasmodium falciparum erythrocytic schizonts. Parasitology. **121 (Pt 3)**, 273-287

29 Hopkins, J., Fowler, R., Krishna, S., Wilson, I., Mitchell, G. and Bannister, L. (1999) The plastid in Plasmodium falciparum asexual blood stages: a three-dimensional ultrastructural analysis. Protist. **150**, 283-295

30 Slomianny, C. and Prensier, G. (1990) A cytochemical ultrastructural study of the lysosomal system of different species of malaria parasites. J Protozool. **37**, 465-470

31 Taraschi, T. F., Trelka, D., Schneider, T. and Matthews, I. (1998) Plasmodium falciparum: characterization of organelle migration during merozoite morphogenesis in asexual malaria infections. Exp Parasitol. **88**, 184-193

32 Jaikaria, N. S., Rozario, C., Ridley, R. G. and Perkins, M. E. (1993) Biogenesis of rhoptry organelles in Plasmodium falciparum. Mol Biochem Parasitol. **57**, 269-279

33 Sim, B. K., Carter, J. M., Deal, C. D., Holland, C., Haynes, J. D. and Gross, M. (1994) Plasmodium falciparum: further characterization of a functionally active region of the merozoite invasion ligand EBA-175. Exp Parasitol. **78**, 259-268

34 Duraisingh, M. T., Triglia, T., Ralph, S. A., Rayner, J. C., Barnwell, J. W., McFadden, G. I. and Cowman, A. F. (2003) Phenotypic variation of Plasmodium falciparum merozoite

proteins directs receptor targeting for invasion of human erythrocytes. EMBO J. **22**, 1047-1057

35 Maier, A. G., Duraisingh, M. T., Reeder, J. C., Patel, S. S., Kazura, J. W., Zimmerman, P. A. and Cowman, A. F. (2003) Plasmodium falciparum erythrocyte invasion through glycophorin C and selection for Gerbich negativity in human populations. Nat Med. **9**, 87-92

36 Baum, J., Richard, D., Healer, J., Rug, M., Krnajski, Z., Gilberger, T. W., Green, J. L., Holder, A. A. and Cowman, A. F. (2006) A conserved molecular motor drives cell invasion and gliding motility across malaria life cycle stages and other apicomplexan parasites. J Biol Chem. **281**, 5197-5208

37 Kyes, S., Horrocks, P. and Newbold, C. (2001) Antigenic variation at the infected red cell surface in malaria. Annu Rev Microbiol. **55**, 673-707

38 Deitsch, K. W. and Wellems, T. E. (1996) Membrane modifications in erythrocytes parasitized by Plasmodium falciparum. Mol Biochem Parasitol. **76**, 1-10

39 Haldar, K., Samuel, B. U., Mohandas, N., Harrison, T. and Hiller, N. L. (2001) Transport mechanisms in Plasmodium-infected erythrocytes: lipid rafts and a tubovesicular network. Int J Parasitol. **31**, 1393-1401

40 Haldar, K. and Mohandas, N. (2007) Erythrocyte remodeling by malaria parasites. Curr Opin Hematol. **14**, 203-209

41 Aikawa, M., Uni, Y., Andrutis, A. T. and Howard, R. J. (1986) Membrane-associated electron-dense material of the asexual stages of Plasmodium falciparum: evidence for movement from the intracellular parasite to the erythrocyte membrane. Am J Trop Med Hyg. **35**, 30-36

42 Atkinson, C. T., Aikawa, M., Rock, E. P., Marsh, K., Andrysiak, P. M., Campbell, G. H., Collins, W. E. and Howard, R. J. (1987) Ultrastructure of the erythrocytic stages of Plasmodium malariae. J Protozool. **34**, 267-274

43 Tilley, L., Sougrat, R., Lithgow, T. and Hanssen, E. (2008) The twists and turns of Maurer's cleft trafficking in P. falciparum-infected erythrocytes. Traffic. **9**, 187-197

44 Hanssen, E., Sougrat, R., Frankland, S., Deed, S., Klonis, N., Lippincott-Schwartz, J. and Tilley, L. (2008) Electron tomography of the Maurer's cleft organelles of Plasmodium falciparum-infected erythrocytes reveals novel structural features. Mol Microbiol. **67**, 703-718

45 Kriek, N., Tilley, L., Horrocks, P., Pinches, R., Elford, B. C., Ferguson, D. J., Lingelbach, K. and Newbold, C. I. (2003) Characterization of the pathway for transport of the cytoadherence-mediating protein, PfEMP1, to the host cell surface in malaria parasite-infected erythrocytes. Mol Microbiol. **50**, 1215-1227

46 Wickham, M. E., Rug, M., Ralph, S. A., Klonis, N., McFadden, G. I., Tilley, L. and Cowman, A. F. (2001) Trafficking and assembly of the cytoadherence complex in Plasmodium falciparum-infected human erythrocytes. EMBO J. **20**, 5636-5649

47 Bhattacharjee, S., van Ooij, C., Balu, B., Adams, J. H. and Haldar, K. (2008) Maurer's clefts of Plasmodium falciparum are secretory organelles that concentrate virulence protein reporters for delivery to the host erythrocyte. Blood. **111**, 2418-2426

48 Gormley, J. A., Howard, R. J. and Taraschi, T. F. (1992) Trafficking of malarial proteins to the host cell cytoplasm and erythrocyte surface membrane involves multiple pathways. J Cell Biol. **119**, 1481-1495

49 Garcia, C. R., Takeuschi, M., Yoshioka, K. and Miyamoto, H. (1997) Imaging Plasmodium falciparum-infected ghost and parasite by atomic force microscopy. J Struct Biol. **119**, 92-98

50 Taraschi, T. F., O'Donnell, M., Martinez, S., Schneider, T., Trelka, D., Fowler, V. M., Tilley, L. and Moriyama, Y. (2003) Generation of an erythrocyte vesicle transport system by Plasmodium falciparum malaria parasites. Blood. **102**, 3420-3426

51 Taraschi, T. F., Trelka, D., Martinez, S., Schneider, T. and O'Donnell, M. E. (2001) Vesicle-mediated trafficking of parasite proteins to the host cell cytosol and erythrocyte surface membrane in Plasmodium falciparum infected erythrocytes. Int J Parasitol. **31**, 1381-1391

52 Hibbs, A. R. and Saul, A. J. (1994) Plasmodium falciparum: highly mobile small vesicles in the malaria-infected red blood cell cytoplasm. Exp Parasitol. **79**, 260-269

53 Kilejian, A. (1979) Characterization of a protein correlated with the production of knob-like protrusions on membranes of erythrocytes infected with Plasmodium falciparum. Proc Natl Acad Sci U S A. **76**, 4650-4653

54 Miller, L. H., Hudson-Taylor, D., Gamain, B. and Saul, A. J. (2002) Definition of the minimal domain of CIDR1alpha of Plasmodium falciparum PfEMP1 for binding CD36. Mol Biochem Parasitol. **120**, 321-323

55 Duffy, P. E. and Fried, M. (2003) Plasmodium falciparum adhesion in the placenta. Curr Opin Microbiol. **6**, 371-376

56 Chasis, J. A. and Schrier, S. L. (1989) Membrane deformability and the capacity for shape change in the erythrocyte. Blood. **74**, 2562-2568

57 Gronowicz, G., Swift, H. and Steck, T. L. (1984) Maturation of the reticulocyte in vitro. J Cell Sci. **71**, 177-197

58 Geminard, C., de Gassart, A. and Vidal, M. (2002) Reticulocyte maturation: mitoptosis and exosome release. Biocell. **26**, 205-215

59 Baruch, D. I., Rogerson, S. J. and Cooke, B. M. (2002) Asexual blood stages of malaria antigens: cytoadherence. Chem Immunol. **80**, 144-162

60 Glenister, F. K., Fernandez, K. M., Kats, L. M., Hanssen, E., Mohandas, N., Coppel, R. L. and Cooke, B. M. (2009) Functional alteration of red blood cells by a megadalton protein of Plasmodium falciparum. Blood. **113**, 919-928

61 Haldar, K., Mohandas, N., Samuel, B. U., Harrison, T., Hiller, N. L., Akompong, T. and Cheresh, P. (2002) Protein and lipid trafficking induced in erythrocytes infected by malaria parasites. Cell Microbiol. **4**, 383-395

62 Cooke, B. M., Lingelbach, K., Bannister, L. H. and Tilley, L. (2004) Protein trafficking in Plasmodium falciparum-infected red blood cells. Trends Parasitol. **20**, 581-589

63 Charpian, S. and Przyborski, J. M. (2008) Protein transport across the parasitophorous vacuole of Plasmodium falciparum: into the great wide open. Traffic. **9**, 157-165

64 Przyborski, J. M. and Lanzer, M. (2005) Protein transport and trafficking in Plasmodium falciparum-infected erythrocytes. Parasitology. **130**, 373-388

65 Trelka, D. P., Schneider, T. G., Reeder, J. C. and Taraschi, T. F. (2000) Evidence for vesicle-mediated trafficking of parasite proteins to the host cell cytosol and erythrocyte surface membrane in Plasmodium falciparum infected erythrocytes. Mol Biochem Parasitol. **106**, 131-145

66 Elmendorf, H. G. and Haldar, K. (1993) Identification and localization of ERD2 in the malaria parasite Plasmodium falciparum: separation from sites of sphingomyelin synthesis and implications for organization of the Golgi. Embo J. **12**, 4763-4773

67 de Castro, F. A., Ward, G. E., Jambou, R., Attal, G., Mayau, V., Jaureguiberry, G., Braun-Breton, C., Chakrabarti, D. and Langsley, G. (1996) Identification of a family of Rab G-proteins in Plasmodium falciparum and a detailed characterisation of pfrab6. Mol Biochem Parasitol. **80**, 77-88

68 Van Wye, J., Ghori, N., Webster, P., Mitschler, R. R., Elmendorf, H. G. and Haldar, K. (1996) Identification and localization of rab6, separation of rab6 from ERD2 and implications for an 'unstacked' Golgi, in Plasmodium falciparum. Mol Biochem Parasitol. **83**, 107-120

69 Pouvelle, B., Gormley, J. A. and Taraschi, T. F. (1994) Characterization of trafficking pathways and membrane genesis in malaria-infected erythrocytes. Mol Biochem Parasitol. **66**, 83-96

70 Elliott, D. A., McIntosh, M. T., Hosgood, H. D., 3rd, Chen, S., Zhang, G., Baevova, P. and Joiner, K. A. (2008) Four distinct pathways of hemoglobin uptake in the malaria parasite Plasmodium falciparum. Proc Natl Acad Sci U S A. **105**, 2463-2468

71 Pouvelle, B., Spiegel, R., Hsiao, L., Howard, R. J., Morris, R. L., Thomas, A. P. and Taraschi, T. F. (1991) Direct access to serum macromolecules by intraerythrocytic malaria parasites. Nature. **353**, 73-75

72 Haldar, K. (1994) Ducts, channels and transporters in Plasmodium-infected erythrocytes. Parasitol Today. **10**, 393-395

73 van Ooij, C., Tamez, P., Bhattacharjee, S., Hiller, N. L., Harrison, T., Liolios, K., Kooij, T., Ramesar, J., Balu, B., Adams, J., Waters, A. P., Janse, C. J. and Haldar, K. (2008) The malaria secretome: from algorithms to essential function in blood stage infection. PLoS Pathog. **4**, e1000084

74 Jenkins, D., Seelow, D., Jehee, F. S., Perlyn, C. A., Alonso, L. G., Bueno, D. F., Donnai, D., Josifova, D., Mathijssen, I. M., Morton, J. E., Orstavik, K. H., Sweeney, E., Wall, S. A., Marsh, J. L., Nurnberg, P., Passos-Bueno, M. R. and Wilkie, A. O. (2007) RAB23 mutations in Carpenter syndrome imply an unexpected role for hedgehog signaling in cranial-suture development and obesity. Am J Hum Genet. **80**, 1162-1170

75 Kins, S., Lauther, N., Szodorai, A. and Beyreuther, K. (2006) Subcellular trafficking of the amyloid precursor protein gene family and its pathogenic role in Alzheimer's disease. Neurodegener Dis. **3**, 218-226

76 Schonthaler, H. B., Fleisch, V. C., Biehlmaier, O., Makhankov, Y., Rinner, O., Bahadori, R., Geisler, R., Schwarz, H., Neuhauss, S. C. and Dahm, R. (2008) The zebrafish mutant lbk/vam6 resembles human multisystemic disorders caused by aberrant trafficking of endosomal vesicles. Development. **135**, 387-399

77 Fromme, J. C., Ravazzola, M., Hamamoto, S., Al-Balwi, M., Eyaid, W., Boyadjiev, S. A., Cosson, P., Schekman, R. and Orci, L. (2007) The genetic basis of a craniofacial disease provides insight into COPII coat assembly. Dev Cell. **13**, 623-634

78 Smith, R., Klein, P., Koc-Schmitz, Y., Waldvogel, H. J., Faull, R. L., Brundin, P., Plomann, M. and Li, J. Y. (2007) Loss of SNAP-25 and rabphilin 3a in sensory-motor cortex in Huntington's disease. J Neurochem. **103**, 115-123

79 Bonifacino, J. S. and Glick, B. S. (2004) The mechanisms of vesicle budding and fusion. Cell. **116**, 153-166

80 Spang, A. (2008) The life cycle of a transport vesicle. Cell Mol Life Sci. **65**, 2781-2789

81 Hong, W. (2005) SNAREs and traffic. Biochim Biophys Acta. **1744**, 120-144

82 McNew, J. A. (2008) Regulation of SNARE-mediated membrane fusion during exocytosis. Chem Rev. **108**, 1669-1686

83 Brunger, A. T. (2005) Structure and function of SNARE and SNARE-interacting proteins. Q Rev Biophys. **38**, 1-47

84 Jahn, R. and Scheller, R. H. (2006) SNAREs--engines for membrane fusion. Nat Rev Mol Cell Biol. **7**, 631-643

85 Pfeffer, S. R. (2007) Unsolved mysteries in membrane traffic. Annu Rev Biochem. **76**, 629-645

86 Glick, B. S. and Rothman, J. E. (1987) Possible role for fatty acyl-coenzyme A in intracellular protein transport. Nature. **326**, 309-312

87 Malhotra, V., Orci, L., Glick, B. S., Block, M. R. and Rothman, J. E. (1988) Role of an N-ethylmaleimide-sensitive transport component in promoting fusion of transport vesicles with cisternae of the Golgi stack. Cell. **54**, 221-227

88 Eakle, K. A., Bernstein, M. and Emr, S. D. (1988) Characterization of a component of the yeast secretion machinery: identification of the SEC18 gene product. Mol Cell Biol. **8**, 4098-4109

89 Beckers, C. J. and Balch, W. E. (1989) Calcium and GTP: essential components in vesicular trafficking between the endoplasmic reticulum and Golgi apparatus. J Cell Biol. **108**, 1245-1256

90 Diaz, R., Mayorga, L. S., Weidman, P. J., Rothman, J. E. and Stahl, P. D. (1989) Vesicle fusion following receptor-mediated endocytosis requires a protein active in Golgi transport. Nature. **339**, 398-400

91 Clary, D. O., Griff, I. C. and Rothman, J. E. (1990) SNAPs, a family of NSF attachment proteins involved in intracellular membrane fusion in animals and yeast. Cell. **61**, 709-721

92 Sollner, T., Whiteheart, S. W., Brunner, M., Erdjument-Bromage, H., Geromanos, S., Tempst, P. and Rothman, J. E. (1993) SNAP receptors implicated in vesicle targeting and fusion. Nature. **362**, 318-324

93 Weber, T., Zemelman, B. V., McNew, J. A., Westermann, B., Gmachl, M., Parlati, F., Sollner, T. H. and Rothman, J. E. (1998) SNAREpins: minimal machinery for membrane fusion. Cell. **92**, 759-772

94 Hu, C., Ahmed, M., Melia, T. J., Sollner, T. H., Mayer, T. and Rothman, J. E. (2003) Fusion of cells by flipped SNAREs. Science. **300**, 1745-1749

95 Paumet, F., Rahimian, V. and Rothman, J. E. (2004) The specificity of SNARE-dependent fusion is encoded in the SNARE motif. Proc Natl Acad Sci U S A. **101**, 3376-3380

96 Varlamov, O., Volchuk, A., Rahimian, V., Doege, C. A., Paumet, F., Eng, W. S., Arango, N., Parlati, F., Ravazzola, M., Orci, L., Sollner, T. H. and Rothman, J. E. (2004) i-SNAREs: inhibitory SNAREs that fine-tune the specificity of membrane fusion. J Cell Biol. **164**, 79-88

97 Jahn, R. and Sudhof, T. C. (1999) Membrane fusion and exocytosis. Annu Rev Biochem. **68**, 863-911

98 Hess, D. T., Slater, T. M., Wilson, M. C. and Skene, J. H. (1992) The 25 kDa synaptosomal-associated protein SNAP-25 is the major methionine-rich polypeptide in

rapid axonal transport and a major substrate for palmitoylation in adult CNS. J Neurosci. **12**, 4634-4641

99 Veit, M. (2000) Palmitoylation of the 25-kDa synaptosomal protein (SNAP-25) in vitro occurs in the absence of an enzyme, but is stimulated by binding to syntaxin. Biochem J. **345 Pt 1**, 145-151

100 Veit, M., Becher, A. and Ahnert-Hilger, G. (2000) Synaptobrevin 2 is palmitoylated in synaptic vesicles prepared from adult, but not from embryonic brain. Mol Cell Neurosci. **15**, 408-416

101 Weimbs, T., Low, S. H., Chapin, S. J., Mostov, K. E., Bucher, P. and Hofmann, K. (1997) A conserved domain is present in different families of vesicular fusion proteins: a new superfamily. Proc Natl Acad Sci U S A. **94**, 3046-3051

102 Rossi, V., Picco, R., Vacca, M., D'Esposito, M., D'Urso, M., Galli, T. and Filippini, F. (2004) VAMP subfamilies identified by specific R-SNARE motifs. Biol Cell. **96**, 251-256

103 Lu, J., Garcia, J., Dulubova, I., Sudhof, T. C. and Rizo, J. (2002) Solution structure of the Vam7p PX domain. Biochemistry. **41**, 5956-5962

104 Fasshauer, D., Sutton, R. B., Brunger, A. T. and Jahn, R. (1998) Conserved structural features of the synaptic fusion complex: SNARE proteins reclassified as Q- and R-SNAREs. Proc Natl Acad Sci U S A. **95**, 15781-15786

105 Katz, L. and Brennwald, P. (2000) Testing the 3Q:1R "rule": mutational analysis of the ionic "zero" layer in the yeast exocytic SNARE complex reveals no requirement for arginine. Mol Biol Cell. **11**, 3849-3858

106 Graf, C. T., Riedel, D., Schmitt, H. D. and Jahn, R. (2005) Identification of functionally interacting SNAREs by using complementary substitutions in the conserved '0' layer. Mol Biol Cell. **16**, 2263-2274

107 Ossig, R., Schmitt, H. D., de Groot, B., Riedel, D., Keranen, S., Ronne, H., Grubmuller, H. and Jahn, R. (2000) Exocytosis requires asymmetry in the central layer of the SNARE complex. EMBO J. **19**, 6000-6010

108 Liu, T., Tucker, W. C., Bhalla, A., Chapman, E. R. and Weisshaar, J. C. (2005) SNARE-driven, 25-millisecond vesicle fusion in vitro. Biophys J. **89**, 2458-2472

109 Woodbury, D. J. and Rognlien, K. (2000) The t-SNARE syntaxin is sufficient for spontaneous fusion of synaptic vesicles to planar membranes. Cell Biol Int. **24**, 809-818

110 Bowen, M. E., Weninger, K., Brunger, A. T. and Chu, S. (2004) Single molecule observation of liposome-bilayer fusion thermally induced by soluble N-ethyl maleimide sensitive-factor attachment protein receptors (SNAREs). Biophys J. **87**, 3569-3584

111 Fasshauer, D., Bruns, D., Shen, B., Jahn, R. and Brunger, A. T. (1997) A structural change occurs upon binding of syntaxin to SNAP-25. J Biol Chem. **272**, 4582-4590

112 Fasshauer, D., Otto, H., Eliason, W. K., Jahn, R. and Brunger, A. T. (1997) Structural changes are associated with soluble N-ethylmaleimide-sensitive fusion protein attachment protein receptor complex formation. J Biol Chem. **272**, 28036-28041

113 Fiebig, K. M., Rice, L. M., Pollock, E. and Brunger, A. T. (1999) Folding intermediates of SNARE complex assembly. Nat Struct Biol. **6**, 117-123

114 Lee, M. C., Miller, E. A., Goldberg, J., Orci, L. and Schekman, R. (2004) Bi-Directional Protein Transport Between the ER and Golgi. Annu Rev Cell Dev Biol

115 Mayer, A. (2001) What drives membrane fusion in eukaryotes? Trends Biochem Sci. **26**, 717-723

116 Pelham, H. R. (2001) SNAREs and the specificity of membrane fusion. Trends Cell Biol. **11**, 99-101

117 Leabu, M. (2006) Membrane fusion in cells: molecular machinery and mechanisms. J Cell Mol Med. **10**, 423-427

118 McNew, J. A., Parlati, F., Fukuda, R., Johnston, R. J., Paz, K., Paumet, F., Sollner, T. H. and Rothman, J. E. (2000) Compartmental specificity of cellular membrane fusion encoded in SNARE proteins. Nature. **407**, 153-159

119 Xue, M. and Zhang, B. (2002) Do SNARE proteins confer specificity for vesicle fusion? Proc Natl Acad Sci U S A. **99**, 13359-13361

120 Fasshauer, D., Eliason, W. K., Brunger, A. T. and Jahn, R. (1998) Identification of a minimal core of the synaptic SNARE complex sufficient for reversible assembly and disassembly. Biochemistry. **37**, 10354-10362

121 Parlati, F., McNew, J. A., Fukuda, R., Miller, R., Sollner, T. H. and Rothman, J. E. (2000) Topological restriction of SNARE-dependent membrane fusion. Nature. **407**, 194-198

122 Sutton, R. B., Fasshauer, D., Jahn, R. and Brunger, A. T. (1998) Crystal structure of a SNARE complex involved in synaptic exocytosis at 2.4 A resolution. Nature. **395**, 347-353

123 Weimbs, T., Mostov, K., Low, S. H. and Hofmann, K. (1998) A model for structural similarity between different SNARE complexes based on sequence relationships. Trends Cell Biol. **8**, 260-262

124 Burri, L. and Lithgow, T. (2004) A complete set of SNAREs in yeast. Traffic. **5**, 45-52

125 Sanderfoot, A. A., Assaad, F. F. and Raikhel, N. V. (2000) The Arabidopsis genome. An abundance of soluble N-ethylmaleimide-sensitive factor adaptor protein receptors. Plant Physiol. **124**, 1558-1569

126 Burri, L., Varlamov, O., Doege, C. A., Hofmann, K., Beilharz, T., Rothman, J. E., Sollner, T. H. and Lithgow, T. (2003) A SNARE required for retrograde transport to the endoplasmic reticulum. Proc Natl Acad Sci U S A. **100**, 9873-9877

127 Borgese, N., Colombo, S. and Pedrazzini, E. (2003) The tale of tail-anchored proteins: coming from the cytosol and looking for a membrane. J Cell Biol. **161**, 1013-1019

128 Abell, B. M., Pool, M. R., Schlenker, O., Sinning, I. and High, S. (2004) Signal recognition particle mediates post-translational targeting in eukaryotes. EMBO J. **23**, 2755-2764

129 High, S. and Abell, B. M. (2004) Tail-anchored protein biosynthesis at the endoplasmic reticulum: the same but different. Biochem Soc Trans. **32**, 659-662

130 Steel, G. J., Brownsword, J. and Stirling, C. J. (2002) Tail-anchored protein insertion into yeast ER requires a novel posttranslational mechanism which is independent of the SEC machinery. Biochemistry. **41**, 11914-11920

131 Stefanovic, S. and Hegde, R. S. (2007) Identification of a targeting factor for posttranslational membrane protein insertion into the ER. Cell. **128**, 1147-1159

132 Wattenberg, B. and Lithgow, T. (2001) Targeting of C-terminal (tail)-anchored proteins: understanding how cytoplasmic activities are anchored to intracellular membranes. Traffic. **2**, 66-71

133 Abell, B. M., Rabu, C., Leznicki, P., Young, J. C. and High, S. (2007) Post-translational integration of tail-anchored proteins is facilitated by defined molecular chaperones. J Cell Sci. **120**, 1743-1751

134 Joglekar, A. P., Xu, D., Rigotti, D. J., Fairman, R. and Hay, J. C. (2003) The SNARE motif contributes to rbet1 intracellular targeting and dynamics independently of SNARE interactions. J Biol Chem. **278**, 14121-14133

135 Banfield, D. K., Lewis, M. J., Rabouille, C., Warren, G. and Pelham, H. R. (1994) Localization of Sed5, a putative vesicle targeting molecule, to the cis-Golgi network involves both its transmembrane and cytoplasmic domains. J Cell Biol. **127**, 357-371

136 Borgese, N., Brambillasca, S. and Colombo, S. (2007) How tails guide tail-anchored proteins to their destinations. Curr Opin Cell Biol. **19**, 368-375

137 Liu, Y., Flanagan, J. J. and Barlowe, C. (2004) Sec22p export from the endoplasmic reticulum is independent of SNARE pairing. J Biol Chem. **279**, 27225-27232

138 Mancias, J. D. and Goldberg, J. (2007) The transport signal on Sec22 for packaging into COPII-coated vesicles is a conformational epitope. Mol Cell. **26**, 403-414

139 Gordon, D. E., Mirza, M., Sahlender, D. A., Jakovleska, J. and Peden, A. A. (2009) Coiled-coil interactions are required for post-Golgi R-SNARE trafficking. EMBO Rep

140 Springer, S. and Schekman, R. (1998) Nucleation of COPII vesicular coat complex by endoplasmic reticulum to Golgi vesicle SNAREs. Science. **281**, 698-700

141 Rein, U., Andag, U., Duden, R., Schmitt, H. D. and Spang, A. (2002) ARF-GAP-mediated interaction between the ER-Golgi v-SNAREs and the COPI coat. J Cell Biol. **157**, 395-404

142 Miller, E. A., Beilharz, T. H., Malkus, P. N., Lee, M. C., Hamamoto, S., Orci, L. and Schekman, R. (2003) Multiple cargo binding sites on the COPII subunit Sec24p ensure capture of diverse membrane proteins into transport vesicles. Cell. **114**, 497-509

143 Mossessova, E., Bickford, L. C. and Goldberg, J. (2003) SNARE selectivity of the COPII coat. Cell. **114**, 483-495

144 Mancias, J. D. and Goldberg, J. (2008) Structural basis of cargo membrane protein discrimination by the human COPII coat machinery. EMBO J. **27**, 2918-2928

145 West, A. E., Neve, R. L. and Buckley, K. M. (1997) Targeting of the synaptic vesicle protein synaptobrevin in the axon of cultured hippocampal neurons: evidence for two distinct sorting steps. J Cell Biol. **139**, 917-927

146 Zeng, Q., Tran, T. T., Tan, H. X. and Hong, W. (2003) The cytoplasmic domain of Vamp4 and Vamp5 is responsible for their correct subcellular targeting: the N-terminal extenSion of VAMP4 contains a dominant autonomous targeting signal for the trans-Golgi network. J Biol Chem. **278**, 23046-23054

147 Dahms, N. M., Lobel, P. and Kornfeld, S. (1989) Mannose 6-phosphate receptors and lysosomal enzyme targeting. J Biol Chem. **264**, 12115-12118

148 Pendyala, P. R., Ayong, L., Eatrides, J., Schreiber, M., Pham, C., Chakrabarti, R., Fidock, D. A., Allen, C. M. and Chakrabarti, D. (2008) Characterization of a PRL protein tyrosine phosphatase from Plasmodium falciparum. Mol Biochem Parasitol. **158**, 1-10

149 Gowda, D. C. and Davidson, E. A. (1999) Protein glycosylation in the malaria parasite. Parasitol Today. **15**, 147-152

150 Dieckmann-Schuppert, A., Bender, S., Odenthal-Schnittler, M., Bause, E. and Schwarz, R. T. (1992) Apparent lack of N-glycosylation in the asexual intraerythrocytic stage of Plasmodium falciparum. Eur J Biochem. **205**, 815-825

151 Lewis, M. J. and Pelham, H. R. (1990) A human homologue of the yeast HDEL receptor. Nature. **348**, 162-163

152 Lewis, M. J. and Pelham, H. R. (1992) Sequence of a second human KDEL receptor. J Mol Biol. **226**, 913-916

153 Lewis, M. J. and Pelham, H. R. (1992) Ligand-induced redistribution of a human KDEL receptor from the Golgi complex to the endoplasmic reticulum. Cell. **68**, 353-364

154 Jackson, M. R., Nilsson, T. and Peterson, P. A. (1990) Identification of a consensus motif for retention of transmembrane proteins in the endoplasmic reticulum. EMBO J. **9**, 3153-3162

155 Jackson, M. R., Nilsson, T. and Peterson, P. A. (1993) Retrieval of transmembrane proteins to the endoplasmic reticulum. J Cell Biol. **121**, 317-333

156 Peterson, M. G., Crewther, P. E., Thompson, J. K., Corcoran, L. M., Coppel, R. L., Brown, G. V., Anders, R. F. and Kemp, D. J. (1988) A second antigenic heat shock protein of Plasmodium falciparum. DNA. **7**, 71-78

157 La Greca, N., Hibbs, A. R., Riffkin, C., Foley, M. and Tilley, L. (1997) Identification of an endoplasmic reticulum-resident calcium-binding protein with multiple EF-hand motifs in asexual stages of Plasmodium falciparum. Mol Biochem Parasitol. **89**, 283-293

158 Lopez-Estrano, C., Bhattacharjee, S., Harrison, T. and Haldar, K. (2003) Cooperative domains define a unique host cell-targeting signal in Plasmodium falciparum-infected erythrocytes. Proc Natl Acad Sci U S A. **100**, 12402-12407

159 van Ooij, C. and Haldar, K. (2007) Protein export from Plasmodium parasites. Cell Microbiol. **9**, 573-582

160 Marti, M., Good, R. T., Rug, M., Knuepfer, E. and Cowman, A. F. (2004) Targeting malaria virulence and remodeling proteins to the host erythrocyte. Science. **306**, 1930-1933

161 Hiller, N. L., Bhattacharjee, S., van Ooij, C., Liolios, K., Harrison, T., Lopez-Estrano, C. and Haldar, K. (2004) A host-targeting signal in virulence proteins reveals a secretome in malarial infection. Science. **306**, 1934-1937

162 Horrocks, P. and Muhia, D. (2005) Pexel/VTS: a protein-export motif in erythrocytes infected with malaria parasites. Trends Parasitol. **21**, 396-399

163 Sargeant, T. J., Marti, M., Caler, E., Carlton, J. M., Simpson, K., Speed, T. P. and Cowman, A. F. (2006) Lineage-specific expansion of proteins exported to erythrocytes in malaria parasites. Genome Biol. **7**, R12

164 Boddey, J. A., Moritz, R. L., Simpson, R. J. and Cowman, A. F. (2009) Role of the Plasmodium export element in trafficking parasite proteins to the infected erythrocyte. Traffic. **10**, 285-299

165 Hiss, J. A., Przyborski, J. M., Schwarte, F., Lingelbach, K. and Schneider, G. (2008) The Plasmodium export element revisited. PLoS ONE. **3**, e1560

166 Ansorge, I., Benting, J., Bhakdi, S. and Lingelbach, K. (1996) Protein sorting in Plasmodium falciparum-infected red blood cells permeabilized with the pore-forming protein streptolysin O. Biochem J. **315 (Pt 1)**, 307-314

167 Gehde, N., Hinrichs, C., Montilla, I., Charpian, S., Lingelbach, K. and Przyborski, J. M. (2009) Protein unfolding is an essential requirement for transport across the

parasitophorous vacuolar membrane of Plasmodium falciparum. Mol Microbiol. **71**, 613-628

168 Winstanley, P. (2001) Modern chemotherapeutic options for malaria. Lancet Infect Dis. **1**, 242-250

169 Warhurst, D. C., Craig, J. C. and Adagu, I. S. (2002) Lysosomes and drug resistance in malaria. Lancet. **360**, 1527-1529

170 Banerjee, R., Liu, J., Beatty, W., Pelosof, L., Klemba, M. and Goldberg, D. E. (2002) Four plasmepsins are active in the Plasmodium falciparum food vacuole, including a protease with an active-site histidine. Proc Natl Acad Sci U S A. **99**, 990-995

171 Shenai, B. R., Sijwali, P. S., Singh, A. and Rosenthal, P. J. (2000) Characterization of native and recombinant falcipain-2, a principal trophozoite cysteine protease and essential hemoglobinase of Plasmodium falciparum. J Biol Chem. **275**, 29000-29010

172 Coombs, G. H., Goldberg, D. E., Klemba, M., Berry, C., Kay, J. and Mottram, J. C. (2001) Aspartic proteases of Plasmodium falciparum and other parasitic protozoa as drug targets. Trends Parasitol. **17**, 532-537

173 Dasaradhi, P. V., Korde, R., Thompson, J. K., Tanwar, C., Nag, T. C., Chauhan, V. S., Cowman, A. F., Mohmmed, A. and Malhotra, P. (2007) Food vacuole targeting and trafficking of falcipain-2, an important cysteine protease of human malaria parasite Plasmodium falciparum. Mol Biochem Parasitol. **156**, 12-23

174 Klemba, M., Gluzman, I. and Goldberg, D. E. (2004) A Plasmodium falciparum dipeptidyl aminopeptidase I participates in vacuolar hemoglobin degradation. J Biol Chem. **279**, 43000-43007

175 Sijwali, P. S., Kato, K., Seydel, K. B., Gut, J., Lehman, J., Klemba, M., Goldberg, D. E., Miller, L. H. and Rosenthal, P. J. (2004) Plasmodium falciparum cysteine protease falcipain-1 is not essential in erythrocytic stage malaria parasites. Proc Natl Acad Sci U S A. **101**, 8721-8726

176 Klemba, M., Beatty, W., Gluzman, I. and Goldberg, D. E. (2004) Trafficking of plasmepsin II to the food vacuole of the malaria parasite Plasmodium falciparum. J Cell Biol. **164**, 47-56

177 Kats, L. M., Black, C. G., Proellocks, N. I. and Coppel, R. L. (2006) Plasmodium rhoptries: how things went pear-shaped. Trends Parasitol. **22**, 269-276

178 Lobo, C. A., Rodriguez, M., Hou, G., Perkins, M., Oskov, Y. and Lustigman, S. (2003) Characterization of PfRhop148, a novel rhoptry protein of Plasmodium falciparum. Mol Biochem Parasitol. **128**, 59-65

179 Topolska, A. E., Lidgett, A., Truman, D., Fujioka, H. and Coppel, R. L. (2004) Characterization of a membrane-associated rhoptry protein of Plasmodium falciparum. J Biol Chem. **279**, 4648-4656

180 Bonifacino, J. S. and Dell'Angelica, E. C. (1999) Molecular bases for the recognition of tyrosine-based sorting signals. J Cell Biol. **145**, 923-926

181 Robinson, M. S. (2004) Adaptable adaptors for coated vesicles. Trends Cell Biol. **14**, 167-174

182 Bhanot, P., Frevert, U., Nussenzweig, V. and Persson, C. (2003) Defective sorting of the thrombospondin-related anonymous protein (TRAP) inhibits Plasmodium infectivity. Mol Biochem Parasitol. **126**, 263-273

183 Meissner, M., Reiss, M., Viebig, N., Carruthers, V. B., Toursel, C., Tomavo, S., Ajioka, J. W. and Soldati, D. (2002) A family of transmembrane microneme proteins of Toxoplasma gondii contain EGF-like domains and function as escorters. J Cell Sci. **115**, 563-574

184 Reiss, M., Viebig, N., Brecht, S., Fourmaux, M. N., Soete, M., Di Cristina, M., Dubremetz, J. F. and Soldati, D. (2001) Identification and characterization of an escorter for two secretory adhesins in Toxoplasma gondii. J Cell Biol. **152**, 563-578

185 Rug, M., Wickham, M. E., Foley, M., Cowman, A. F. and Tilley, L. (2004) Correct promoter control is needed for trafficking of the ring-infected erythrocyte surface antigen to the host cytosol in transfected malaria parasites. Infect Immun. **72**, 6095-6105

186 Le Roch, K. G., Zhou, Y., Blair, P. L., Grainger, M., Moch, J. K., Haynes, J. D., De La Vega, P., Holder, A. A., Batalov, S., Carucci, D. J. and Winzeler, E. A. (2003) Discovery of gene function by expression profiling of the malaria parasite life cycle. Science. **301**, 1503-1508

187 Bozdech, Z., Llinas, M., Pulliam, B. L., Wong, E. D., Zhu, J. and DeRisi, J. L. (2003) The transcriptome of the intraerythrocytic developmental cycle of Plasmodium falciparum. PLoS Biol. **1**, E5

188 Bozdech, Z., Zhu, J., Joachimiak, M. P., Cohen, F. E., Pulliam, B. and DeRisi, J. L. (2003) Expression profiling of the schizont and trophozoite stages of Plasmodium falciparum with a long-oligonucleotide microarray. Genome Biol. **4**, R9

189 Emanuelsson, O. and von Heijne, G. (2001) Prediction of organellar targeting signals. Biochim Biophys Acta. **1541**, 114-119

190 Emanuelsson, O., von Heijne, G. and Schneider, G. (2001) Analysis and prediction of mitochondrial targeting peptides. Methods Cell Biol. **65**, 175-187

191 Neupert, W. and Brunner, M. (2002) The protein import motor of mitochondria. Nat Rev Mol Cell Biol. **3**, 555-565

192 Hoogenraad, N. J., Ward, L. A. and Ryan, M. T. (2002) Import and assembly of proteins into mitochondria of mammalian cells. Biochim Biophys Acta. **1592**, 97-105

193 Bender, A., van Dooren, G. G., Ralph, S. A., McFadden, G. I. and Schneider, G. (2003) Properties and prediction of mitochondrial transit peptides from Plasmodium falciparum. Mol Biochem Parasitol. **132**, 59-66

194 Waller, R. F., Keeling, P. J., Donald, R. G., Striepen, B., Handman, E., Lang-Unnasch, N., Cowman, A. F., Besra, G. S., Roos, D. S. and McFadden, G. I. (1998) Nuclear-encoded proteins target to the plastid in Toxoplasma gondii and Plasmodium falciparum. Proc Natl Acad Sci U S A. **95**, 12352-12357

195 Sato, S., Clough, B., Coates, L. and Wilson, R. J. (2004) Enzymes for heme biosynthesis are found in both the mitochondrion and plastid of the malaria parasite Plasmodium falciparum. Protist. **155**, 117-125

196 Waller, R. F., Reed, M. B., Cowman, A. F. and McFadden, G. I. (2000) Protein trafficking to the plastid of Plasmodium falciparum is via the secretory pathway. EMBO J. **19**, 1794-1802

197 Foth, B. J., Ralph, S. A., Tonkin, C. J., Struck, N. S., Fraunholz, M., Roos, D. S., Cowman, A. F. and McFadden, G. I. (2003) Dissecting apicoplast targeting in the malaria parasite Plasmodium falciparum. Science. **299**, 705-708

198 Gorlich, D., Henklein, P., Laskey, R. A. and Hartmann, E. (1996) A 41 amino acid motif in importin-alpha confers binding to importin-beta and hence transit into the nucleus. EMBO J. **15**, 1810-1817

199 Gorlich, D. and Mattaj, I. W. (1996) Nucleocytoplasmic transport. Science. **271**, 1513-1518

200 Lanford, R. E., Kanda, P. and Kennedy, R. C. (1986) Induction of nuclear transport with a synthetic peptide homologous to the SV40 T antigen transport signal. Cell. **46**, 575-582

201 Robbins, J., Dilworth, S. M., Laskey, R. A. and Dingwall, C. (1991) Two interdependent basic domains in nucleoplasmin nuclear targeting sequence: identification of a class of bipartite nuclear targeting sequence. Cell. **64**, 615-623

202 Dang, C. V. and Lee, W. M. (1988) Identification of the human c-myc protein nuclear translocation signal. Mol Cell Biol. **8**, 4048-4054

203 Weighardt, F., Biamonti, G. and Riva, S. (1995) Nucleo-cytoplasmic distribution of human hnRNP proteins: a search for the targeting domains in hnRNP A1. J Cell Sci. **108 (Pt 2)**, 545-555

204 Przyborski, J. M., Bartels, K., Lanzer, M. and Andrews, K. T. (2003) The histone H4 gene of Plasmodium falciparum is developmentally transcribed in asexual parasites. Parasitol Res. **90**, 387-389

205 Xu, X., Yamasaki, H., Feng, Z. and Aoki, T. (2002) Molecular cloning and characterization of Plasmodium falciparum transportin. Parasitol Res. **88**, 391-394

206 Mohmmed, A., Kishore, S., Dasaradhi, P. V., Patra, K., Malhotra, P. and Chauhan, V. S. (2003) Cloning and characterization of Plasmodium falciparum homologs of nuclear import factors, karyopherin alpha and karyopherin beta. Mol Biochem Parasitol. **127**, 199-203

207 Gardner, M. J., Hall, N., Fung, E., White, O., Berriman, M., Hyman, R. W., Carlton, J. M., Pain, A., Nelson, K. E., Bowman, S., Paulsen, I. T., James, K., Eisen, J. A., Rutherford, K.,

Salzberg, S. L., Craig, A., Kyes, S., Chan, M. S., Nene, V., Shallom, S. J., Suh, B., Peterson, J., Angiuoli, S., Pertea, M., Allen, J., Selengut, J., Haft, D., Mather, M. W., Vaidya, A. B., Martin, D. M., Fairlamb, A. H., Fraunholz, M. J., Roos, D. S., Ralph, S. A., McFadden, G. I., Cummings, L. M., Subramanian, G. M., Mungall, C., Venter, J. C., Carucci, D. J., Hoffman, S. L., Newbold, C., Davis, R. W., Fraser, C. M. and Barrell, B. (2002) Genome sequence of the human malaria parasite Plasmodium falciparum. Nature. **419**, 498-511

208 Gardner, M. J., Shallom, S. J., Carlton, J. M., Salzberg, S. L., Nene, V., Shoaibi, A., Ciecko, A., Lynn, J., Rizzo, M., Weaver, B., Jarrahi, B., Brenner, M., Parvizi, B., Tallon, L., Moazzez, A., Granger, D., Fujii, C., Hansen, C., Pederson, J., Feldblyum, T., Peterson, J., Suh, B., Angiuoli, S., Pertea, M., Allen, J., Selengut, J., White, O., Cummings, L. M., Smith, H. O., Adams, M. D., Venter, J. C., Carucci, D. J., Hoffman, S. L. and Fraser, C. M. (2002) Sequence of Plasmodium falciparum chromosomes 2, 10, 11 and 14. Nature. **419**, 531-534

209 Florens, L., Washburn, M. P., Raine, J. D., Anthony, R. M., Grainger, M., Haynes, J. D., Moch, J. K., Muster, N., Sacci, J. B., Tabb, D. L., Witney, A. A., Wolters, D., Wu, Y., Gardner, M. J., Holder, A. A., Sinden, R. E., Yates, J. R. and Carucci, D. J. (2002) A proteomic view of the Plasmodium falciparum life cycle. Nature. **419**, 520-526

210 Wilson, R. J. and Williamson, D. H. (1997) Extrachromosomal DNA in the Apicomplexa. Microbiol Mol Biol Rev. **61**, 1-16

211 Wilson, R. J., Denny, P. W., Preiser, P. R., Rangachari, K., Roberts, K., Roy, A., Whyte, A., Strath, M., Moore, D. J., Moore, P. W. and Williamson, D. H. (1996) Complete gene

map of the plastid-like DNA of the malaria parasite Plasmodium falciparum. J Mol Biol. **261**, 155-172

212 Meissner, M., Breinich, M. S., Gilson, P. R. and Crabb, B. S. (2007) Molecular genetic tools in Toxoplasma and Plasmodium: achievements and future needs. Curr Opin Microbiol. **10**, 349-356

213 Aravind, L., Iyer, L. M., Wellems, T. E. and Miller, L. H. (2003) Plasmodium biology: genomic gleanings. Cell. **115**, 771-785

214 Blackman, M. J. (2003) RNAi in protozoan parasites: what hope for the Apicomplexa? Protist. **154**, 177-180

215 Tonkin, C. J., van Dooren, G. G., Spurck, T. P., Struck, N. S., Good, R. T., Handman, E., Cowman, A. F. and McFadden, G. I. (2004) Localization of organellar proteins in Plasmodium falciparum using a novel set of transfection vectors and a new immunofluorescence fixation method. Mol Biochem Parasitol. **137**, 13-21

216 O'Donnell, R. A., Freitas-Junior, L. H., Preiser, P. R., Williamson, D. H., Duraisingh, M., McElwain, T. F., Scherf, A., Cowman, A. F. and Crabb, B. S. (2002) A genetic screen for improved plasmid segregation reveals a role for Rep20 in the interaction of Plasmodium falciparum chromosomes. EMBO J. **21**, 1231-1239

217 Wu, Y., Kirkman, L. A. and Wellems, T. E. (1996) Transformation of Plasmodium falciparum malaria parasites by homologous integration of plasmids that confer resistance to pyrimethamine. Proc Natl Acad Sci U S A. **93**, 1130-1134

218 Crabb, B. S. and Cowman, A. F. (1996) Characterization of promoters and stable transfection by homologous and nonhomologous recombination in Plasmodium falciparum. Proc Natl Acad Sci U S A. **93**, 7289-7294

219 Fidock, D. A. and Wellems, T. E. (1997) Transformation with human dihydrofolate reductase renders malaria parasites insensitive to WR99210 but does not affect the intrinsic activity of proguanil. Proc Natl Acad Sci U S A. **94**, 10931-10936

220 Deitsch, K., Driskill, C. and Wellems, T. (2001) Transformation of malaria parasites by the spontaneous uptake and expression of DNA from human erythrocytes. Nucleic Acids Res. **29**, 850-853

221 O'Donnell, R. A., Preiser, P. R., Williamson, D. H., Moore, P. W., Cowman, A. F. and Crabb, B. S. (2001) An alteration in concatameric structure is associated with efficient segregation of plasmids in transfected Plasmodium falciparum parasites. Nucleic Acids Res. **29**, 716-724

222 Nkrumah, L. J., Muhle, R. A., Moura, P. A., Ghosh, P., Hatfull, G. F., Jacobs, W. R., Jr. and Fidock, D. A. (2006) Efficient site-specific integration in Plasmodium falciparum chromosomes mediated by mycobacteriophage Bxb1 integrase. Nat Methods. **3**, 615-621

223 Balu, B., Shoue, D. A., Fraser, M. J., Jr. and Adams, J. H. (2005) High-efficiency transformation of Plasmodium falciparum by the lepidopteran transposable element piggyBac. Proc Natl Acad Sci U S A. **102**, 16391-16396

224 Gattiker, A., Gasteiger, E. and Bairoch, A. (2002) ScanProsite: a reference implementation of a PROSITE scanning tool. Appl Bioinformatics. **1**, 107-108

225 Sigrist, C. J., Cerutti, L., Hulo, N., Gattiker, A., Falquet, L., Pagni, M., Bairoch, A. and Bucher, P. (2002) PROSITE: a documented database using patterns and profiles as motif descriptors. Brief Bioinform. **3**, 265-274

226 Arai, M., Mitsuke, H., Ikeda, M., Xia, J. X., Kikuchi, T., Satake, M. and Shimizu, T. (2004) ConPred II: a consensus prediction method for obtaining transmembrane topology models with high reliability. Nucleic Acids Res. **32**, W390-393

227 Chakrabarti, D., Da Silva, T., Barger, J., Paquette, S., Patel, H., Patterson, S. and Allen, C. M. (2002) Protein farnesyltransferase and protein prenylation in Plasmodium falciparum. J Biol Chem. **277**, 42066-42073

228 Elandalloussi, L. M. and Smith, P. J. (2002) Preparation of pure and intact Plasmodium falciparum plasma membrane vesicles and partial characterisation of the plasma membrane ATPase. Malar J. **1**, 6

229 Bradford, M. M. (1976) A rapid and sensitive method for the quantitation of microgram quantities of protein utilizing the principle of protein-dye binding. Anal Biochem. **72**, 248-254

230 Fidock, D. A., Nomura, T. and Wellems, T. E. (1998) Cycloguanil and its parent compound proguanil demonstrate distinct activities against Plasmodium falciparum malaria parasites transformed with human dihydrofolate reductase. Mol Pharmacol. **54**, 1140-1147

231 Lee, M. C., Moura, P. A., Miller, E. A. and Fidock, D. A. (2008) Plasmodium falciparum Sec24 Marks Transitional ER that Exports a Model Cargo via a Diacidic Motif. Mol Microbiol

232 Mumberg, D., Muller, R. and Funk, M. (1994) Regulatable promoters of Saccharomyces cerevisiae: comparison of transcriptional activity and their use for heterologous expression. Nucleic Acids Res. **22**, 5767-5768

233 Miller, E. A., Liu, Y., Barlowe, C. and Schekman, R. (2005) ER-Golgi transport defects are associated with mutations in the Sed5p-binding domain of the COPII coat subunit, Sec24p. Mol Biol Cell. **16**, 3719-3726

234 Ito, H., Fukuda, Y., Murata, K. and Kimura, A. (1983) Transformation of intact yeast cells treated with alkali cations. J Bacteriol. **153**, 163-168

235 McNew, J. A., Sogaard, M., Lampen, N. M., Machida, S., Ye, R. R., Lacomis, L., Tempst, P., Rothman, J. E. and Sollner, T. H. (1997) Ykt6p, a prenylated SNARE essential for endoplasmic reticulum-Golgi transport. J Biol Chem. **272**, 17776-17783

236 Besteiro, S., Coombs, G. H. and Mottram, J. C. (2006) The SNARE protein family of Leishmania major. BMC Genomics. **7**, 250

237 Hong, W. (2005) SNAREs and traffic. Biochim Biophys Acta

238 Dacks, J. B. and Doolittle, W. F. (2004) Molecular and phylogenetic characterization of syntaxin genes from parasitic protozoa. Mol Biochem Parasitol. **136**, 123-136

239 Paek, I., Orci, L., Ravazzola, M., Erdjument-Bromage, H., Amherdt, M., Tempst, P., Sollner, T. H. and Rothman, J. E. (1997) ERS-24, a mammalian v-SNARE implicated in vesicle traffic between the ER and the Golgi. J Cell Biol. **137**, 1017-1028

240 Tang, B. L., Low, D. Y. and Hong, W. (1998) Hsec22c: a homolog of yeast Sec22p and mammalian rsec22a and msec22b/ERS-24. Biochem Biophys Res Commun. **243**, 885-891

241 Uemura, T., Ueda, T., Ohniwa, R. L., Nakano, A., Takeyasu, K. and Sato, M. H. (2004) Systematic analysis of SNARE molecules in Arabidopsis: dissection of the post-Golgi network in plant cells. Cell Struct Funct. **29**, 49-65

242 Ballensiefen, W., Ossipov, D. and Schmitt, H. D. (1998) Recycling of the yeast v-SNARE Sec22p involves COPI-proteins and the ER transmembrane proteins Ufe1p and Sec20p. J Cell Sci. **111 (Pt 11)**, 1507-1520

243 Chang, H. H., Falick, A. M., Carlton, P. M., Sedat, J. W., DeRisi, J. L. and Marletta, M. A. (2008) N-terminal processing of proteins exported by malaria parasites. Mol Biochem Parasitol. **160**, 107-115

244 Gupta, G. D. and Brent Heath, I. (2002) Predicting the distribution, conservation, and functions of SNAREs and related proteins in fungi. Fungal Genet Biol. **36**, 1-21

245 Schilde, C., Wassmer, T., Mansfeld, J., Plattner, H. and Kissmehl, R. (2006) A multigene family encoding R-SNAREs in the ciliate Paramecium tetraurelia. Traffic. **7**, 440-455

246 Beilharz, T., Egan, B., Silver, P. A., Hofmann, K. and Lithgow, T. (2003) Bipartite signals mediate subcellular targeting of tail-anchored membrane proteins in Saccharomyces cerevisiae. J Biol Chem. **278**, 8219-8223

247 Watson, R. T. and Pessin, J. E. (2001) Subcellular compartmentalization and trafficking of the insulin-responsive glucose transporter, GLUT4. Exp Cell Res. **271**, 75-83

248 Hayashi, M., Taniguchi, S., Ishizuka, Y., Kim, H. S., Wataya, Y., Yamamoto, A. and Moriyama, Y. (2001) A homologue of N-ethylmaleimide-sensitive factor in the malaria parasite Plasmodium falciparum is exported and localized in vesicular structures in the cytoplasm of infected erythrocytes in the brefeldin A-sensitive pathway. J Biol Chem. **276**, 15249-15255

249 Arnold, K., Bordoli, L., Kopp, J. and Schwede, T. (2006) The SWISS-MODEL workspace: a web-based environment for protein structure homology modelling. Bioinformatics. **22**, 195-201

250 Fidock, D. A., Nomura, T., Talley, A. K., Cooper, R. A., Dzekunov, S. M., Ferdig, M. T., Ursos, L. M., Sidhu, A. B., Naude, B., Deitsch, K. W., Su, X. Z., Wootton, J. C., Roepe, P. D. and Wellems, T. E. (2000) Mutations in the P. falciparum digestive vacuole transmembrane protein PfCRT and evidence for their role in chloroquine resistance. Mol Cell. **6**, 861-871

251 Ayong, L., Pagnotti, G., Tobon, A. B. and Chakrabarti, D. (2007) Identification of Plasmodium falciparum family of SNAREs. Mol Biochem Parasitol. **152**, 113-122

252 Orci, L., Perrelet, A., Ravazzola, M., Wieland, F. T., Schekman, R. and Rothman, J. E. (1993) "BFA bodies": a subcompartment of the endoplasmic reticulum. Proc Natl Acad Sci U S A. **90**, 11089-11093

253 Orci, L., Tagaya, M., Amherdt, M., Perrelet, A., Donaldson, J. G., Lippincott-Schwartz, J., Klausner, R. D. and Rothman, J. E. (1991) Brefeldin A, a drug that blocks secretion, prevents the assembly of non-clathrin-coated buds on Golgi cisternae. Cell. **64**, 1183-1195

254 Benting, J., Ansorge, I., Paprotka, K. and Lingelbach, K. R. (1994) Chemical and thermal inhibition of protein secretion have stage specific effects on the intraerythrocytic development of Plasmodium falciparum in vitro. Trop Med Parasitol. **45**, 303-307

255 Przyborski, J. M., Miller, S. K., Pfahler, J. M., Henrich, P. P., Rohrbach, P., Crabb, B. S. and Lanzer, M. (2005) Trafficking of STEVOR to the Maurer's clefts in Plasmodium falciparum-infected erythrocytes. Embo J. **24**, 2306-2317

256 Klein, D. J., Moore, P. B. and Steitz, T. A. (2004) The contribution of metal ions to the structural stability of the large ribosomal subunit. Rna. **10**, 1366-1379

257 Chehab, E. W., Patharkar, O. R. and Cushman, J. C. (2007) Isolation and characterization of a novel v-SNARE family protein that interacts with a calcium-dependent protein kinase from the common ice plant, Mesembryanthemum crystallinum. Planta. **225**, 783-799

258 Spycher, C., Rug, M., Klonis, N., Ferguson, D. J., Cowman, A. F., Beck, H. P. and Tilley, L. (2006) Genesis of and trafficking to the Maurer's clefts of Plasmodium falciparum-infected erythrocytes. Mol Cell Biol. **26**, 4074-4085

259 Dixon, M. W., Hawthorne, P. L., Spielmann, T., Anderson, K. L., Trenholme, K. R. and Gardiner, D. L. (2008) Targeting of the ring exported protein 1 to the Maurer's clefts is mediated by a two-phase process. Traffic. **9**, 1316-1326

260 Saridaki, T., Frohlich, K. S., Braun-Breton, C. and Lanzer, M. (2009) Export of PfSBP1 to the Plasmodium falciparum Maurer's clefts. Traffic. **10**, 137-152

261 Gonzalez, L. C., Jr., Weis, W. I. and Scheller, R. H. (2001) A novel snare N-terminal domain revealed by the crystal structure of Sec22b. J Biol Chem. **276**, 24203-24211

262 Tsui, M. M. and Banfield, D. K. (2000) Yeast Golgi SNARE interactions are promiscuous. J Cell Sci. **113 (Pt 1)**, 145-152

263 Klausner, R. D., Donaldson, J. G. and Lippincott-Schwartz, J. (1992) Brefeldin A: insights into the control of membrane traffic and organelle structure. J Cell Biol. **116**, 1071-1080

264 Wiser, M. F., Lanners, H. N., Bafford, R. A. and Favaloro, J. M. (1997) A novel alternate secretory pathway for the export of Plasmodium proteins into the host erythrocyte. Proc Natl Acad Sci U S A. **94**, 9108-9113

265 Hohenstein, A. C. and Roche, P. A. (2001) SNAP-29 is a promiscuous syntaxin-binding SNARE. Biochem Biophys Res Commun. **285**, 167-171

266 Fasshauer, D., Antonin, W., Margittai, M., Pabst, S. and Jahn, R. (1999) Mixed and non-cognate SNARE complexes. Characterization of assembly and biophysical properties. J Biol Chem. **274**, 15440-15446

267 Aoki, T., Kojima, M., Tani, K. and Tagaya, M. (2008) Sec22b-dependent assembly of endoplasmic reticulum Q-SNARE proteins. Biochem J. **410**, 93-100

268 Aury, J. M., Jaillon, O., Duret, L., Noel, B., Jubin, C., Porcel, B. M., Segurens, B., Daubin, V., Anthouard, V., Aiach, N., Arnaiz, O., Billaut, A., Beisson, J., Blanc, I., Bouhouche, K., Camara, F., Duharcourt, S., Guigo, R., Gogendeau, D., Katinka, M., Keller, A. M., Kissmehl, R., Klotz, C., Koll, F., Le Mouel, A., Lepere, G., Malinsky, S., Nowacki, M., Nowak, J. K., Plattner, H., Poulain, J., Ruiz, F., Serrano, V., Zagulski, M., Dessen, P., Betermier, M., Weissenbach, J., Scarpelli, C., Schachter, V., Sperling, L., Meyer, E., Cohen, J. and Wincker, P. (2006) Global trends of whole-genome duplications revealed by the ciliate Paramecium tetraurelia. Nature. **444**, 171-178

269 Elias, E. V., Quiroga, R., Gottig, N., Nakanishi, H., Nash, T. E., Neiman, A. and Lujan, H. D. (2008) Characterization of SNAREs determines the absence of a typical Golgi apparatus in the ancient eukaryote Giardia lamblia. J Biol Chem. **283**, 35996-36010

270 Kloepper, T. H., Kienle, C. N. and Fasshauer, D. (2008) SNAREing the basis of multicellularity: consequences of protein family expansion during evolution. Mol Biol Evol. **25**, 2055-2068

271 Kloepper, T. H., Kienle, C. N. and Fasshauer, D. (2007) An elaborate classification of SNARE proteins sheds light on the conservation of the eukaryotic endomembrane system. Mol Biol Cell. **18**, 3463-3471

272 Elmendorf, H. G. and Haldar, K. (1994) Plasmodium falciparum exports the Golgi marker sphingomyelin synthase into a tubovesicular network in the cytoplasm of mature erythrocytes. J Cell Biol. **124**, 449-462

273 Spielmann, T., Fergusen, D. J. and Beck, H. P. (2003) etramps, a new Plasmodium falciparum gene family coding for developmentally regulated and highly charged membrane proteins located at the parasite-host cell interface. Mol Biol Cell. **14**, 1529-1544

274 McMahon, H. T. and Gallop, J. L. (2005) Membrane curvature and mechanisms of dynamic cell membrane remodelling. Nature. **438**, 590-596

275 Bonnefoy, S. and Menard, R. (2008) Deconstructing export of malaria proteins. Cell. **134**, 20-22

276 de Koning-Ward, T. F., Gilson, P. R., Boddey, J. A., Rug, M., Smith, B. J., Papenfuss, A. T., Sanders, P. R., Lundie, R. J., Maier, A. G., Cowman, A. F. and Crabb, B. S. (2009) A newly discovered protein export machine in malaria parasites. Nature. **459**, 945-949

277 Adisa, A., Albano, F. R., Reeder, J., Foley, M. and Tilley, L. (2001) Evidence for a role for a Plasmodium falciparum homologue of Sec31p in the export of proteins to the surface of malaria parasite-infected erythrocytes. J Cell Sci. **114**, 3377-3386

278 Adisa, A., Rug, M., Foley, M. and Tilley, L. (2002) Characterisation of a delta-COP homologue in the malaria parasite, Plasmodium falciparum. Mol Biochem Parasitol. **123**, 11-21

279 Albano, F. R., Berman, A., La Greca, N., Hibbs, A. R., Wickham, M., Foley, M. and Tilley, L. (1999) A homologue of Sar1p localises to a novel trafficking pathway in malaria-infected erythrocytes. Eur J Cell Biol. **78**, 453-462